A LABORATORY METHOD FOR INVESTIGATION OF DIFFUSION AND TRANSFORMATION OF VOLATILE ORGANIC COMPOUNDS IN LOW PERMEABILITY MEDIA

by

Susan Lynne Gordon

A thesis
presented to the University of Waterloo
in fulfilment of the
thesis requirement for the degree of
Doctor of Philosophy
in
Earth Sciences

Waterloo, Ontario, Canada, 1999

The University of Waterloo requires the signatures of all persons using or photocopying this thesis. Please sign below, and give address and date.

ABSTRACT

A laboratory diffusion cell technique is presented that provided effective diffusion coefficients (D_e) and first order rate constants (k) of volatile organic compounds (VOCs) in one sample of reactive low permeability media based on the temporal VOC concentration measurements of both a reservoir source and a porous medium column. A sealed stainless steel cylinder contained a vapour reservoir overlying an artificial, low permeability medium under slight negative porewater pressure. Vapour-filled horizontal "mini-boreholes" were established along the length of the porous medium. Nonreactive experiments (Ottawa sand crushed to fine silt and clay size) with 5 VOCs (carbon disulphide (CS_2), chloroform (CCl_3H), 1,2-dichloroethane (1,2-DCA), carbon tetrachloride (CCl_4) and perchloroethylene (PCE)) and reactive experiments (the nonreactive material amended with 17% (w/w) pyrite) with CCl_4 transforming to CCl_3H and CS_2 were conducted in duplicate, each for one month.

Reservoir concentrations and borehole profiles were obtained within a few minute of collecting a 1 minute sample utilizing Solid Phase Microextraction fibres coated with 1 of 2 tested poly(dimethylsiloxane) thicknesses (7 μm and 100 μm). For VOCs with greater fibre coating partitioning values (CCl_4 and PCE), the thinner coating was better suited because it reduced the mass extracted from the reservoir and the porewater. For application to field samples, the core container itself could be utilized as the diffusion cell to ensure a tight seal with the cylinder walls.

D_e values, which ranged from 4×10^{-6} to 7×10^{-6} cm^2/sec, are within the range of literature values for nonsorbing and nonreactive compounds in natural silt and clay deposits. The 4 estimated first order rate constants for the CCl_4-pyrite reactions were within the same order of magnitude as results by others. The overall rate constant for CCl_4 was within experimental precision in the duplicate diffusion cells. The rate constant for the formation of the transformation products were up to 1.6 times different in the two diffusion cells and this may reflect the reaction mechanism's sensitivity to slight differences in reaction conditions, as reported by others. CCl_4 transformation is overpredicted in the first few cm of diffusive transport with a first order reaction kinetic model (with respect to CCl_4 concentration model) and may be better predicted with a zero order kinetic model and/or a decrease in assumed pyrite reactivity with time.

ACKNOWLEDGMENTS

I thank my family, friends, supervisors and committee members. All of you have had an important role at some point in my reaching this final stage. Also thanks to the many colleagues that were willing to provide advice on the various components of the research.

Much has been gained by this experience. Of course, as in all things in life, some things have been lost. I have given so little time to those I consider dear while they have kept me focussed and sane. So many memories to take with me on my new life path.....

TABLE OF CONTENTS

List of Tables

List of Figures

List of Appendices

CHAPTER 1
INTRODUCTION

The diffusion and fate of Volatile Organic Compounds (VOCs) in low permeability media may have a significant impact on groundwater contaminant remediation. Natural low permeability media can act as long term sources of contaminants (Parker et al., 1994) and contaminant migration on a scale typical of the thickness of engineered waste disposal site liners can occur solely as a result of diffusive fluxes (Johnson et al., 1989; Shackelford, 1991; Devlin and Parker, 1996).

The fate of VOCs in natural or engineered low permeability media has not been extensively studied (Devlin and Parker, 1996; Major 1997) but it is recognized that their transformation could be an important process in reducing the breakthrough of contaminants out of low permeability media. Laboratory studies of VOC transformation by reactive media (Kreigman-King and Reinhard, 1991; Gillham and O'Hannesin, 1994) have shown that the rates of abiotic heterogeneous transformations (reactions that occur without microrganisms and occur at least in part at a solid surface) of certain types of VOCs, i.e. halogenated organic compounds (HOCs), are several orders of magnitude faster than abiotic homogeneous reactions (occuring solely in the aqueous phase). In general, the low hydraulic conductivities of low permeability media, which result in contaminant transport dominanted by diffusion through fine grained porous media, appear well suited to generate conditions favourable to the abiotic heterogeneous transformation of HOCs, i.e. low oxygen conditions, long contact times between contaminant and solid surface, and high solid surface areas (Schwarzenbach et al., 1993; Nicholson, 1994; Kreigman-King and Reinhard, 1994). Thus, abiotic heterogeneous reactions would be expected to be important in controlling the fate and transport of some VOCs in low permeability media.

The diffusive fluxes of the members of an abiotic heterogeneous transformation series formed in reactive, low permeability media are controlled by their rates of generation, diffusion and subsequent transformation, all of which may be difficult to predict *a priori*. Thus, our ability to exploit transformation processes in the remediation of VOCs in low permeability media would benefit from a laboratory diffusion cell technique that allows for the fast and efficient measurement of sequential diffusion profiles in one core sample with minimal disturbance to the processes being studied.

The more common laboratory diffusion cell techniques are not well suited to the temporal measurements of a VOC transformation series because they are destructive, i.e. contaminated cores are sliced or micro-cored (Parker, 1996; Ball et al., 1997), and are best

suited for "snap shot" sampling to obtain concentrations on a one time basis. Another method, which measures the declining concentrations in an aqueous source reservoir (Myrand et al., 1992), does not include the measurement of diffusion profiles and, thus, leads to the inevitable uncertainty whether the unaccounted mass for has actually diffused within the column as assumed.

1.1 Goals, Structure and Scope of the Thesis

One goal of this thesis is to develop a method to temporally study diffusion and other processes such as transformation in a single sample of low permeability media. Thus, this goal involves collecting samples for analysis in such a way that there is minimal impact of the sampling procedure on the VOC's diffusive transport and transformation in the low permeability medium. This requires that any advective effects on the profiles caused by the sampling process are insignificant, and that the solute mass removed creates an insignificant disturbance of the concentration gradients. Another goal was improved accuracy and precision of the experimentally determined effective diffusion coefficients and reaction coefficients. In addition, improved insight into the possible time dependence of processes that may affect VOC transformations was sought.

The new diffusion cell design employs a vapour reservoir source and utilizes negative porewater pressures in the porous medium column to create "mini-boreholes" containing vapour in equilibrium with the surrounding porewater. The sampling of the vapour in the reservoir and in the boreholes uses a microsampling technique called Solid Phase Microextraction or SPME (Pawliszyn, 1997). This sampling technique employs a polymer coated fibre (in this study a poly(dimethylsiloxane) coating) that "microextracts" VOC mass after insertion into a sample that can then be quantified by various analytical techniques such as the gas chromatography used in this study.

The thesis has been written as two manuscripts (Chapters 2 and 3) each with separate introduction, methodology, results, conclusions and references. Chapters 1 and 4 have been written as the introduction and conclusions, respectively, of the thesis. The first manuscript (Chapter 2) focuses on the description of the new diffusion cell technique and its application to the diffusion of a suite of five VOCs (carbon disulphide (CS_2), chloroform (CCl_3H), 1,2-dicholoroethane (1,2-DCA), carbon tetrachloride (CCl_4) and perchloroethylene (PCE)) through a nonreactive artificial porous medium comprised of water-saturated packed silica solids with a low permeability. These packed columns of water-saturated, fine silt- and clay-sized particles are anticipated to yield effective diffusion coefficient estimates similar to

those from field cores of natural silt or clay. The second manuscript (Chapter 3) describes the diffusion of a heterogeneous transformation series (CCl_4 transforming to CCl_3H and CS_2) and a tracer (1,2-DCA) through a reactive artificial low permeability medium comprised of a mixture of pyrite and silica solids with a similar grain size distribution as used in the nonreactive study.

The thesis has the following components: 1) constructing duplicate diffusion cells that allow for temporal measurements of diffusion profiles; 2) creating an artificial and idealized low permeability medium for use in the initial testing of the experimental approach; 3) developing and undertaking of calibration methods for the reservoir and borehole samples; 4) conducting nonreactive (control) diffusion experiments to obtain reservoir concentration decreases with time and sequential diffusion profiles; 5) conducting reactive-diffusion experiments to obtain reservoir concentration changes with time and sequential diffusion profiles; 6) assessing the reproducibility of the technique in the investigation of diffusion and transformation processes; 7) conducting model fitting simulations of the reservoir and profile results to obtain estimates of effective diffusion coefficients and reaction coefficients for solutes within the artificial low permeability medium and 8) comparing these estimates of diffusion coefficients and reaction coefficients from the model fitting of the experimental results to other studies.

CHAPTER 2
A LABORATORY METHOD FOR THE INVESTIGATION OF THE DIFFUSION OF VOLATILE ORGANIC COMPOUNDS IN LOW PERMEABILITY MEDIA

2.1 INTRODUCTION

Recent studies have suggested that the diffusion of Volatile Organic Compounds (VOCs) into low permeability media may have a significant impact on groundwater quality. Significant contaminant migration, on a scale typical of the thickness of waste disposal site liners, can occur solely as a result of diffusive fluxes (Johnson et al., 1989; Shackelford, 1991; Devlin and Parker, 1996). Diffusive losses into low permeability zones in fractured media could reduce the feasibility of remediation of DNAPL and LNAPL contaminated sites (Parker et al., 1994). The fate of VOCs in low permeability media has not been extensively studied (Devlin and Parker, 1996) but it is recognized that sorption and in particular transformations could be important processes in reducing the breakthrough of contaminants from low permeability media. To investigate both diffusion and fate in low permeability media, there is a need to provide accurate, repeatable and efficient methods to quantify diffusion, sorption and transformation processes in both natural and engineered low permeability media.

Current laboratory methods used to study diffusion in low permeability media are summarized by Shackelford (1991). Two of the more common methods to estimate diffusion coefficients use 1) diffusion profiles obtained by slicing or micro-coring of contaminated cores (Parker, 1996; Ball, 1997) or 2) declining concentrations in an aqueous source reservoir (Myrand et al., 1992). Because the first method is destructive, it is best suited for "snap shot" sampling to obtain concentrations on a one time basis. Although a number of cores can be sacrificed at different times to develop temporal data, there is variability between cores that is difficult to quantify. In addition, slicing or coring increases the potential for loss of volatile compounds during the sampling and extraction process. The second method, although less labour intensive, also has limitations because of the requirement of a well-mixed reservoir (Van Rees et al., 1991), the potential for mass loss due to the sampling procedure (Myrand et al., 1992), and the inevitable uncertainty whether the mass not accounted for has actually diffused within the column as assumed.

This chapter describes a new diffusion cell design that employs a vapour reservoir source and utilizes negative porewater pressures in the porous medium sample to create "mini-boreholes" containing vapour in equilibrium with the surrounding porewater. The sampling of the vapour in the reservoir and in the boreholes uses a microsampling technique

called Solid Phase Microextraction or SPME (Pawliszyn, 1997). SPME consists of a sample probe, similar in size to a syringe needle, that is thinly coated with a polymer (the solid phase) into which the analyte is "micro-extracted" when the syringe is inserted into a sample. This laboratory diffusion cell and microsampling technique allows for the generation of diffusion profiles over time for a single column of low permeability medium.

The performance of the experimental approach is illustrated for a nonreactive artificial low permeability medium by the results of duplicate experiments conducted with five VOCs: carbon disulphide (CS_2), chloroform (CCl_3H), 1,2-dicholoroethane (1,2-DCA), carbon tetrachloride (CCl_4) and perchloroethylene (PCE). The experimental compounds were selected for two reasons: 1) they have a relatively wide range in partitioning properties (e.g. volatilities and hydrophobicities) that are well suited to evaluate the experimental method and 2) four of these compounds were to be studied in the subsequent reactive-diffusion experiments (described in Chapter 3). An artificial porous medium is utilized as a controlled analogue of natural low permeability media and engineered low permeability barriers to minimize the occurrence of processes other than diffusion (e.g., sorption). The medium is comprised of packed silica grains composed of silt- and clay-sized particles. Effective diffusion coefficients for the five compounds in the water-saturated artificial low permeability medium are estimated from the fitting of the two different types of temporal data collected: 1) reservoir concentrations over time, and 2) sequential concentration profiles within the low permeability medium. The success of the diffusion cell technique is determined by an agreement of 1) the experimental results with model simulations of the experimental conditions, and 2) the experimental estimates of effective diffusion coefficients for this artificial low permeability medium with literature values for similar types of low permeability media.

2.1.1 Goals and Objectives of the Study

One goal of this study is to develop a technique for making successive profile measurements over time using a single sample of a low permeability medium. Another goal is the improved accuracy and precision of the experimentally determined effective diffusion coefficients. Thus, an additional goal is to collect samples for analysis in such a way that there is minimal impact of the sampling procedure on the diffusive transport in the low permeability medium. This requires that any advective effects on the profiles caused by the sampling process be insignificant, and that the solute mass removed creates an insignificant disturbance of the concentration gradients.

The specific objectives of the study presented in this chapter are: 1) to construct a

diffusion cell that allows for temporal measurements of diffusion profiles within the cell; 2) to create an artificial and idealized low permeability medium for use in the initial testing of the experimental approach; 3) to develop and undertake calibration methods for the reservoir and borehole samples; 4) to conduct nonreactive (control) diffusion experiments to obtain reservoir concentration decreases with time and sequential diffusion profiles; and 5) to conduct model fitting simulations of the reservoir and profile results to obtain estimates of effective diffusion coefficients for solutes within the artificial low permeability medium.

2.2 METHOD

2.2.1 Materials

Analytical reagent grade chemicals were used for stock standards for the 5 VOCs. Standard stocks were prepared by dissolving the organic solvents in analytical grade methanol. Vapour and water calibration standards were prepared by dissolving specific volumes of the standard stocks in known volumes of vapour or water. All laboratory experiments were conducted with nanopure water produced by an Easypure UV filter.

To create a homogeneous, nonsorbing and nonreactive artificial low permeability medium, Ottawa sand was crushed with a ball mill and sieved through a 325 mesh screen to obtain grains less than 44 μm in diameter. This resulted in a medium that was comprised of fine silt- to clay-sized particles. Pore diameter distribution was estimated to range from 5 μm to 20 μm with the assumption that the medium was comprised mostly of grains with a diameter near the large end of the range (e.g. approximately 40 μm). This pore diameter estimate was based on the assumptions of "closest" packing of the grains, that the narrowest openings are expected to have a diameter approximately 1/10 of the grain diameter and the widest opening are expected to have a diameter approximately 1/2 of this grain diameter (personal communication, Dr. P. Groenvelt, University of Guelph). The mineralogy was approximately 95 % silica according to XRD analysis and these grains had a specific surface area of 0.6 m^2/g based on N_2-BET analysis. The solid organic carbon content of the medium (f_{oc}) was 0.07%. Batch sorption studies with dissolved PCE (the most hydrophobic contaminant used in this work) and the crushed Ottawa sand, indicated minimal mass loss from solution (≤ 10%) and a loss that was similar to control samples (only solution no solid). This provided confirmation that sorption should insignificant in the diffusion experiments.

2.2.2 Physicochemical Properties of the Compounds

Table 2.1 provides a summary of various physicochemical properties of the organic chemicals studied in this work. These literature properties are expected to control the diffusion and partitioning processes that occur in the diffusion experiments. The experimentally determined values, derived from this work, are discussed in Section 2.4.

Diffusion coefficients for porewater in saturated porous media are commonly lower in magnitude than those in bulk water because of the tortuous nature of pores in porous media. The diffusion coefficient in a porous medium is referred to as the effective diffusion coefficient (D_e) and is related to the diffusion coefficient in the bulk water (or the aqueous or free-solution

diffusion coefficient D_w) by the following equation

$$D_e = D_w \tau \qquad [2.1]$$

where τ, an empirical parameter, is termed the tortuosity factor. The tortuosity factor is reported to range from 0.0 to 1.0 (Bear,1972). D_w values for the 5 compounds in this study were estimated by the method of Wilke and Chang (1955):

$$\frac{D_{w1}}{D_{w2}} = \left(\frac{M_2 \rho_1}{M_1 \rho_2} \right)^{0.6} \qquad [2.2]$$

where M and ρ refer to the molecular weights and densities of the two compounds, respectively. A D_{w2} value at 20 °C for tricholoroethylene of 9.0 x 10^{-6} cm^2/s (Perry, 1984) was used to calculate the D_{w1} for the experimental compounds. As evident in Table 2.1, the D_w values are expected to fall in a narrow range for the five compounds; the D_w are all estimated to be approximately 10 x 10^{-6} cm^2/sec. Note that vapour diffusion coefficients (D_v, not shown in Table 2.1) are typically 10^4 times greater than those in water (Schwarzenbach et al., 1993).

These compounds (measured at 25 °C) have moderate vapour pressures (V_p) that range from 0.02 to 0.4 atm and moderate solubilities (S) ranging from approximately 1 to 85 mM. Vapour-water equilibrium partition coefficient (H) values for the five compounds range from 0.04 to 0.8. The octanol-water partitioning coefficient (K_{ow}) varies from 30 to 400. Thus, while the 5 analytes are likely to have similar rates of diffusion, they are widely varying in other properties, which would be expected to affect their behaviour in the diffusion cell experiments, as discussed in detail later. This range in properties was desirable to allow for the evaluation of the applicability of the experimental method.

2.2.3 Experimental Apparatus and Design

Figure 2.1 illustrates the key features of the diffusion cell design: a vapour reservoir overlying a vertical soil column, a series of sample ports, and a connection to a hanging water column.

Diffusion Cell

Two cylindrical cells were constructed of 316 grade stainless steel, each 20 cm long, 6.4 cm O.D. and 5.1 cm I.D. The cells were sealed with end caps having a narrow groove into which a teflon gasket was fitted. Threaded rods tightened the end caps to an outside ring in the middle of the cell. In order to minimize the influence of laboratory temperature fluctuations, the cells were covered with insulating styrofoam boxes. In addition, water from a

heated bath was continuously pumped through copper tubing that was tightly wrapped around the cells.

Sample ports were installed through the wall of each of the diffusion cells, arranged in 4 or 5 columns along the length of the cell. The spacing of the ports was such that samples could be obtained at 1 cm intervals. Figure 2.2 shows a schematic diagram for a port and borehole. A 316 grade stainless steel, 1.5 mm I.D. diameter Swagelok® fitting was used to cap the port. It contained a Vespel® ferrule that either sealed against a stainless steel wire when the port was not in use for sampling, or sealed against the SPME device when sampling was underway (Figure 2.2 inset).

Preliminary experiments confirmed that the cell and ports had good seals, and that the compounds did not sorb significantly to the silica solids used to pack the cells. These preliminary experiments were as follows. The sealed cell was pressurized with up to 40 psi of He gas pressure and no leaks (i.e. no bubbles) were observed when the cell was immersed in a water bath. PCE mass loss from the sealed diffusion cell containing the PCE in a N_2 gas was less than 10 % over a 2 week period. PCE mass decrease in borehole samples of the uniformly contaminated, water-saturated silica solids packed into the diffusion cell was less than 10 % over a 2.5 week period. Finally, PCE mass loss from a batch sorption study using the silica solids, with a solid to water ratio of 0.8 g/ml, was less than 10 % over a 2 week period. In addition, experiments by others (Reynolds et al., 1990) confirmed that the compounds did not react at a discernible rate with the materials of which the experimental cell was constructed.

Packing and Water Saturation of Solids

The idealized nonreactive porous medium was created by packing the crushed and sieved silica grains into the diffusion cells. Prior to packing, the solids were prewet with water (3 percent by mass) to enhance the attraction between grains. The solids were packed in shallow lifts (i.e. approximately 1 cm in thickness) to minimize packing heterogeneity. Each lift was compressed with a plunger with a diameter just slightly smaller than that of the cell in an attempt to minimize edge effects from the packing procedure. The air was removed from the pores by displacement with CO_2. The porous medium was then saturated with organic-free water pumped from bottom to top at a flow rate of 0.4 ml/min. A minimum of 10 pore volumes was displaced. The porosity was determined by the difference of the weight of the wet solids in the cell to the initial weight of the solids in the cell (corrected for the water added to prewet the solids).

Establishment of Negative Water Pressures

After the completion of the saturation process, the bottom of the cell was connected to a hanging water bottle. The top of the cell was opened and water was allowed to drain out of the cell into the bottle. Once a hydraulic connection was established between the cell and the hanging water bottle, the water left in the reservoir was removed and the cell was resealed at the top. Because the bottle was vented to the atmosphere, it served as a hanging water column. This process established negative water pressures in the medium. The negative water pressure at the top of the cell (in terms of height above the hanging water column) is estimated to be approximately -50 cm. The negative pressure required to drain the pores at this height was estimated with the following equation

$$h_c = \frac{2\sigma}{\rho g r} \qquad [2.3]$$

where h_c is the capillary rise (or height above a water table, or in this experiment, height above the hanging water column), σ is the air-water interfacial tension (7.2×10^{-2} N/m^2), ρg is the weight density of water (9.8×10^3 N/m^3) and r is the radius of the pores. Although the pore size was not known, if the maximum of the estimated range (stated previously as a diameter range of approximately 5 to 20 μm) is used in the calculation, the h_c is estimated to be 150 cm for the larger pores. These calculations suggest that the pores in the medium used in the diffusion should have been able to sustain the negative pressures established through the connection to the hanging water column.

Borehole Construction

After the negative pore pressures were established, boreholes were constructed by inserting a 1.5 mm diameter rod through the Swagelok fitting, and pushing it 1.2 cm into the water saturated porous medium. The rod was then carefully removed and the port was resealed with the ferrule and Swagelok cap. The tension of the porewater prevented the collapse of the solids and/or the drainage of water. The boreholes, therefore, remained open and free of water during the experiment, allowing the vapour in the borehole to be in direct contact with the surrounding water.

Vapour Source Reservoir

A well-defined vapour phase source was established by flushing the reservoir (the space left above the water saturated porous medium provided a volume of approximately 55

mls) with approximately 3 litres of a vapour stock source. The vapour stock source was made by spiking specific volumes of the compounds of interest into a 4 litre Tedlar bag filled with N_2 gas (Zero Oxygen Grade) and mixing it by shaking the bag (which contained 2 glass beads to facilitate mixing). The vapour stock source was added to the reservoir by first connecting the tedlar bag to a port in the top end cap and then compressing the bag. The vapour was vented out another port in the top end cap. This process took between 5 and 10 minutes.

2.2.4 Sampling Methodology

Solid Phase Microextraction (SPME) Sampling of Diffusion Cells

The SPME technique has been used as an analyte preconcentration step in the gas chromatographic analysis of a wide range of organic compounds, e.g. chlorinated hydrocarbons, polyaromatic hydrocarbons, phenols, various pesticides, and polychlorinated biphenyls, in a variety of sample matrixes (Pawliszyn, 1997). The SPME extraction is similar in concept to pentane-water extraction although the phase to be extracted can be vapour as well as water. The extraction is conducted by inserting a needle containing a fine fibre into the sample matrix and exposing the fibre. The fibre has a thin hydrophobic polymer coating which serves as the extracting phase. Typically the coating has a known and uniform thickness (100 μm or less) and is 1 cm long; the total coating volume is thus 10^{-3} ml (for a 100 μm thickness) or less. Thus, even with high coating-sample partition coefficients, the SPME method extracts only a small total mass of analyte. The mass extracted into the coating is typically quantified by thermal desorption in an injection port of a conventional gas chromatograph (details of the specific method used in this work are described later).

Diffusion Cell Sampling Techniques

Figure 2.2A shows a schematic of the SPME device inserted into a borehole sample port in the cell. The sampling procedure as described also applies to the reservoir samples. SPME fibres with either 100 μm or 7 μm thick poly(dimethylsiloxane) coatings were used to collect samples from the boreholes (or reservoir). As shown in Figure 2.2 (inset), the fibre is contained in a specially designed syringe with a plunger that, when depressed, exposes the fibre and its polymer coating to the vapour to be sampled. To collect a sample, the stainless steel wire used to seal the port during non-sampling times was removed from the ferrule as the SPME needle in its place and the ferrule was immediately sealed around the needle by tightening the swagelok cap. This procedure took less than 5 seconds and this short time

combined with the tiny diameter of the opening in the ferrule (0.5 mm) was expected to minimize vapour losses from the borehole. The needle was advanced into the port and the polymer coated fibre exposed to the vapour sample in the borehole for 1 minute. The procedure was reversed to remove the fibre and reseal the port. The fibre was immediately inserted into the heated injector of the gas chromatograph (GC) for analysis of the mass sorbed from the borehole into the fibre coating. This technique minimized vapour losses during sampling as indicated by measured concentrations that were constant for repeated sample collection in the borehole calibration experiments. As the mass remaining in the fibre coating after desorption by the heated GC injector was less than 1 % mass of the mass sorbed from a sample extraction, the same fibre could be used to sample all the ports.

Diffusion Cell Sampling Schedule

Two diffusion experiments ran simultaneously for approximately one month in "duplicate" cells. Cell 1 was the principal cell and Cell 2 was used for periodic checks on the reproducibility of data from Cell 1. Eight sampling events were undertaken.

The reservoir was sampled with a fibre that had the 7 μm thick coating so that the amount of mass removed in a sample would be minimized. For the borehole samples, both the 100 μm and 7 μm fibres were utilized although the latter were only used for sample events near the end of the experiment. As will be discussed later, sampling boreholes with the thinner coated fibres is recommended over the thicker coated fibre to minimize mass extraction.

2.2.5 Analytical Technique

A Varian 3400 gas chromatograph (GC) with a Septum Programmable Injector (SPI) was used for the analysis of the five compounds. The injector temperature was 250°C. The GC was equipped with a J & W 30 m x 0.32 mm x 5 μm DB1 column and an Photoionization Detector (PID) with a 11.7 eV lamp. UHP Helium gas was used as the carrier and make-up gas. The temperature program was as follows: hold at 35°C for 1 minute, ramp at 12°C /minute to 120°C, and hold for 10 minutes at the final temperature.

The PID was calibrated using 0.2 to 0.6 μl direct methanolic stock injections. Calibration curves of detector peak area versus mass injected into the GC were used to determine the PID response. The precision was approximately ± 5%.

On every sampling day, gas standards were prepared and analyzed using two stocks

and two fibres. One of the fibres was rarely used for sampling and thus tested the PID response over time. The other, the borehole sample fibre, was tested for changes in its partitioning capacity over time.

2.2.6 Modelling of Diffusion Processes

Conceptualization of Diffusion Processes in Diffusion Cell Experiments

The mass transport process from the reservoir into and through the porous medium in the diffusion cell is conceptualized as follows. Diffusion within the vapour reservoir is fast because of the large diffusion coefficient therein, i.e. on the order of 10^{-1} cm^2/s Schwarzenbach et al. (1993). Consequently, we consider this volume to be well-mixed and assume that only one concentration measurement is needed to represent the total reservoir volume at any point in time. At the interface between the reservoir and the water-saturated homogeneous porous medium, it is assumed that equilibrium partitioning occurs from the vapour into the water menisci. This assumption has been used by others, e.g. for headspace gases over enclosed water (Pankow, 1986). For the nonsorbing, nonreactive media, the solutes are assumed to undergo one-dimensional diffusion, unaffected by sorption or other reactions.

The governing equation for the change in vapour reservoir concentrations with time for well-mixed conditions is taken from Van Rees et al. (1991) with a modification to account for equilibrium partitioning from a vapour reservoir to the porewater in the porous medium and is given by:

$$\frac{\partial C_R^t}{\partial t} = \frac{D_e \theta}{z_{PM} H} \frac{\partial C_R^t}{\partial z_{PM}} \quad \text{at } z_{PM} = 0, t \qquad [2.4]$$

$$\text{for } C_{PW}^t = \frac{C_R^t}{H} \text{ at } z_{PM} = 0, t$$

where C_R^t is the analyte concentration in the reservoir at time t, D_e the effective diffusion coefficient, θ the porosity of the porous medium, z_R the height of the reservoir, H the vapour-water equilibrium partition coefficient, C_{PW}^t the analyte concentration in the porewater at time (t) and z_{PM} the depth in the porous medium.

The governing equation for the one-dimensional diffusion of nonreactive solutes in the porewater of a saturated, homogeneous porous medium can be represented by Fick's Second Law (Crank, 1975).

$$\frac{\partial C^t_{PW}}{\partial t} = D_e \frac{\partial^2 C^t_{PW}}{\partial z^2_{PM}} \qquad [2.5]$$

Modelling of Diffusion Cell Reservoir and Porewater Concentrations

The analytical solutions to equations [2.4] and [2.5] for the reservoir and porewater concentrations, respectively, are taken from Rees et al. (1991) with a modification to boundary conditions to account for equilibrium partitioning from the vapour reservoir to the porewater in the porous medium. The following initial and boundary conditions were used in the derivation.

$$C_{PW}(z_{PM}, 0) = 0$$

$$C_R(0) = C^0_R$$

$$C_{PW}(\infty, t) = 0$$

$$C^t_{PW} = \frac{C^t_R}{H} \text{ at } z_{PM} = 0, t$$

The following is the analytical solution for the contaminant concentration in the well-mixed vapour reservoir.

$$C^t_R = C^0_R \exp\left(\frac{D_e t}{\alpha^2}\right)\left(\operatorname{erfc}\frac{\sqrt{D_e t}}{\alpha}\right) \qquad [2.6]$$

$$\text{where } \alpha = \frac{z_R H}{\theta}$$

The following is the analytical solution for one-dimensional diffusion within the porewater of a nonsorbing and nonreactive analyte with a vapour source.

$$C^t_{PW} = C^0_{PW} \exp\left(\frac{z_{PM}}{\alpha} + \frac{D_e t}{\alpha^2}\right)\left(\operatorname{erfc}\left[\frac{z_{PM}}{\sqrt{D_e t}} + \frac{\sqrt{D_e t}}{\alpha}\right]\right) \qquad [2.7]$$

$$\text{where } \alpha = \frac{z_R H}{\theta}$$

The parameters needed to solve these equations were: C^0_R, H, z_R, θ, z_{PM} and D_e. All parameters except D_e were measured experimentally. The diffusion cell properties used in the model simulations were z_R of 2.6 cm and θ of 0.47. The equations were solved using a commercially available math software program Mathcad.

Model simulations with an H value equal to unity (i.e. simulating a water source) agreed with those based on another analytical model (Martin, 1992) simulating a declining water reservoir source.

Modelling of Borehole Extraction by SPME

Modelling was conducted to evaluate the mass redistribution between the porewater, the borehole and the coating after sampling. The goal was to determine whether the SPME borehole sampling technique was likely to significantly affect the diffusion of analytes within the bulk of the porewater in the diffusion cells (i.e. affect "bulk porewater diffusion"). The model simulations were used for comparing distributions of concentration and mass before and after the SPME borehole extraction. A conceptual diagram of the mass extraction process during a borehole extraction by SPME is shown in Figure 2.2.B.

A one-dimensional linear diffusion model presented in Appendix A3.2 of Pawliszyn (1997) was used in this assessment. The model accounts for the diffusion from a water phase to a vapour phase and then into a fibre coating. Diffusive transport in each phase is represented by Fick's Second Law and is solved analytically for the following conditions. The model assumes that equilibrium is established between the porewater and the borehole concentrations before sampling and that there are zero flux boundaries at the outer water boundary and inner coating boundary. At each of the two interfaces, the partitioning from one phase to the other was represented by the following equilibrium equations:

$$C^t_{PW}H = C^t_B \quad \text{at porewater-borehole interface} \qquad [2.8]$$

$$C^t_B K_V = C^t_C \quad \text{at borehole-coating interface} \qquad [2.9]$$

where C^t_{PW} is the porewater concentration adjacent to the borehole at time (t), C^t_B the borehole vapour concentration at time (t), C^t_C the coating concentration at time (t), H the vapour-water equilibrium partition coefficient, and K_V the coating-vapour equilibrium partition coefficient.

Pawliszyn's one-dimensional linear model may underestimate the rates of diffusion in our system (in and near the borehole) because it assumes a constant cross-sectional area along the diffusion path. Under the borehole sampling conditions, diffusion is radial inwards toward the fibre and, thus, the cross-sectional area decreases with diffusion distance. The model can compensate for a reduction in cross-sectional area at the borehole-coating interface through the use of a shape factor (F) that represents the ratio of surface areas; for cylindrical geometry, F is the ratio of the radii (r_C/r_{BH})

2.2.7 Fibre Calibration Methods

The calibration methods are illustrated in Figure 2.3. A vapour medium was sampled in both the reservoir and borehole cases. However, as will be shown later, separate

calibration techniques were required for the two types of sampling locations. A water calibration method was utilized as part of the borehole calibration method.

The calculation for the vapour reservoir calibration and the water calibration is based on a mass balance for sampling conditions that reach equilibrium between the sample matrix and the fibre coating. Shown below is a mass balance equation for a simple example using a vapour matrix that is sampled with the fibre coating.

$$C_V^0 V_V = C_V^{EQ} V_V + C_C^{EQ} V_C \qquad [2.10a]$$

where C_V^0 is the initial concentration in the vapour, C_V^{EQ} the equilibrium concentration in the vapour, C_C^{EQ} is the equilibrium concentration in the fibre coating, V_V is the vapour volume, and V_C is the volume of the coating. The concentrations in the two phases at equilbrium can be related to each other through an equilibrium partition coefficient (K_V)

$$K_V = \frac{C_C^{EQ}}{C_V^{EQ}} \qquad [2.10b]$$

By rearranging equation [2.10b] to solve for C_V^{EQ} and substituting this rearranged equation into equation [2.10a], the mass balance equation [2.10a] can be rewritten:

$$C_V^0 V_V = \frac{C_C^{EQ}}{K_V} V_V + C_C^{EQ} V_C \qquad [2.10c]$$

By rearranging equation [2.10c], K_V can then be determined with the following equation.

$$K_V = \frac{C_C^{EQ} V_V}{C_V^0 V_V - C_C^{EQ} V_C} \qquad [2.10d]$$

The same type of derivation was used to determine the coating-water equilibrium partition coefficient (K_W) for the water calibration provided in equation [2.12a].

Reservoir Calibration

For the reservoir calibrations, 160 ml glass vials, air-filled and sealed with mininert valves, were spiked with known volumes of methanolic stock standards to obtain a range in vapour concentrations. The precision for the reservoir samples was determined from the relative standard deviation of least 10 replicate samples and was calculated to be ± 5%. Sampling times sufficient to reach equilibrium conditions were used (e.g. 1 to 2 minutes). For these equilibrium samples, the coating-vapour equilibrium coefficient (K_V) was determined. A slight simplification to the calculation described above was possible because of the large vapour volume in the vials and the small mass extracted by the fibre. For this calibration, the initial concentration, C_V^0, is essentially identical to the equilibrium value C_V^{EQ} fibre. Thus the following approximation may be made:

$$K_V = \frac{C_C^{EQ}}{C_V^0} \qquad [2.11a]$$

Using this K_V calibration value and the measured fibre coating concentration (C_C^{EQ}) obtained from a sample of the reservoir in the diffusion experiments, a reservoir concentration (C_R^t) at sample time (t) was obtained using the following equation.

$$C_R^t = \frac{C_C^{EQ}}{K_V} \qquad [2.11b]$$

As was the case for the reservoir calibration vial volume, the volume of the reservoir in the diffusion cell (55 mls) was large enough to allow for the assumption that the reservoir concentration at the time of sampling (C_R^t) was essentially identical to the reservoir concentration after sampling.

Borehole Calibration

The borehole calibration experiment was conducted in the cell with the artificial porous medium in place. The borehole calibration was conducted for a range of porewater concentrations that overlapped those expected in the diffusion experiment. The precision for the borehole samples was determined from the relative standard deviation of least 10 borehole samples from a calibration experiment and was calculated to be ± 15%. As will be discussed later, the mass extracted with the 100 μm fibre seemed to be sensitive to the porosity of the porous medium. Thus, it is important to ensure that the same procedure to pack and saturate the solids is used for both the calibration and diffusion experiments.

Uniform porewater concentrations (C_{PW}^0) were established by pumping a spiked water source through the packed solids in the cell until the influent and effluent concentrations were the same (no vapour reservoir was created during the calibration). The porewater concentrations were determined from a water calibration that was conducted prior to conducting the borehole calibration. The water calibration was conducted as follows. A 2.5 ml standard was transferred to a 5 ml bottle. The 2.5 ml headspace in these bottles was sampled with the SPME fibre for 15 minutes while the water was stirred. Stirring was used to reduce times to equilibrium (Zhang and Pawliszyn, 1993). In the current work, a 15 minute exposure time resulted in equilibrium between the coating and the sample. From analyses of the standard samples, an equilibrium partition coefficient K_W was calculated using the following equation:

$$K_W = \frac{C_C^{EQ}(V_W + HV_{HS})}{C_W^o V_W - C_C^{EQ} V_C} \qquad [2.12a]$$

where C_W^o is the initial concentration in the vapour, C_C^{EQ} is the equilibrium concentration in the fibre coating, H is the equilibrium partition coefficient for air-water, V_W is the water volume, V_{HS} is the headspace volume and V_C is the volume of the coating. Unlike the vapour reservoir calibration method, because of the smaller sample volume of water in the vials, the calculation for K_W has to take into account that the initial water concentration has been decreased due to the fibre sample extraction. By reorganizing equation [2.12a] to solve for the concentration in water in the vials, in this case for influent and effluent samples collected in the calibration experiment, the concentration in the porewater (C_{PW}^0) could be determined. The rearranged equation is as follows.

$$C_{PW}^o = \frac{C_C^{EQ}\left(\frac{V_W}{K_W} + \frac{HV_{HS}}{K_W} + V_C\right)}{V_W} \qquad [2.12b]$$

The boreholes for the borehole calibration experiments, were constructed in the same way as for the diffusion experiments. The same borehole sampling technique was also used, i.e. short sample durations (1 minute) to minimize the mass extracted from the porewater. Thus, the concentrations in the coating were not necessarily at equilibrium with the porewater concentrations for some of the 5 compounds.

For each borehole calibration experiment, typically 5 to 10 boreholes were sampled by SPME with at least 2 measurements taken from each borehole. Using the average fibre coating concentration for the 1 minute borehole samples (C_C^1) and the measured initial porewater concentration (C_{PW}^0), an empirical nonequilibrium calibration coefficient was calculated as follows:

$$K_B = \frac{C_C^1}{C_{PW}^o} \qquad [2.13a]$$

This borehole calibration coefficient K_B was used in the diffusion experiments to convert the fibre coating concentration for a 1 minute sample of the borehole (C_C^1) into the porewater concentration surrounding the borehole (C_{PW}^t) at time (t) by using the following equation.

$$C_{PW}^t = \frac{C_C^1}{K_B} \qquad [2.13b]$$

2.3 MODEL SIMULATIONS OF SPME SAMPLES OF BOREHOLES

Borehole extraction simulations of the five experimental compounds illustrated the relative influence of their H values (vapour-water equilibrium partition coefficient) versus their K_v values (coating-vapour equilibrium partition coefficient) on depleting the mass from the porewater adjacent to the borehole. Since the 100 μm fibre would have the greatest influence on porewater concentrations, the modelling assessment assumed this coating thickness. Shown in Figure 2.4 are simulated concentration profiles in the porewater, vapour borehole and coating before and after a 1 minute SPME sample. The concentrations were normalized to the initial source concentration in the porewater and were plotted on a logarithmic scale because of the wide range in concentrations among the three media. The simulations are shown for 1,2-DCA and CCl_4 to illustrate the range in behaviour of the experimental compounds; these two compounds have the lowest and highest H (0.05 and 0.8, respectively). The values of the parameters used in the model simulations are reported with Figure 2.4. These simulations used the K_v and H values measured experimentally in this study (Section 2.4). The D_e values were those obtained from the diffusion experiments. These D_e values differed by only a factor of 1.5, with 1,2-DCA having the larger value. The same diffusion coefficients for the vapour in the borehole (D_v) and for the coating (D_c) were used for the two compounds to enable a clearer comparison of the effect of the partition coefficients at the two interfaces. D_v and D_c values were obtained from Zhang and Pawliszyn (1993) for their VOC modelling analyses.

As shown in Figure 2.4, there is significantly more CCl_4 extracted into the coating than 1,2-DCA, even though the K_v value for CCl_4 is only 1.5 times greater than that of 1,2-DCA. This has occurred because, with a significantly greater H value, the CCl_4 borehole concentrations are greater than those of 1,2-DCA which results in CCl_4 coating concentrations that are greater than for 1,2-DCA. For a 1 minute extraction, borehole and porewater concentrations for both 1,2-DCA and CCl_4 are affected. The vapour in the borehole is depleted from its initial concentration because the porewater cannot supply mass as fast as it is transported through the vapour in the borehole to the coating. The 1 minute extraction simulations suggest that there is equilibrium between the concentration in vapour in the borehole and the concentration in the coating. This fast equilibrium time is due to the fast diffusion in vapour in the borehole and the thinness of the coating. Although a zone of depletion is predicted in the porewater, even for CCl_4, the depletion is predicted to be insignificant beyond about 0.1 cm from the borehole-porewater interface. Thus, only a

localized effect on the porewater concentrations is expected. Experimental data (not shown) indicated that repeated sampling of the same borehole with 4 hours or less of recovery time gave indistinguishable measured concentrations. This provided further indication that the extraction has a minimal effect on the bulk porewater concentrations.

2.4 CALIBRATION RESULTS AND DISCUSSION

Table 2.1 lists the experimentally determined values of the calibration coefficients (K_v and K_B) for the 100 μm and 7 μm fibres. Recall that K_v and K_B are used in the analysis of the vapour reservoir and vapour borehole concentrations, respectively. Further, K_v is an equilibrium coefficient, whereas K_B is an empirical coefficient determined from 1 minute borehole samples. Table 2.1 also lists the K_w values, the coating-water equilibrium partition coefficients used to calculate porewater concentrations during the borehole calibration exercise. Since only the 100 μm fibre was used for measuring the porewater calibration concentrations, the K_w was experimentally measured only for this fibre. The K_w values for the 7 μm fibre were assumed to be proportional to the K_w values for the 100 μm fibre, with the constant of proportionality being the ratio of the partitioning capacities of the two fibres (this ratio was determined in the K_v calibration). Values for H, the vapour-water equilibrium partition coefficient, were calculated from $K_v / K_w = H$. These experimentally derived H values (Table 2.1) are similar to those reported in the literature.

2.4.1 Reservoir Calibration Results

K_v values used for the sampling of the reservoir with the 100 μm fibre range from 90-1400 (Table 2.1). The 7 μm fibre had a similar range in K_v values.

For the reservoir samples, because of the large volume of the reservoir (55 ml) relative to that contained in the very small fibre coating (100 μm coating volume of 7×10^{-4} ml and 7 μm coating volume of 3×10^{-5} ml), a fibre extraction resulted in very little mass removed relative to that initially present. Because it had the largest K_v, the greatest mass extracted was for PCE with 1.4 % of the initial mass removed in a 100 μm fibre sample. For all compounds, a 100 μm fibre reservoir sample removed, on average, about 20 times more mass than a 7 μm fibre reservoir sample.

2.4.2 Borehole Calibration Results

Typical 100 μm borehole calibration results (concentrations in the coating (for a 1 minute borehole sample) versus initial porewater concentrations) are shown in Figure 2.5. A linear regression of these results yielded the 100 μm K_B reported in Table 2.1. The K_B values were lower than the K_v values and ranged from 32 to 245. The compounds can be grouped into two categories based on the magnitude of their K_B values. CS_2, CCl_3H and 1,2-DCA have

low values whereas the K_B values for CCl_4 and PCE were up to 20 times greater for the 100 μm fibre (both compounds having a value of about 240).

For the borehole samples, because of the small volume of the borehole (0.02 ml), a 100 μm fibre extraction resulted in all compounds having mass contributions from the porewater. This is indicated in Table 2.2 where the mass extracted in the coating is greater for all five compounds than the mass estimated to be initially present in the borehole. The greatest mass extracted relative to that estimated to be initially present in the borehole was for PCE with almost 20 times more mass in the 100 μm coating than was initially present in the borehole. As indicated in Table 2.2, when the 7 μm fibre was used, the mass extracted from the porewater was significantly reduced; e.g., the PCE mass removed into the 7 μm coating was then about 3 times more than estimated to be initially present in the borehole. Figure 2.6 is a plot of the mass of analyte extracted by the 100 μm fibre versus the mass of analyte extracted by the 7 μm fibre. On the basis solely of the equilibrium partitioning capacities of the two fibre coatings i.e. the ratio of the two coating volumes, the plots would be expected to have a slope of about 25. As shown in Figure 2.6, 3 of the analytes conformed close to this expectation, with slopes of about 15. However, the slope was half or less of this expected value for CCl_4 and PCE. This suggests that, for these 2 compounds, slow diffusion in the porewater, and thus slow replenishment of the analyte in the vapor borehole, significantly restricts the amount of mass that can be extracted in 1 minute by the 100 μm coated fibre.

At equilibrium the K_B should be equal to K_w. However, for these studies, as indicated in Table 2.1, the 100 μm K_B values were less than the 100 μm K_w values, e.g. up to 2.5 times less for PCE. As suggested in Figure 2.7, with 1,2-DCA and PCE presented as typical of the range in behavior for the experimental compounds, for equilibrium to have been reached for all five compounds extracted in the 100 μm fibre coating, sample times greater than 30 minutes would have been required because of the longer times to equilibrium required for PCE. Even for 1,2-DCA, which had the lowest K_w and, thus, had the fastest time to equilibrium, 15 minutes were required to reach these equilibrium concentrations. Thus 1,2-DCA as compared to PCE had times to equilibrium for the borehole samples that were significantly closer to those for the stirred water-headspace samples in vials (Figure 2.7). As also shown in Figure 2.7, these times to equilibrium for the borehole samples were significantly greater than those for the reservoir samples in which equilibrium concentrations were reached after 1 minute.

The observed nonequilibrium conditions for the 1 minute 100 μm fibre illustrate why a separate borehole calibration was necessary for the diffusion experiments. However, as indicated in Table 2.2, by comparing the concentration in coating after a 1 minute borehole sample to that estimated for equilibrium coating concentrations, the discrepancy is much less for the 7 μm fibre. Apparently the 7 μm fibre borehole samples were closer to equilibrium with the surrounding porewater concentrations than were samples with the 100 μm fibre. The significance of the nonequilibrium sampling of the porewater by the 2 different fibres is evaluated In the later discussion of diffusion experimental results.

2.5 DIFFUSION EXPERIMENT RESULTS AND DISCUSSION

The diffusion experiments with nonreactive media were conducted for two primary reasons. The first was to examine the suitability of the porewater calibration method for obtaining diffusion profiles; this was to be accomplished by comparing experimentally obtained diffusion profiles with model simulations. The second was to obtain diffusion coefficients for use in the interpretation of subsequent experiments with reactive media.

The diffusion experiment was conducted in duplicate: each ran for just over one month with eight sampling events. For this one-month period, the diffusion cells functioned as designed. The negative porewater pressures were maintained and the boreholes remained functional throughout. To minimize the mass extracted in the reservoir samples, only the 7 μm fibre was used. The total mass removed for all samples collected, both reservoir and boreholes, for the entire experiment, was at most 5 % of the total mass added to the source reservoir at the beginning of the experiment. The quantitation limits for both the reservoir and porewater samples are provided in Table 2.3. These were calculated by dividing the obtained quantifiable concentrations in the coatings by the appropriate K_v or K_s for each compound.

The concentrations obtained over time in the reservoir (C_R^t) or in the porewater (C_{PW}^t) are presented as values normalized to the initial concentrations. The initial concentration in the reservoir (C_R^0) in each cell (Table 2.3) was determined from the average of two measurements, i.e. that of the vapour source in the tedlar bag and that of a vial collecting the effluent vapour from the reservoir. The results for these two sample types were within experimental error, suggesting no significant difference. The initial porewater concentration (C_{PW}^0) just below the interface between the reservoir and the artificial porous medium was calculated from the following equation:

$$C_{PW}^0 = \frac{C_R^0}{H} \qquad [2.14]$$

The values for the various compound parameters used in the modelling assessments are reported in Table 2.1 (experimentally derived H) and Table 2.3 (D_e). The z_R and θ values were provided in section 2.2.6. To fit the model simulations to the experimental data, the D_e was adjusted by eye.

2.5.1 Reservoir Results

The reservoir concentration decreases with time for the 5 compounds for both cells are shown in Figure 2.8. As expected (Equation [2.4]), the measured reservoir concentrations decreased at a rate roughly inversely proportional to H. This trend was observed in the data for all 5 compounds over a duration of a month. These reservoir concentration data were compared with model simulations generated with equation [2.5] and fit to the reservoir concentrations by modifying the D_e. As shown in Figure 2.8, a good correspondence was observed between the model simulations and the reservoir concentration results over the duration of the experiment.

The best fit D_e values for each of the 5 compounds were the same in both diffusion cells and ranged for the various compounds from 4×10^{-6} to 7×10^{-6} cm^2/sec (Table 2.3). As would be expected, the fitted D_e decreased with increasing estimated molecular size (based on molecular weight) i.e. $CS_2 > CCl_3H \geq$ 1,2-DCA $> CCl_4 \cong$ PCE. This expectation is based on the correlation observed between the molecular mass (which is related to molecular weight) and the diffusion coefficient in water (Hayduk and Laudie, 1974). These D_e values were within the range of values reported previously for nonsorbing and nonreactive compounds diffusing through natural silty and clayey deposits (e.g. Johnson et al., 1989; Barone et al., 1989). The fitted D_e for the 5 compounds were equal, within experimental error, to values calculated using equation [2.1] and an average τ of 0.5. The values of τ calculated using the fitted D_e values and the D_w values from Table 2.1 range from 0.47 to 0.62 (Table 2.3) with an average value of 0.56 ± 0.08. These values of τ are within the range reported in the literature for saturated porous media of 0.01 to 0.84 (Shackelford and Daniel, 1991) and for clays and clay-till 0f 0.28 to 0.63 (Parker et al., 1994).

These results indicate that 1) D_e can be determined in an artificial, low permeability medium for VOCs with a range in physicochemical properties (those properties values listed in Table 2.1) using sequential fibre extractions of a vapour reservoir and 2) the obtained D_e values are similar to those from studies of natural silty and clayey deposits.

2.5.2 Diffusion Profiles

Figures 2.9A-C show profiles of the porewater concentrations obtained with the 100 μm fibre for all 5 compounds, at early times (Day 6) and at later times (Day 20). The porewater concentrations in these figures were normalized to the initial porewater concentrations just below the interface of the vapour reservoir and the porous medium

(calculated using equation [2.14]). The other sample events yielded profiles that are consistent with the trends presented in Figures 2.9A-C and the conclusions drawn from them are found in the following discussion and thus are not included here for the sake of brevity.

The concentration profiles in Figures 2.9A-B have little scatter in the data and have the shape and, for the most part, the rates of change with time expected for diffusive transport. Reproducible results were obtained from repeated samples of individual boreholes collected within a one-day period and from different ports sampling the same depth in the profile. In addition, boreholes constructed at the end of the experiment produced samples with concentrations similar, i.e. within 15 %, to those determined by sampling ports at the same (or nearly the same) depths which had been constructed at the onset of experiment. Figure 2.9C indicates that the results were similar between the two diffusion cells as illustrated by the concentration profiles for 1,2-DCA and CCl_3H for sample days 6 and 20. Thus, the technique employing SPME to sample boreholes held open by slight negative water pressures (increasing in negativity upwards from approximately -30 to -50 cm) generated reproducible diffusion profiles for the suite of VOCs examined.

To examine this technique on a more quantitative basis, model simulations of the concentration profiles were compared to the experimental results. These simulations were generated using equation [2.7] and the same parameters as those used for the reservoir model, including the D_e estimated from the fit of the reservoir data (referred to hereafter as D_{e-R}). As shown in Figure 2.9A and 2.9B, the Day 6 data, for the most part, corresponded well with the simulated profiles for all five compounds. Sampling and/or analytical difficulties were suspected of plaguing the shallowest CS_2 data point in the soil profile. For later times, e.g. for Day 20, the data fit the model expectations well for CS_2, CCl_3H and 1,2-DCA, but less well for CCl_4 and PCE. Thus we conclude that the experimental technique was successful using a 100 μm fibre in measuring diffusion profiles for CS_2, CCl_3H, and 1,2-DCA for a series of sampling events spanning a month period.

The experimental technique did not yield CCl_4 or PCE profile data that corresponded well to model simulations for times greater than one week using the effective diffusion coefficients determined from the reservoir concentration decline (D_{e-R}). The disparities between data and simulation were generally restricted to the top 4 cm of the profile. The disparities increased with time such that, by Day 20, experimentally obtained concentrations were 3 and 4 times less than model predictions for CCl_4 and PCE, respectively (Figure 2.9B). In deeper portions of the profile and at z_{PM}=0 (converted from the reservoir data) the results agreed reasonably well, for the most part, with model predictions using the D_{e-R}. No

significant improvement in the fit of the simulations was achieved by small changes in the model parameters i.e. 10 % changes for D_e, H, L_R, and θ. In order for there to be a significant improvement in the CCl_4 and PCE results in the upper profile for times Day 20 and later, the D_e needed to be reduced to 50 % of the $D_{e\text{-}R}$ to a value of 2×10^{-6} cm^2/s. However, as illustrated in Figure 2.9B, using the lower D_e improved the fit with the upper profile results but worsened the fit with the lower profile results and the converted reservoir value. In addition, the model simulations with this lower D_e did not correspond well with the early time results. Thus, no significant improvement in the correspondence of this model with the CCl_4 and PCE 100 μm experimental data could be achieved with model parameter modifications.

For other, later times (Days 27 and 33), results were also available for both the 7 μm and 100 μm fibres (Figure 2.10). Disparities between the CCl_4 and PCE 100 μm porewater results and the model were similar or slightly greater to that of Day 20 in the upper profile zone. With the thinner fibre coating, the CCl_4 and PCE concentration profiles agree better with model predictions. There was still a discrepancy between the 7 μm experimental concentrations and that of the model in the upper profile. They were, however, reduced by half from the 100 μm results with the greatest discrepancy. With increasing depth in the profile, the correspondence with the model improved and the fit was better, for the most part, for the 7 μm results as compared to the 100 μm results. For the other three compounds, CS_2, CCl_3H and 1,2-DCA, there was essentially no difference between the diffusion profiles obtained with either the 100 μm or 7 μm fibres and all their results corresponded well to model prediction using $D_{e\text{-}R}$.

Detailed Assessment of CCl_4 and PCE 100 μm Fibre Borehole Sample Results

Although the majority of the CCl_4 and PCE profile data could be fitted moderately well with simulations using the $D_{e\text{-}R}$ value, the cause of the disparities with the 100 μm samples for later times in the upper profile was investigated. Mass balances were calculated for 6 of the 100 μm sample events over the month-long diffusion experiment (Figure 2.11). The equations used are provided in Appendix A. The calculated mass for each compound for each sample event was obtained by adding the mass in the reservoir, which was calculated by multiplying the concentration in the reservoir by the volume of the reservoir, to the mass in the porewater, which was calculated by integrating the area under the concentration curves for the porewater profile. This mass was divided by the initial mass added to the reservoir to obtain the relative mass for each sample event. For CS_2, CCl_3H and 1,2-DCA, a constant

relative mass close to 100 % was estimated for the duration of the experiment. For CCl_4 and PCE, relative mass decreased slightly with time such that by the end of the experiment about 80 % of the initial was accounted for by this method. The lower relative mass for CCl_4 and PCE is consistent with the lower than expected concentrations in the top portion of the profile. As was shown with the model fitting assessment, it appears that the technique provided CCl_4 and PCE concentration measurements at other locations that were accurate and thus corresponded relatively well to expectations.

It may be that the CCl_4 and PCE mass may actually have been present in the upper portion of the profile but were underestimated by the sampling/analytical method. This would mean that the mass extracted by a borehole fibre sample was lower than expected from the calibration experiments. Recall that the porewater concentrations were calculated (as in equation [13b]) as the concentration in the fibre coating (after sampling a borehole) divided by the K_B; the latter was calculated from calibration experiments using equation [13a]. It is not known what process could have reduced the CCl_4 and PCE mass extracted into the fibre. But, since the greatest uptake of mass from the porewater was for CCl_4 and PCE with the 100 μm fibre and since the poorest correspondence with the diffusion profile model simulations was for these types of extractions, the disparities appear to be related to the mass transfer from the porewater. It follows that if there was a change in some property of the porous medium in the upper part of the profile in the diffusion experiment that resulted in a lower mass transfer rate or equilibrium partitioning coefficient than that which occurred in the calibration experiment, the mass extracted into the fibre coating would be reduced from the calibrated values. If it were primarily a rate change, then CCl_4 and PCE 100 μm fibre results would be most significantly affected because these samples types extract the greatest mass from the porewater.

An increase in sorption and/or a decrease in porosity seem to be the two most likely processes that would result in a decrease with time of the mass transfer rate from the porewater and that may conceivably have occurred in these experiments. Sorption can reduce the diffusion rate by reducing the concentration gradients in the porewater. However, the medium was initially found to be only weakly sorptive and there is no reason to assume that changed significantly. The porosity may have decreased with time since from our observations of the porous medium before and after the diffusion experiment, it was noted that some sample reconsolidation (on the order of 0.5 cm) occurred during the progression of the experiment. Whether this small reconsolidation could decrease the porosity enough to lower the tortuosity and thus the diffusion rate through the porewater is not known. If the

reconsolidation occurred over some interval that may have corresponded roughly to the 4 cm zone where the greatest CCl_4 and PCE porewater discrepancies were observed, the porosity in this zone could have been reduced by about 15 % (i.e. from 0.47 to 0.40). Some calibration experiments conducted in this study suggest that for this amount of porosity decrease, the mass extracted into the coating might be reduced even in greater amounts. For two calibration experiments with different porosities, the CCl_4 and PCE mass extracted by the 100 μm fibre decreased proportionally to 2 times the amount the porosity decreased, i.e. when the porosity was decreased 20 %, the mass extracted into the 100 μm coating was decreased by 40 % for CCl_4 and PCE. This decrease in porosity did not reduce the amount of CS_2, CCl_3H and 1,2-DCA, extracted into the 100 μm coating in any observable amount. It is further noted that if the porosity did decrease in the top of the profile compared to that in the calibration experiments, then the K_s value used to convert the mass extracted into the coating (which may be lower than expected from calibrations) may be too large because it was determined from calibration experiments with a higher porosity. Thus there is some possibility that the lower CCl_4 and PCE concentrations may be related to a decrease in porosity in the upper profile.

In summary, it may be that a better fit between CCl_4 and PCE data (from the 100 μm fibre) and model simulations would be obtained if the model accounted for porosity and D_e that varied with depth and time. Such a model was not available for use in this work.

2.5.3 Suitability of Technique to the Study of Diffusion in Low Permeability Media

With the experimental technique explored in this chapter, one diffusion experiment yields two types of temporal data that allow for the estimation of D_e by two separate techniques thus improving the precision of the D_e estimate. The data were generated by two types of sequential SPME measurements: 1) the equilibrium extraction of the well-mixed, relatively large vapour reservoir and 2) the extraction of a well-mixed, vapour-filled "mini-borehole". The latter measurements may yield more accurate data if the 7 μm fibre is utilized rather than the 100 μm fibre; the diffusion cell design appears to be too sensitive to porosity differences for compounds with a large capacity to partition from the porewater to the fibre coating, i.e., those with a large K_w. An improved packing and saturation technique has been developed which minimizes the subsequent consolidation of the porous medium. This technique utilizes a vibration table that provides a means to pack and saturate the soil without requiring the pumping of water through the soil. It was used in subsequent experiments, one

of which is the focus of Chapter 3.

To further improve the general applicability of the technique to a wider range of compounds, the design needs to be modified so that less analyte mass is extracted from the porewater. To reduce the mass contribution from the porewater, the borehole volume could be increased and/or a thinner coated fibre utilized. There may be limitations to both these modifications because a larger borehole will be more susceptible to collapsing and a thinner coating may result in undesirably high detection limits for some compounds. The most appropriate sampling time should be considered with these design modifications. The ideal borehole sampling time is obviously one that allows a close enough approach to equilibrium so that no special borehole calibration technique is required, i.e., when the borehole calibration simply uses the K_v (coating-vapour equilibrium partition coefficient) or K_w (coating-water equilibrium partition coefficient). The most appropriate calibration coefficient will depend on the extent to which the mass extracted into the fibre has come from the porewater. If the SPME sampling of the diffusion cell can be refined to reduce the biases that can occur under some circumstances, then the technique proposed herein would be more broadly applicable to the study of VOCs in low permeability media, including core samples of natural silty or clayey deposits.

2.6 CONCLUSIONS

The diffusion cell design and micro-sampling SPME technique proved to be an efficient method to temporally sample for VOCs in both the reservoir and boreholes of the diffusion experiment. Results were obtained within several minutes after sample collection thus allowing for flexibility in modifying the sampling scheme and suggesting that this technique could be used to measure rapid rates of changes in concentration. Concentrations ranging over at least three orders of magnitude were measured with this method. This range was sufficient for our current needs. If wider concentration ranges were required, a different GC detector and/or chromatography conditions could be used.

The decreases in vapour reservoir concentration over time allowed for effective diffusion coefficients (termed $D_{e\text{-}R}$ herein) to be estimated for 5 VOCs. The values obtained are in the range reported for other nonsorbing and nonreactive compounds in natural silty and clayey deposits (Johnson et al., 1989; Barone et al. 1989). The use of a vapour source, instead of the more commonly utilized water source, reduces the restrictions on reservoir size if well-mixed conditions are desired. For this experimental design, results suggest that well-mixed conditions existed for reservoir volumes up to 100 ml. With the small mass extracted by SPME vapour reservoir samples, simple model fitting assessments are possible because the mass removed is negligible and, therefore does not need to be incorporated into the calculation. SPME fibres with both 100 μm and 7 μm thick poly(dimethylsiloxane) coatings can be used for these reservoir measurements but if the thicker coated fibre is used, the number of samples should be restricted in order to minimize the mass removed from the system. The calibration techniques for the reservoir samples utilize standard gas standard bottles and a range in VOCs could be used for these types of measurements.

The technique employing SPME to sample boreholes, which are held open by slight negative water pressures (-30 to -50 cm), yielded a series of concentration profiles that could be used to generate independent estimates of D_e. The values thus obtained compared well with those estimated by fitting concentration decreases observed in the vapour reservoir. The technique was most successfully applied for borehole extractions that removed the least mass from the porewater; this was for compounds with low K_w (i.e., 50) or for small fibre coating volumes (i.e., fibres with 7 μm thick coatings). The D_e estimates for compounds with larger K_w values (i.e., 10 times larger), particularly when sampled with the 100 μm fibre, are apparently sensitive to small differences in the porosity between the calibration and diffusion experiments. For example, differences caused by medium consolidation during the diffusion

experiments. To minimize differences in porosity with depth and time in the column when using artificial or previously disturbed material, the use of a vibration table and the addition of a soil and water mixture to the cell is recommended. To increase the wider application of the technique, 1) the contribution of mass from the porewater should be reduced through the use of larger borehole volumes and/or thin coated fibres, and/or 2) the sampling times should be designed to more closely approach equilibrium conditions.

This technique as designed is most successful for less hydrophobic and/or less volatile compounds. However, it could be applied to other kinds of concentration profile measurements. Diffusion profiles within field cores of low permeability media could be obtained or other processes such as transformations could be investigated. To successfully apply the technique to cores of natural silty or clayey deposits (for both clean and contaminated samples), which must remain intact and thus cannot be packed into the diffusion cell, several challenges remain: 1) a method for obtaining a well-defined and unchanging volume above the sample to serve as the vapour reservoir, 2) a method for ensuring that there is a tight "seal" between the sample and the wall of the diffusion cell to avoid short circuiting of the diffusive transport, and 3) a method to set up negative porewater pressures. Depending on the natural medium's properties it may be possible to meet these challenges. For application to natural media collected in cores (both clean and uncontaminated samples), this method would ideally use the coring container as the diffusion cell. This would minimize the disturbance to the cores and likely ensure a much tighter seal between medium and cell walls. In addition, the concern over consolidation with the packed medium is not likely to be a significant issue with natural aquitard cores.

REFERENCES

Ball, W.P., Liu, C., Xia, G. and Young, D.F. 1997. A Diffusion-Based Interpretation of Tetrachloroethene and Trichloroethene Concentration Profiles in a Groundwater Aquitard. Water Resources Research, 33(12):2741-2757.

Barone, F.S., Yanful, E.K., Quigley, R.M. and Rowe, R.K. 1989. Effect of Multiple Contaminant Migration on Diffusion and Adsorption of Some Domestic Waste Contaminants in a Natural Clayey Soil. Can. Geotech. J. 26:189-198.

Bear, J. 1972. Dynamics of Fluids in Porous Media. Elsevier, New York.

Crank, J. 1975. The Mathematics of Diffusion. Clarendon Press, Oxford, 2nd Ed.

Devlin, J.F. and Parker, B.L. 1996. Optimum Hydraulic Conductivity to Limit Contaminant Flux through Cutoff Walls. Ground Water 34(4):719-726.

Hayduk, W. and Laudie, H. 1974. Prediction Of Diffusion Coefficients For Non-Electrolytes In Dilute Aqueous Solutions. AIChE, J., 20:611-615.

Johnson, R.L., Cherry, J.A. and Pankow, J.F. 1989. Diffusive Contaminant Transport in Natural Clay: A Field Example and Implications for Clay-Lined Waste Disposal Sites. ES&T 23(3):340.

Mackay, D and Shiu, Wan Ying. 1981. A Critical Review of Henry's Law Constants for Chemicals of Environmental Interest. J. Pys. Chem. Ref. Data 10(4):1175-1193.

Martin, P. 1992. One-Dimensional Diffusion Through a Column from One Reservoir to Another. Unpublished Term Project, University of Waterloo, Department of Earth Science.

Montgomery, J.H. 1990. Groundwater Chemicals Desk Reference Vol 1. John Wiley & Sons Inc., Toronto.

Myrand, D., Gillham, R.W., Sudicky, E.A., O'Hannesin, S.F., and Johnson, R.L. 1992. Diffusion of Volatile Organic Compounds in Natural Clay Deposits. J. of Contaminant Hydrology, 10:159-177.

Pankow, J.F. 1986. Magnitude of Artifacts Caused by Bubbles and Headspace in the Determination of Volatile Compounds in Water. Anal Chem. 58:1822-1826.

Parker. B.L.. 1996. Effects of Molecular Diffusion on the Persistence of Dense, Immiscible Phase Organic Liquids in Fractured Porous Geologic Media. Ph.D. thesis, University of Waterloo, Waterloo Ont., Canada.

Parker, B.L., Gillham, R.W., and Cherry, J.A. 1994. Diffusive Disappearance of Immiscible Phase Organic Liquids in Fractured Geologic Media. Groundwater 32(5):805.

Pawliszyn, J. 1997. Solid Phase Microextraction: Theory and Practice. Wiley-VCH, New York.

Perry, R.H. 1984. Perry's Handbook of Chemical Engineering. Sixth Edition. McGraw-Hill, New York.

Reynolds, G.W., Hoff, J.T., and Gillham, R.W. 1990. Sampling Bias Caused by Materials Used to Monitor Halocarbons in Groundwater. ES&T 24(1):135.

Schwarzenbach, R.P., Gschwend, P.M., and Imboden, D.M. 1993. Environmental Organic Chemistry. John Wiley and Sons, Inc., Toronto.

Shackelford, C.D. 1991. Laboratory Diffusion Testing for Waste Disposal - A Review. J. of Contaminant Hydrology 7:177-217.

Schackelford, C.D. and Daniel, D.E. 1991. Diffusion in Saturated Soi, I. Background. Am. Soc. Civ. Eng. Geotech. Eng., 117(3):440.

Van Rees, K.C., Sudicky, E.A., Rao, S.C., and Reddy, K.R. 1991. Evaluation of Laboratory Techniques for Measuring Diffusion Coefficients in Sediments. ES&T 25(9):1605:1611.

Wilke, C.R., and Chang, P. 1955. Correlation of Diffusion Coefficients in Dilute Solutions. A.I.Ch.E. Journal 1(2):264-270.

Zhang, Z. and Pawliszyn, J. 1993. Headspace Solid-Phase Microextraction. Anal. Chem. 65:1842.

Table 2.1 Physicochemical Properties of Compounds

Literature Values						Experimental Values				
Compound	D_W	V_P	S	K_{ow}	H	K_V	K_W	K_B		H_{exp}
						100 µm	100 µm	100 µm	7 µm	
CS_2	11.3	0.39	40 (2900)	70	0.5	90	46	32	55	0.5
$CHCl_3$	9.9	0.21	85 (1000)	90	0.13	230	35	31	46	0.15
1,2-DCA	9.7	0.11	85 (5100)	30	0.04	315	15	12	15	0.05
CCl_4	8.5	0.12	5 (1150)	250	0.82	405	325	245	540	0.8
PCE	8.4	0.02	0.84 (140)	400	0.51	1400	620	235	1000	0.4

NOTES:

D_W Estimated Free Solution Diffusion Coefficient (value x 10^{-6} cm^2/s)

V_P Vapour Pressure atm 25°C (Mackay and Shui, 1981; Montgomery, 1990)

S Water Solubility mM (µg/l) 25°C (Mackay and Shui, 1981; Montgomery, 1990)

K_{ow} Octanol-Water Partition Coefficient 25°C (Schwarzenbach et al., 1993; Montgomery, 1990)

H Conc. in Vapour / Conc. in Water Equilibrium Partition Coefficients 25°C (Mackay and Shui, 1981; Montgomery, 1990)

K_V Conc. in Coating / Conc. in Vapour Equilibrium Partition Coefficient (22°C ± 1.5°C)

K_W Conc. in Coating / Conc. in Water Equilibrium Partition Coefficients (22°C ± 1.5°C)

K_B Conc. in Coating / Conc. in Porewater Calibration Coefficient (22°C ± 1.5°C)

H_{exp} $K_{W\ 100\ \mu m}$ / $K_{V\ 100\ \mu m}$

Table 2.2 Comparison of 100 μm and 7 μm SPME Samples of Borehole

Borehole Sampling	CS_2		CCl_3H		1,2-DCA		CCl_4		PCE	
	100 μm	7 μm	100 μm	7 μm	100 μm	7 μm	100 μm	7 μm	100 μm	7 μm
Mass in coating after 1 min. sample / Estimated initial mass in borehole [a]	2	0.1	5	0.4	6	0.4	8	0.9	18	3.2
Conc. In coating after 1 min. sample / Conc. in coating at equilibrium [b]	0.70	0.96	0.82	1.06	0.80	0.95	0.74	1.15	0.34	1.07

[a] Estimated initial mass in borehole (m^0_{BH}) calculated from $m^0_{BH}=C^0_{PW}HV_{BH}$ for an estimated borehole volume of 0.02 ml

[b] Concentration in coating at equilibrium (C_C^{EQ}) calculated from $C_C^{EQ}=C^0_{PW}K_W$ where the porewater is assumed to be infinite in volume

Table 2.3 Experimental and Model Parameter Values for Nonreactive Diffusion Experiment

	Units	CS_2	CCl_3H	1,2-DCA	CCl_4	PCE
Diffusion Cell Experimental Parameters						
Quantitation limits for conc. in reservoir - 7 μm fibre	μg/L	30	105	25	80	5
Quantitiation limits for conc. in porewater -7 μm fibre	μg/L	58	657	481	67	5
Quantitiation limits for conc. in porewater -100 μm fibre	μg/L	5	40	25	5	1
Initial concentration in reservoir – Cell 1	μg/L	8400	8200	9100	4800	2800
Initial concentration in reservoir – Cell 2	μg/L	6700	6700	7400	4600	2200
Diffusion Model Parameter						
Effective diffusion coefficient (D_e) - Cell 1 and Cell 2 [a]	$x10^{-6}$ cm^2s^{-1}	7	6	6	4	4
$\tau = D_e / D_W$ [b]	unitless	0.62	0.61	0.62	0.47	0.48

[a] $D_{e\text{-}R}$ from section 2.5.1
[b] D_W from Table 2.1

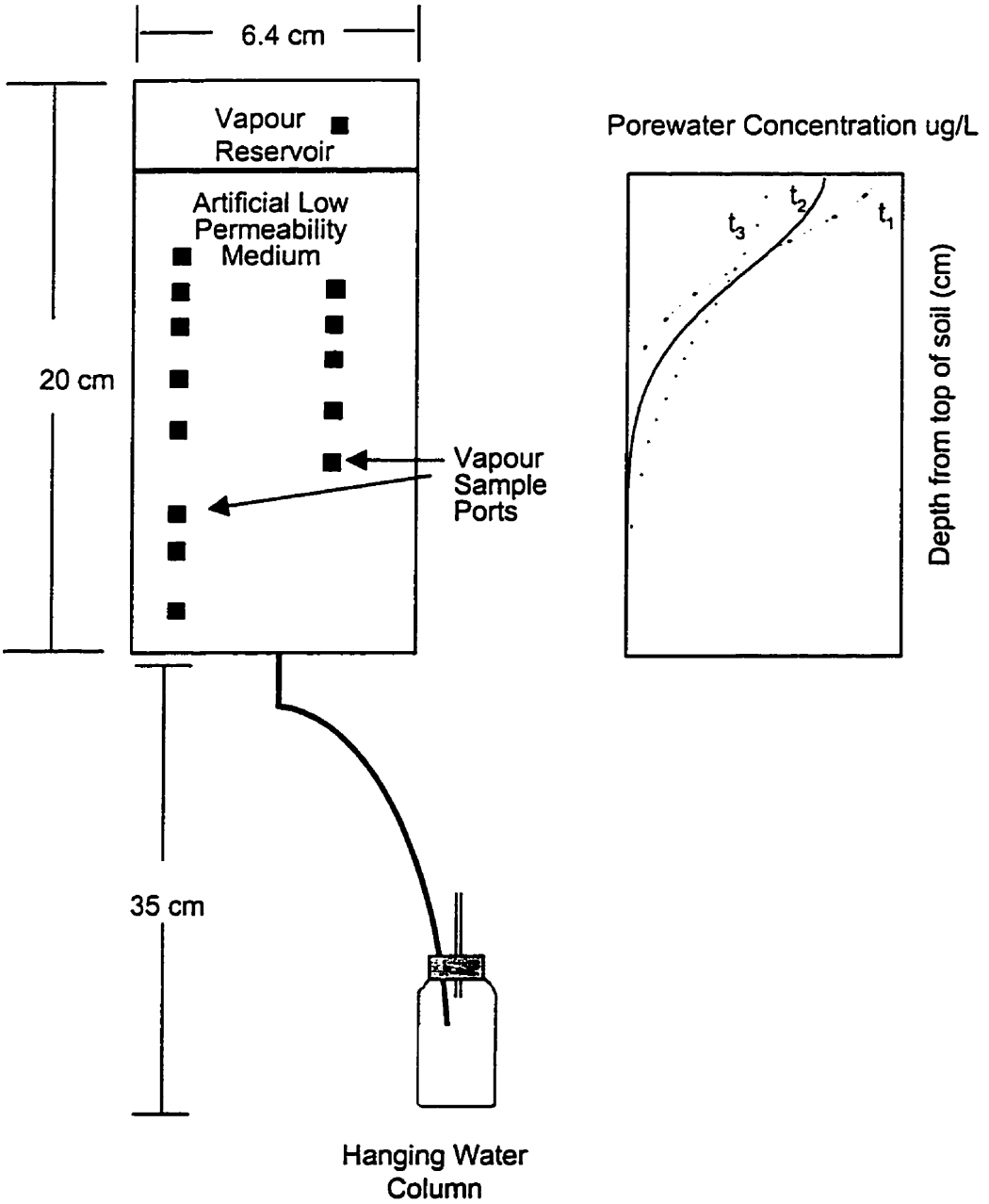

Figure 2.1. Schematic of Diffusion Cell Apparatus. Figure on right is example of sequential diffusion profiles in the porewater (t_1, t_2 and t_3) obtained from temporal sampling of vapour in boreholes created in the artificial low permeability medium.

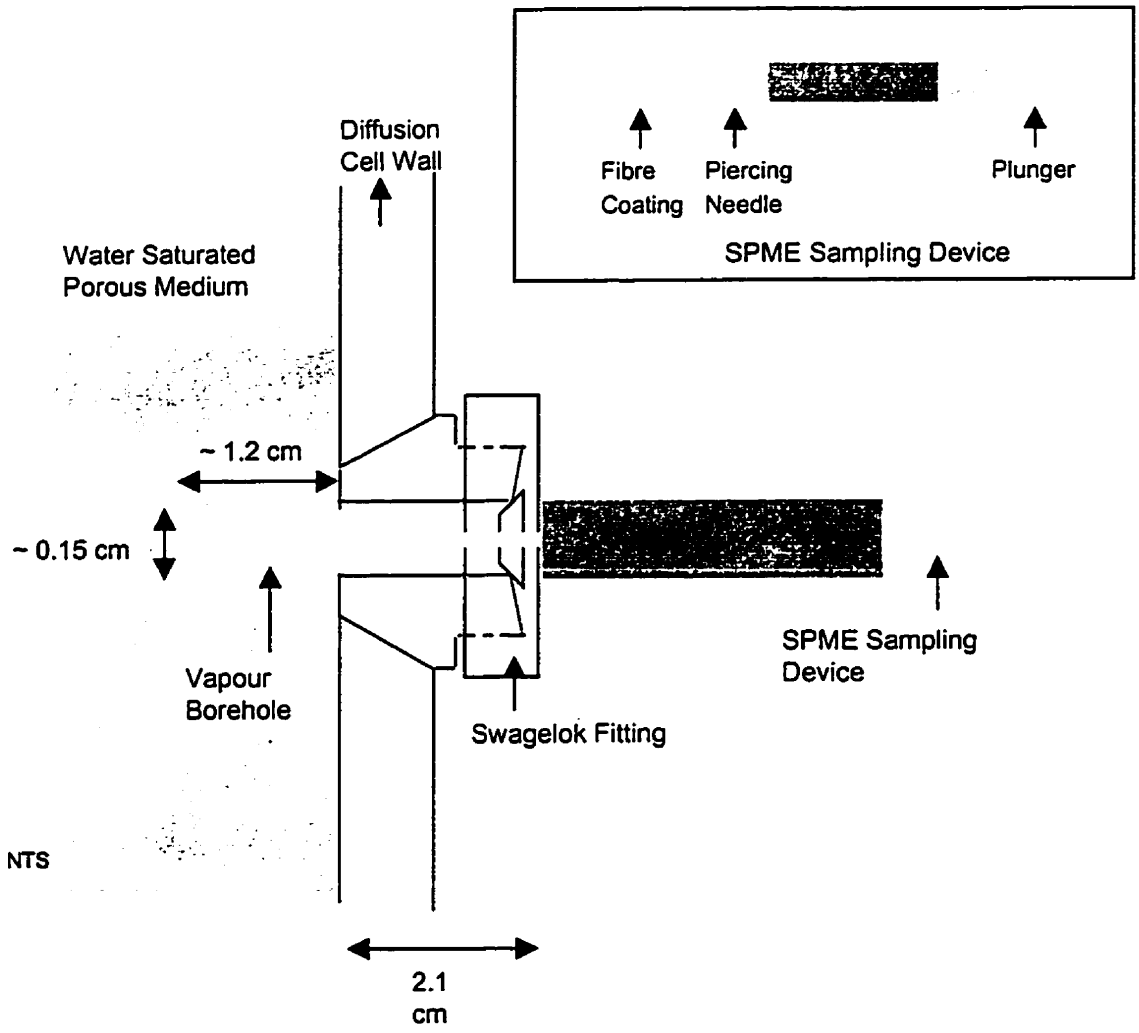

Figure 2.2A. Schematic of Vapour Sample Port and SPME Sampling Device. SPME sampling device is inserted through sample port, the coated fibre is extended into the borehole, the fibre is exposed to vapour in borehole, and the fibre coating extracts analyte mass from vapour. Inset above provides the key features of the SPME Sampling Device.

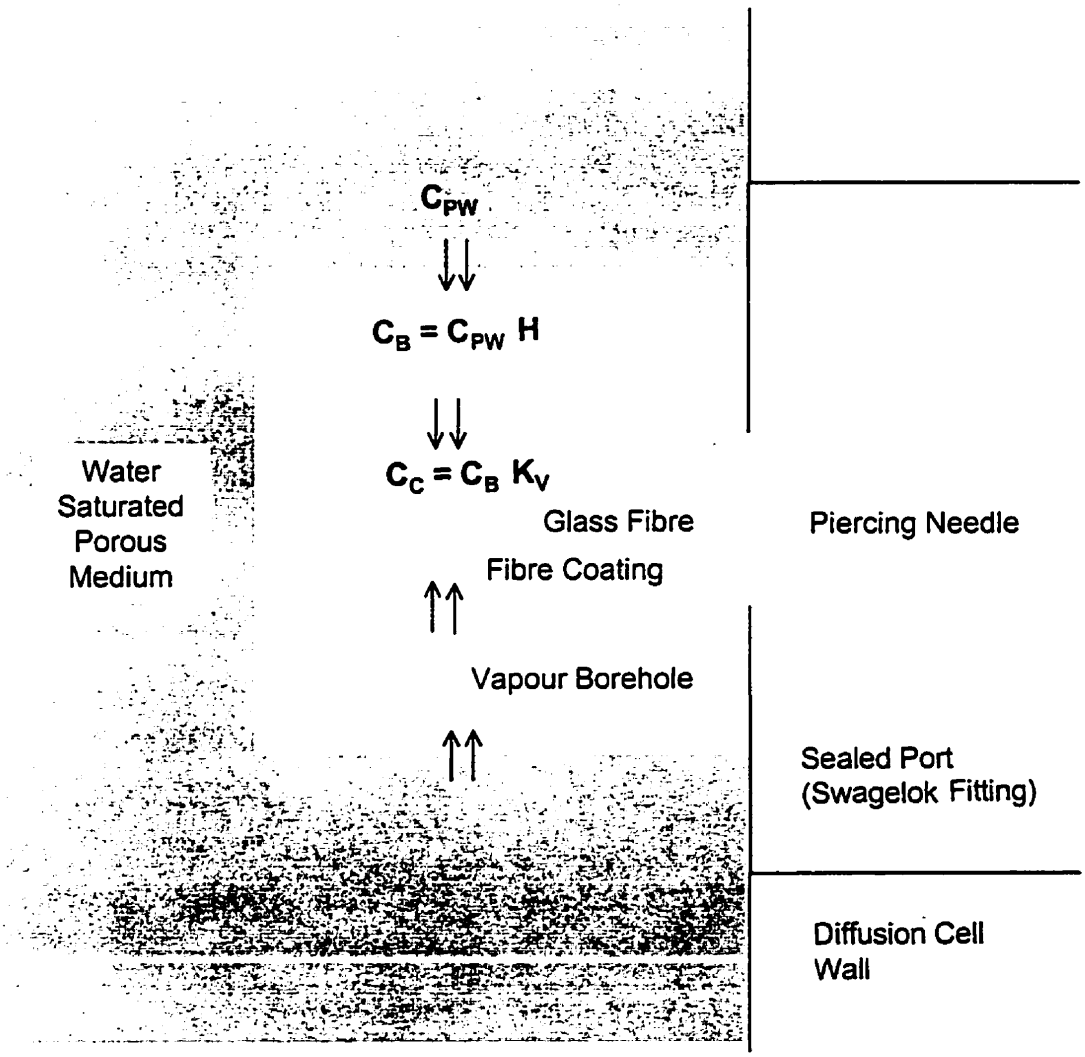

Figure 2.2B. Schematic of Analyte Transport During Vapour Borehole Sample Collection with SPME Sampling Device. Analyte partitions from porewater in porous medium into vapour in borehole and then analyte partitions from vapour in borehole to polymer coating of SPME sampling device (as indicated by arrows). Equilibrium partitioning is assumed to occur at each interface (porewater-vapour in borehole and vapour in borehole-polymer coating interfaces). C_{PW} = concentration in porewater, C_B = concentration in vapour in borehole, C_C = concentration in fibre coating, H = vapour-water equilibrium partitioning coefficient and K_V = coating-vapour equilibrium partitioning coefficient.

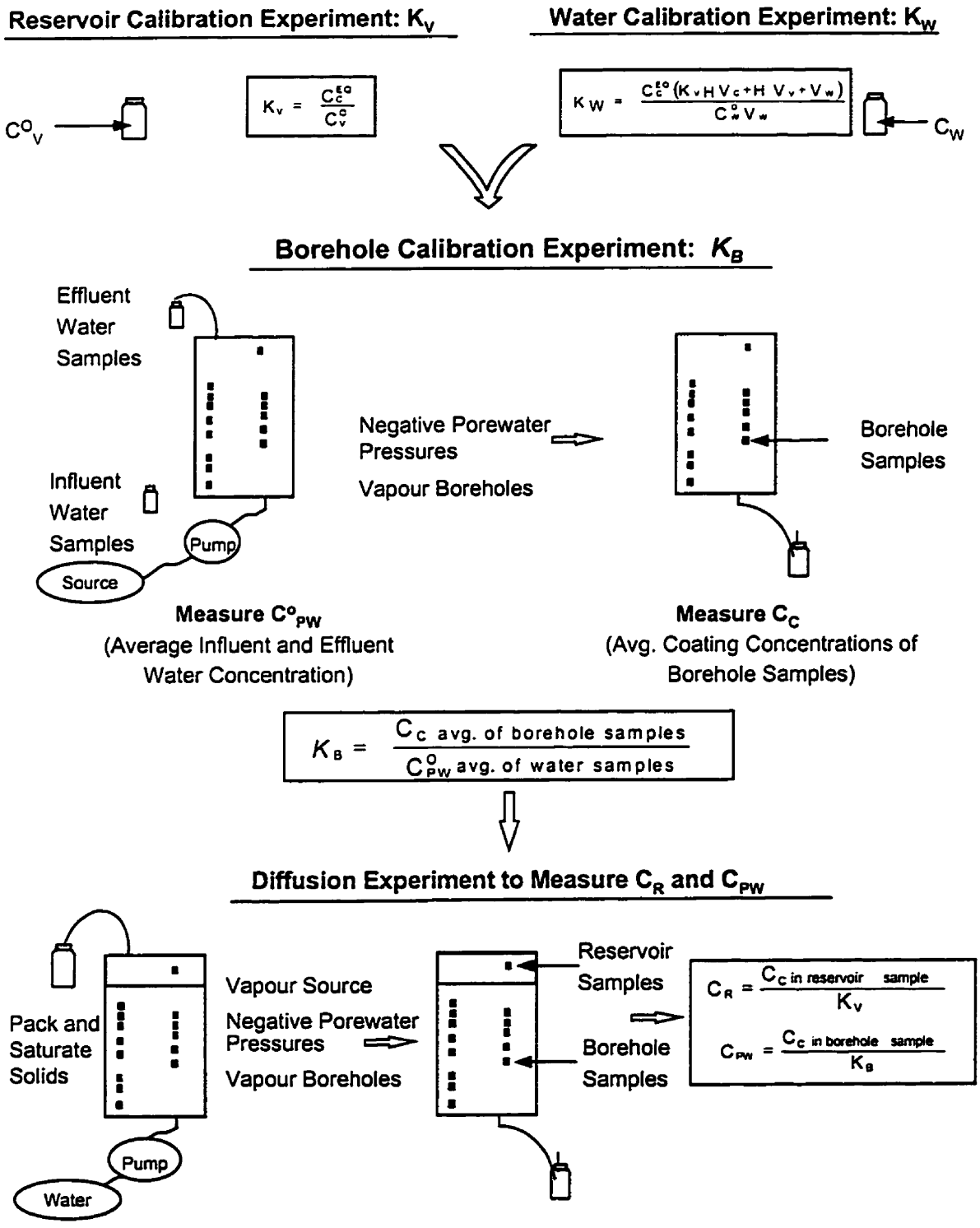

Figure 2.3. Schematic Summary of Methods for Calibration. Reservoir (K_V) and borehole (K_B) calibration coefficients determined for obtaining concentration in reservoir (C_R) and in porewater (C_{PW}) in diffusion experiment. Water calibration coefficient (K_W) required for porewater concentration in borehole calibration.

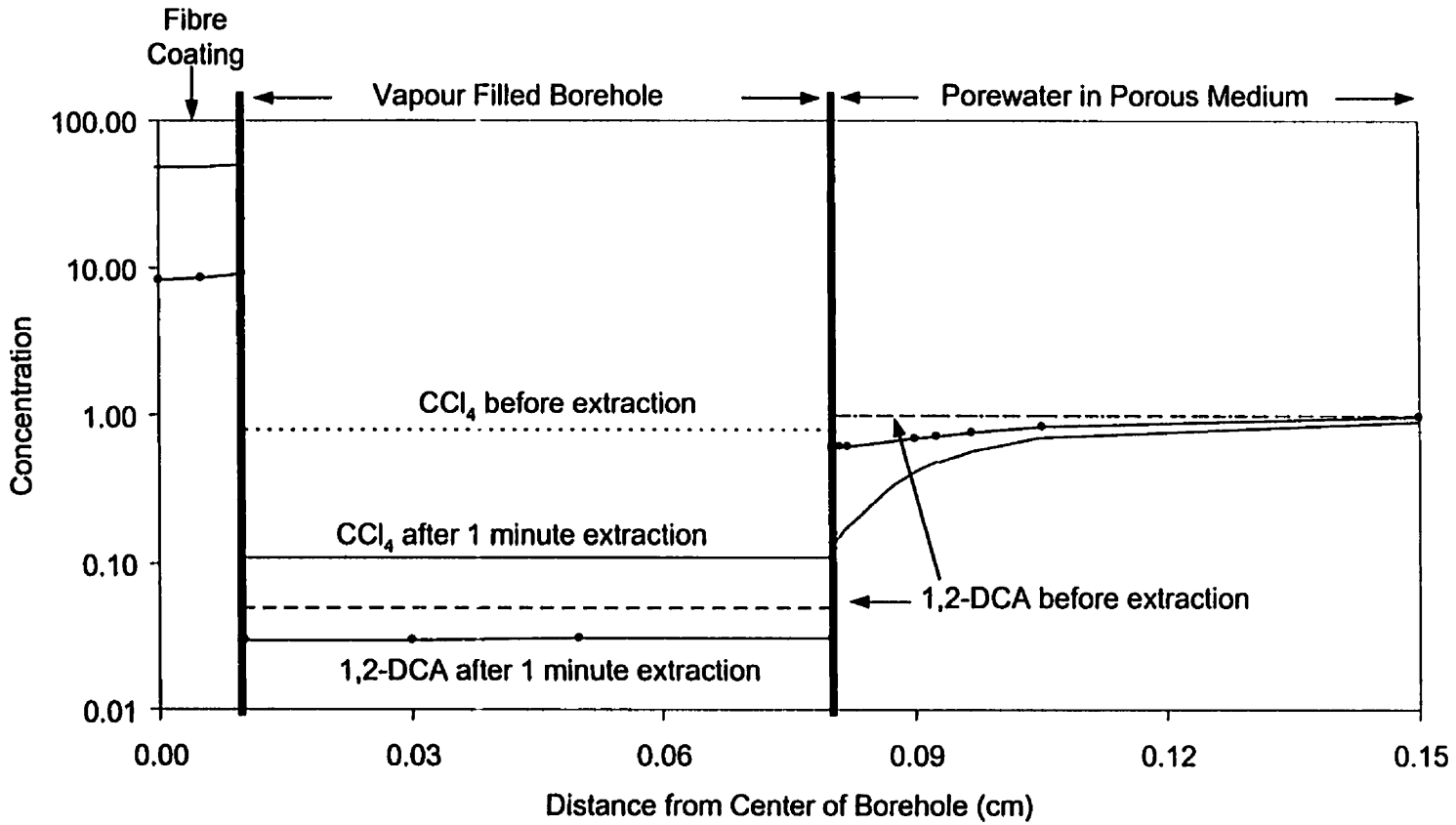

Figure 2.4. Model Diffusion Profiles Before and After a One Minute 100 μm SPME Sample of a Borehole. Figure assumes the following parameter values: 1,2-DCA: H=0.05, K_v=315, D_e=6 x 10^{-6} cm^2/sec; CCl_4: H=0.8, K_v=450, D_e=4 x 10^{-6} cm^2/sec. For both compounds, it is assumed that D_V=8 x 10^{-2} cm^2/sec and D_C=3 x 10^{-6} cm^2/sec. Note log scale for Y axis. Porewater profiles before extraction for 1,2-DCA and CCl_4 overlap each other.

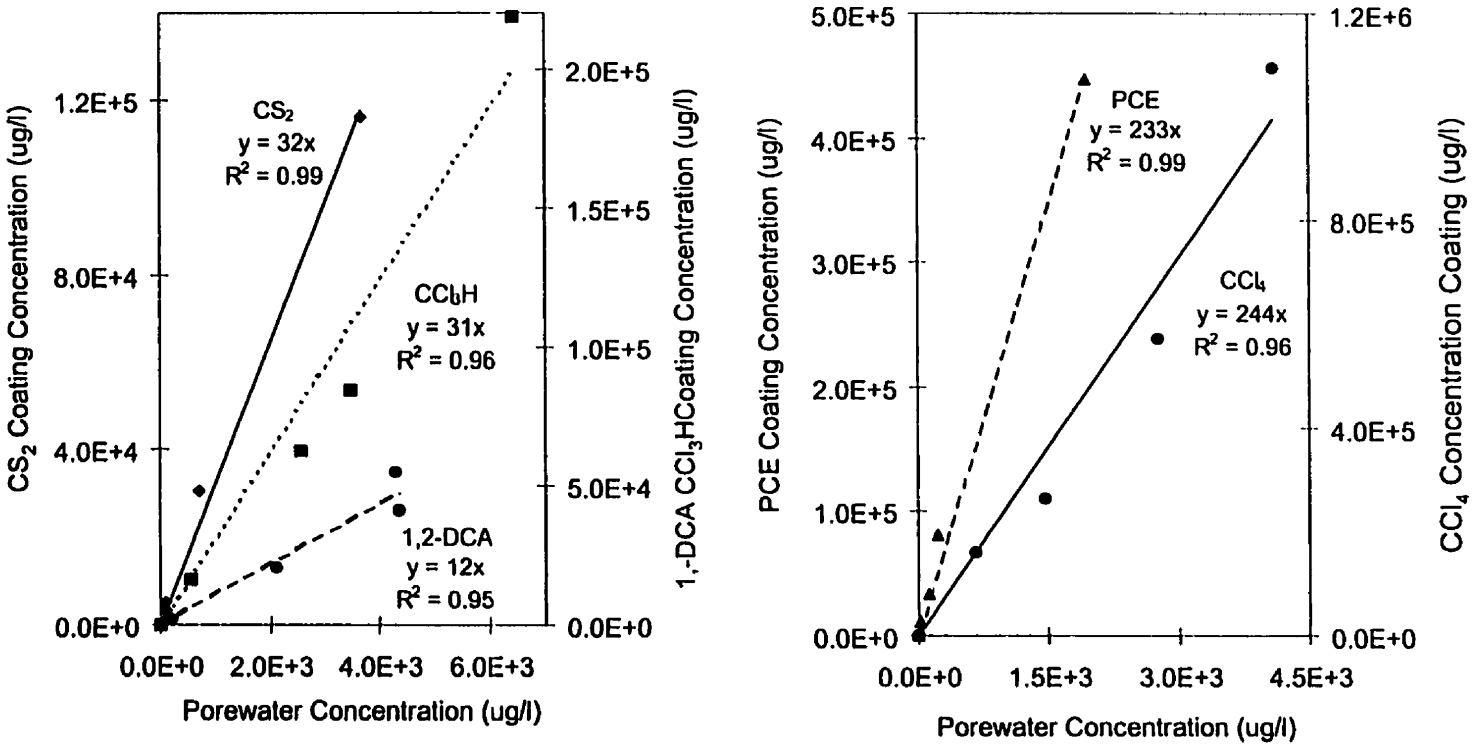

Figure 2.5. CS_2, CCl_3H, 1,2-DCA, CCl_4 and PCE 100 μm Fibre Coating Concentrations for a Range of Porewater Concentrations in the Borehole Calibration Experiments. The linear regressions yield the 100 μm K_B values summarized in Table 2.1.

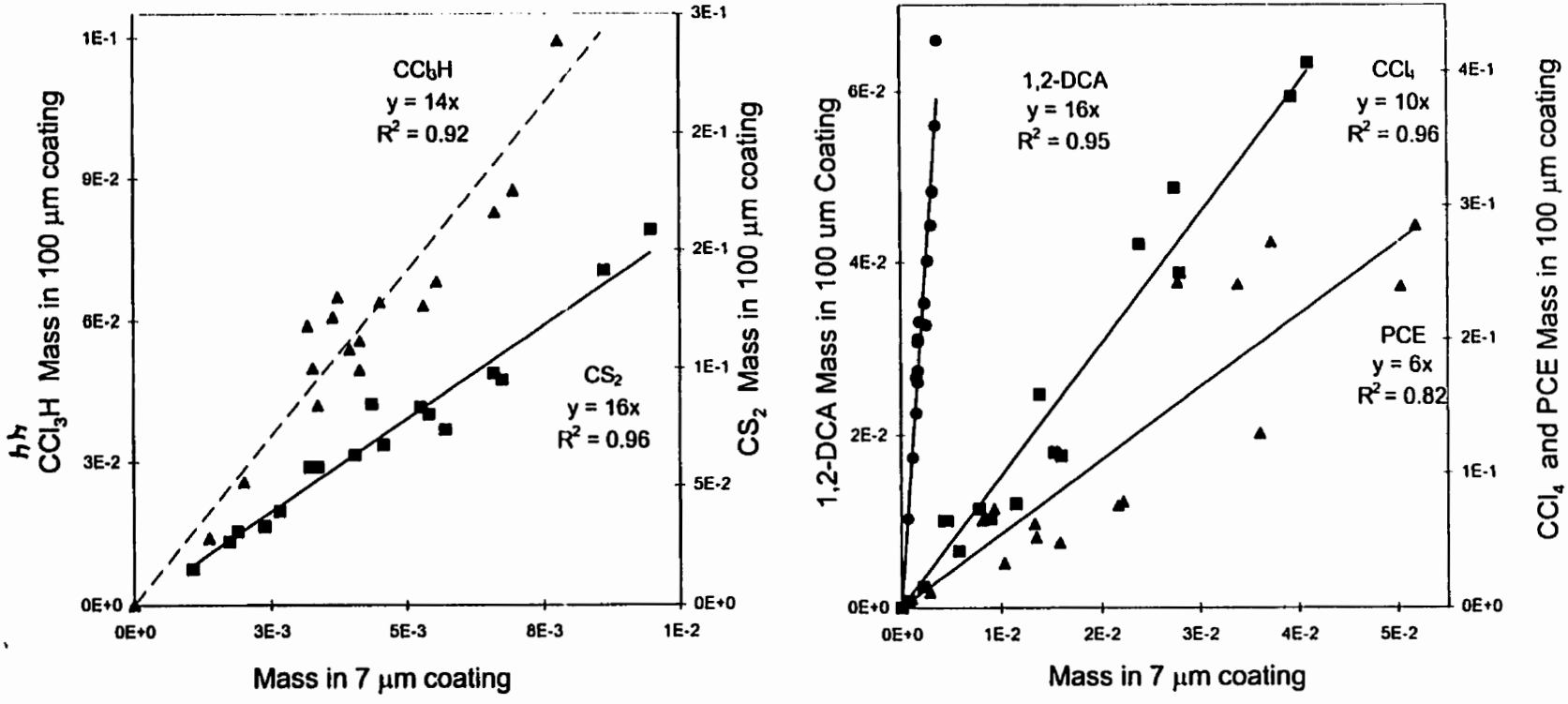

Figure 2.6. Plot of Mass Extracted by 7 µm Fibre versus Mass Extracted by 100 µm Fibre.
Data are for a one minute extraction of the same borehole.

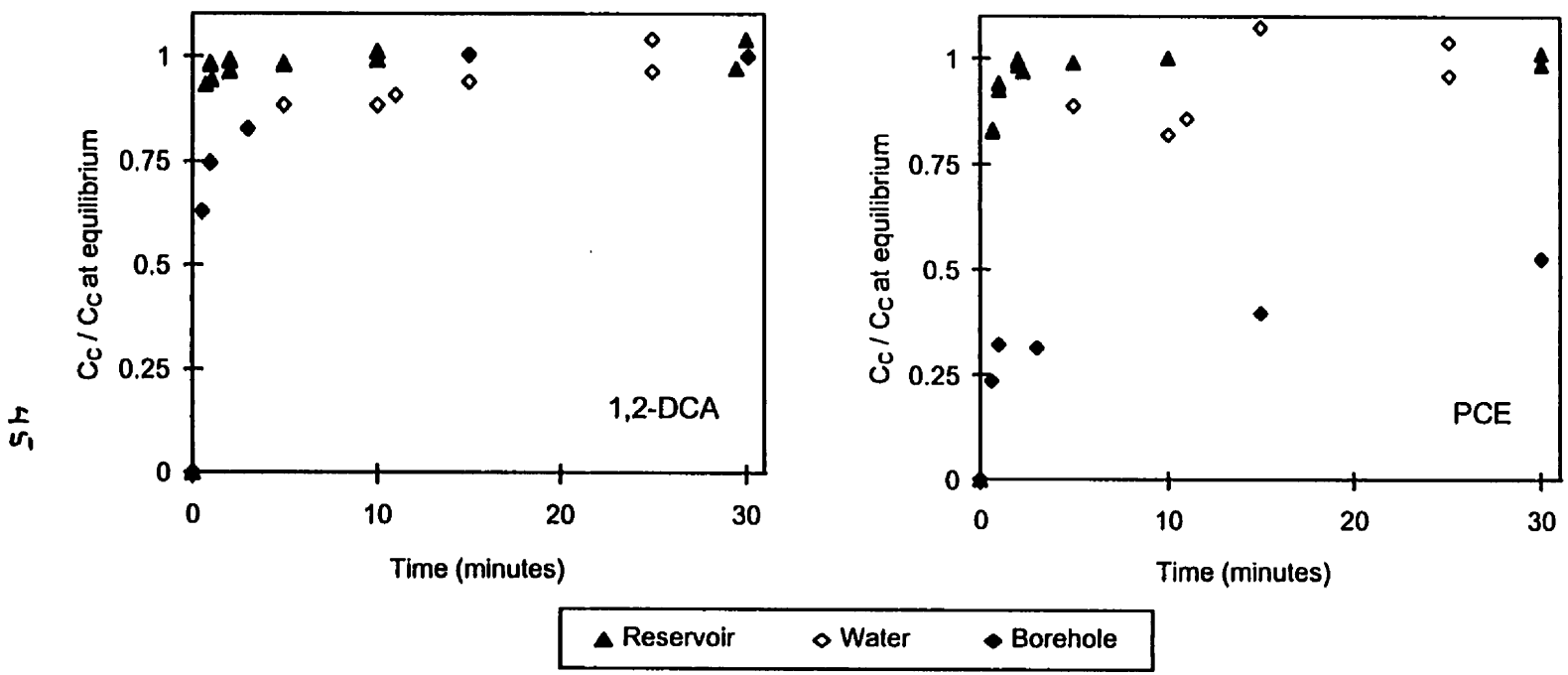

Figure 2.7. 1,2-DCA and PCE Time to Equilibrium Plots for Concentrations in 100 μm Fibre Coating for Reservoir, Water and Borehole Calibrations.

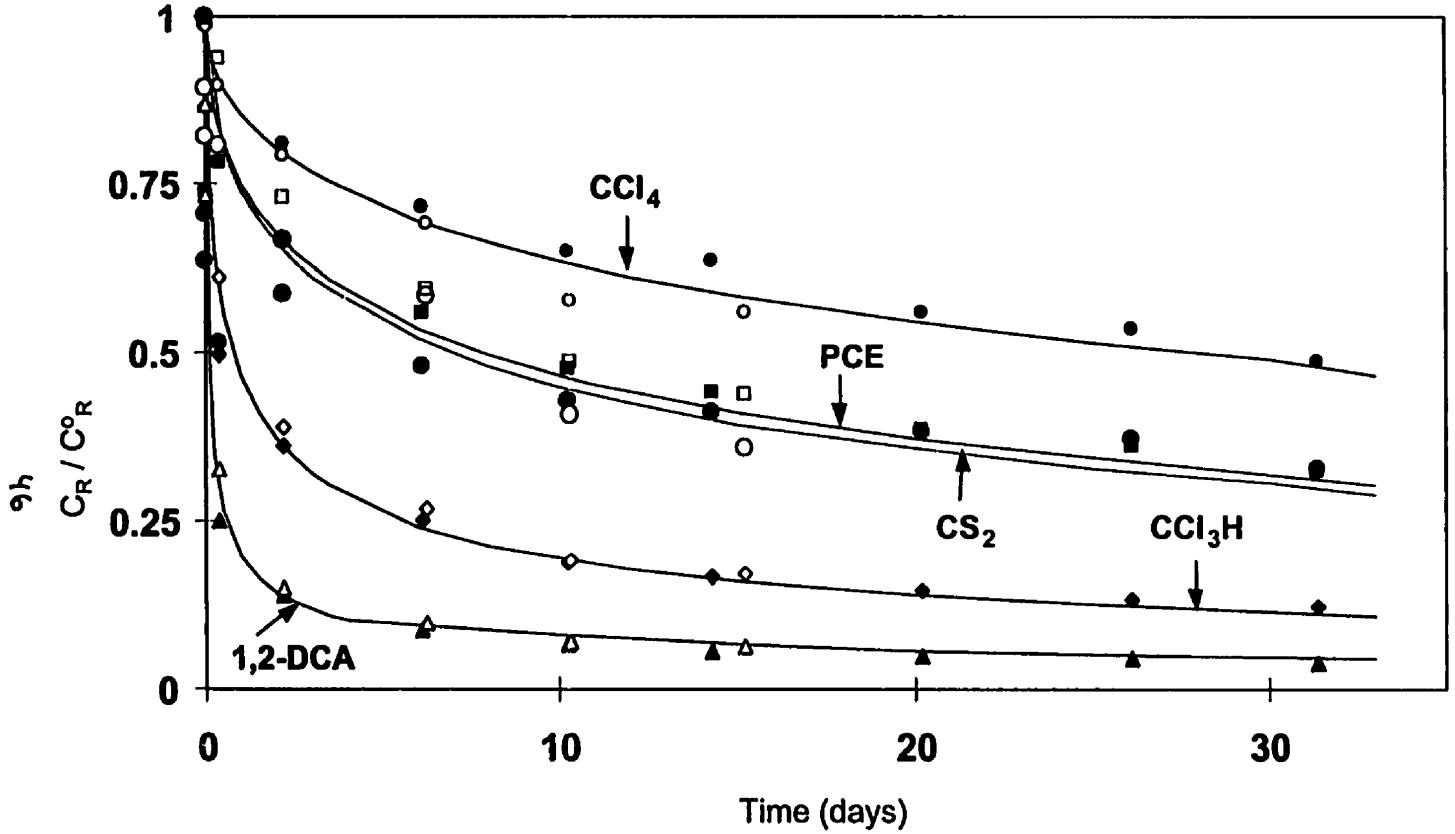

Figure 2.8. Reservoir Diffusive Losses with Time For CS_2, CCl_3H, 1,2-DCA, CCl_4 and PCE. Cell 1 = Closed Symbols, Cell 2 = Open Symbols, Model = Lines. D_e for model: CS_2 = 7x 10^{-6} cm^2/s, CCl_3H = 6 x 10^{-6} cm^2/s, 1,2-DCA = 6 x 10^{-6} cm^2/s, CCl_4 = 4 x 10^{-6} cm^2/s and PCE = 4 x 10^{-6} cm^2/s.

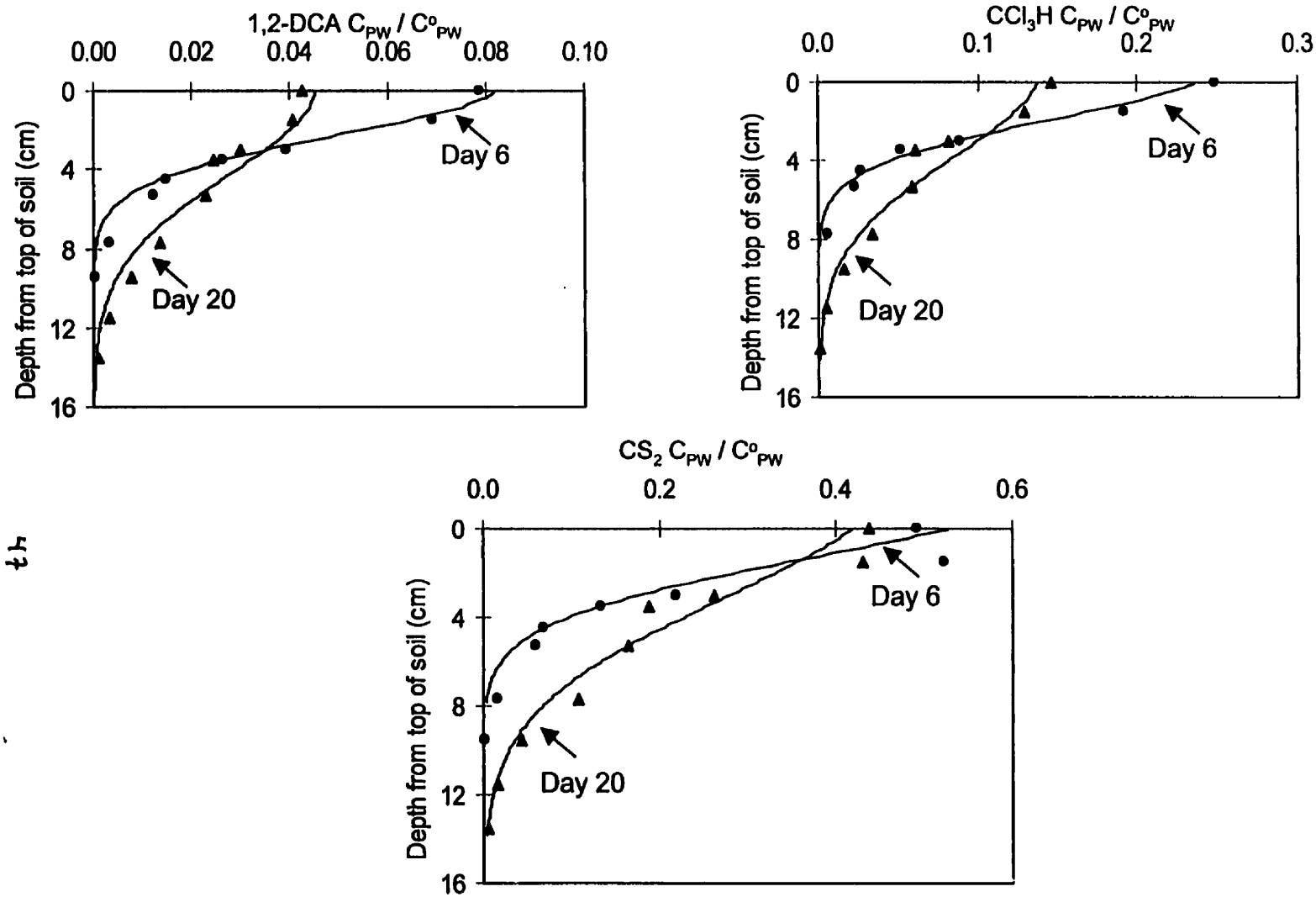

Figure 2.9A. 1,2-DCA, CCl_3H and CS2 Diffusion Profiles for Days 6 and 20. Boreholes Sampled with 100 μm Fibre. Cell 1 = Symbols, Model = Lines. Model D_e same as in Figure 2.8 (i.e. best fit D_{eR} from reservoir concentration data).

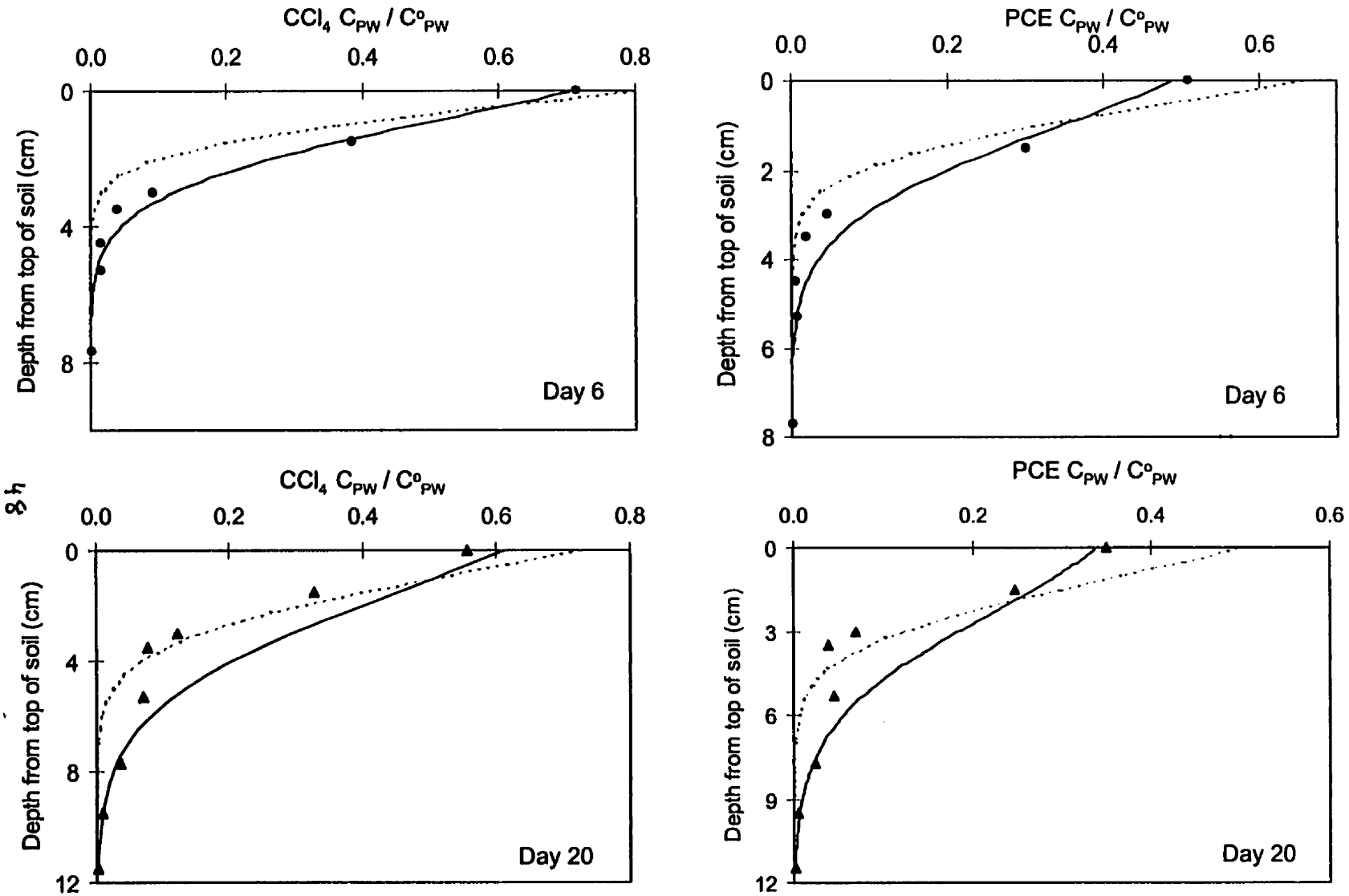

Figure 2.9B. CCl_4 and PCE Diffusion Profiles Day 6 and Day 20. Boreholes sampled with 100 μm Fibre, Cell 1 = Symbols, Model = Lines. Model $D_e = D_{eR} = 4 \times 10^{-6}$ cm²/s = Solid Line, Model $D_e = 2 \times 10^{-6}$ cm²/s = Dashed Line.

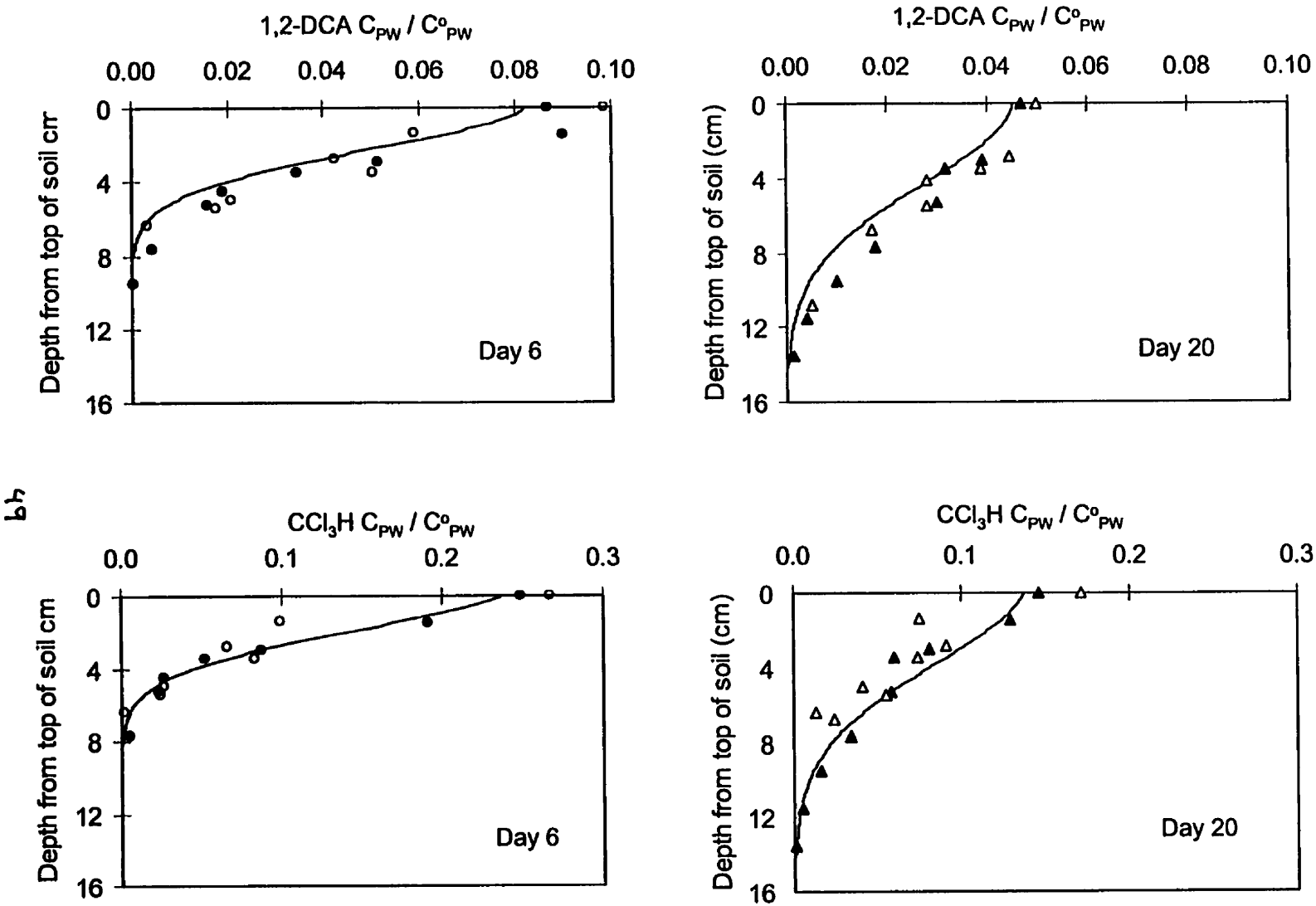

Figure 2.9C. 1,2-DCA and CCl_3H Diffusion Profiles for Cell 1 and Cell 2. Boreholes Sampled with 100 μm Fibre. Cell 1 = Closed Symbols, Cell 2 = Open Symbols, Model = Lines (Model D_e same as in Figure 2.8, i.e. best fit D_e from reservoir concentration data).

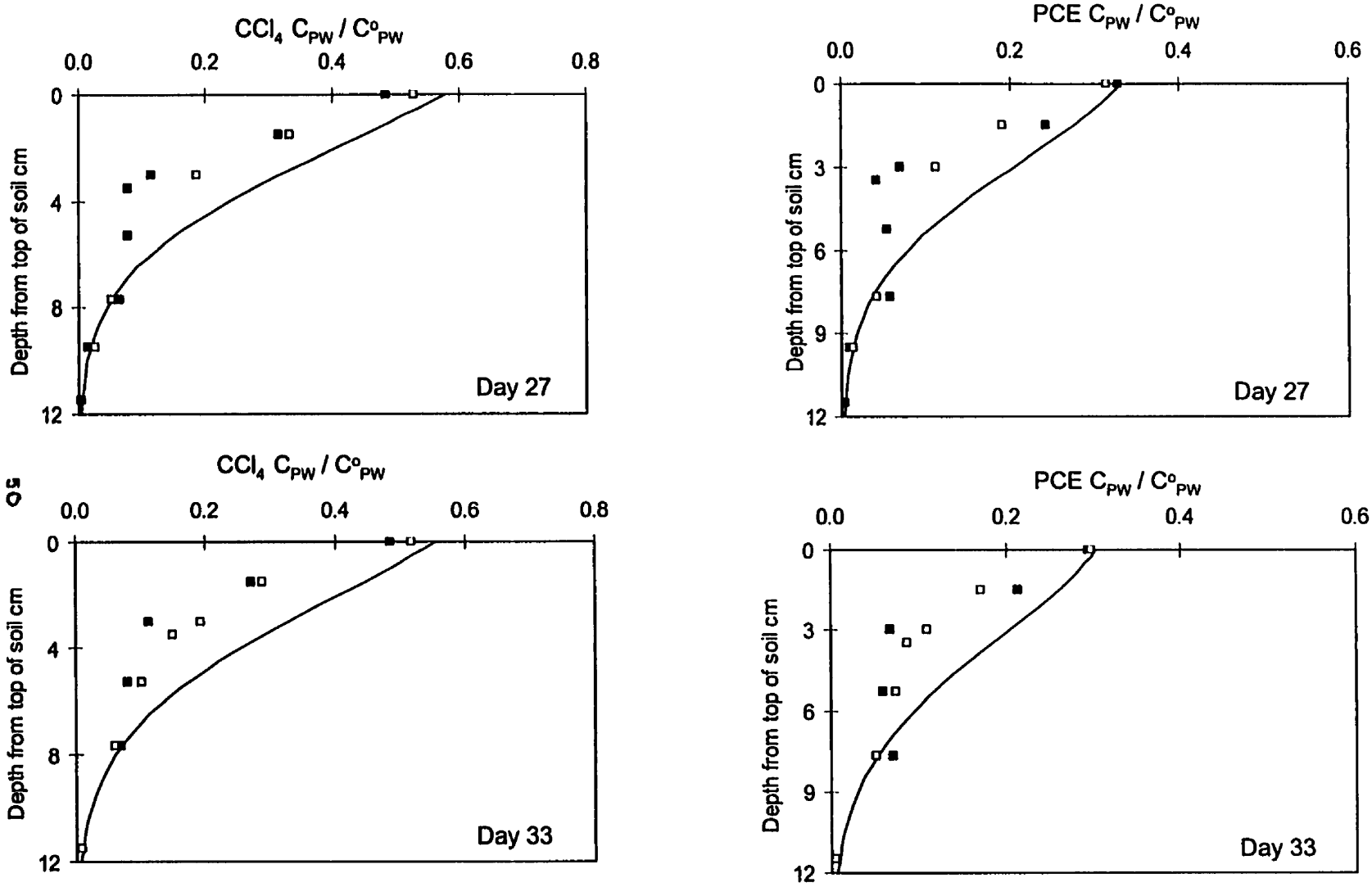

Figure 2.10. 100 μm and 7 μm Fibre Diffusion Profiles for Days 27 and 33. 100 μm fibre = Closed symbols, 7 μm fibre = Open symbols, Model = Lines, Model $D_e = D_{eR} = 4 \times 10^{-6}$ cm²/s

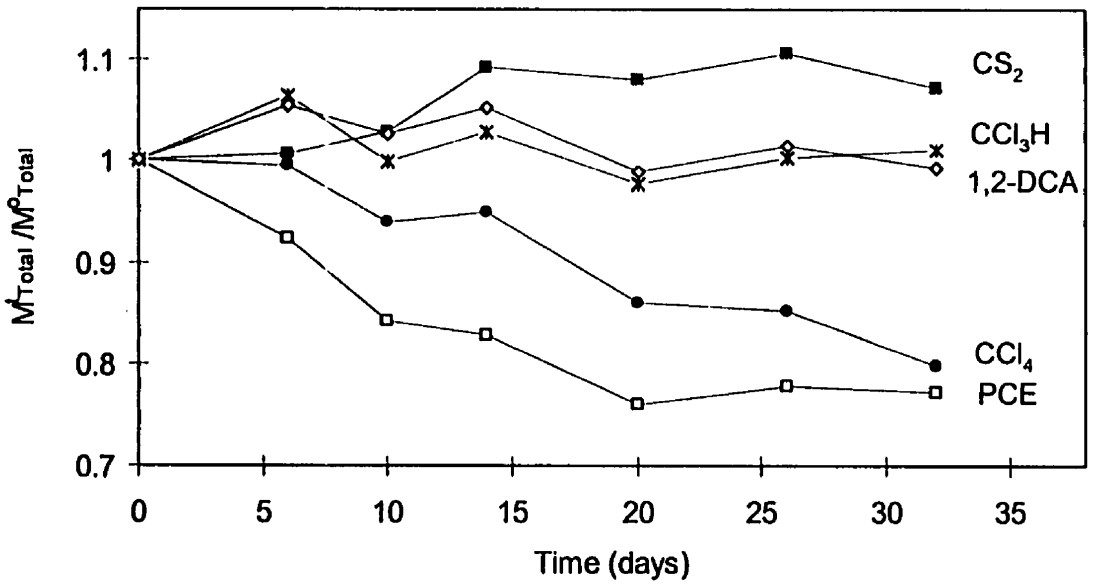

Figure 2.11. Relative Mass in Diffusion Cell Versus Time. Relative Mass is estimated total mass in cell (see text) divided by mass initially added to reservoir.

CHAPTER 3
A LABORATORY METHOD TO STUDY THE HETEROGENEOUS ABIOTIC TRANSFORMATION OF HALOGENATED ORGANIC COMPOUNDS IN LOW PERMEABILITY MEDIA

3.1 INTRODUCTION

Halogenated organic compounds (HOCs) are common groundwater contaminants and are often components of hazardous wastes and landfill leachate (Vogel et al., 1987). HOCs are susceptible to both biotic and abiotic transformations, but subsurface conditions do not always allow biotic transformations to occur or proceed at significant rates. In such cases, only the abiotic reactions may be of significance. However, some abiotic reactions such as hydrolysis can be relatively slow in aqueous solutions, with half lives on the order of hundreds to thousands of years estimated for some chlorinated groundwater contaminants (e.g. perchloroethylene and carbon tetrachloride) at temperatures typical of groundwater environments (Vogel et al., 1987). Nevertheless, when contaminants are present in the subsurface they are exposed to a wide variety of solid surfaces and recent studies have shown that some HOCs can have significantly faster abiotic transformation rates when certain reactive solid surfaces are present (Kreigman-King and Reinhard ,1992; Gillham and O'hannesin, 1994)

Reactions which occur, in part, at the surface of solids are termed heterogeneous reactions. Apparent half lives of chlorinated 1 or 2 carbon aliphatics on the order of a week or less have been measured in the presence of reduced iron-containing solids such as clay minerals; biotite and vermiculite (Kreigman-King and Reinhard, 1991), iron sulphides; pyrite and marcasite (Kreigman-King and Reinhard, 1991), and zero valent iron filings (Gillham and O'Hannesin, 1994). These half lives are at least several orders of magnitude less than those of reactions in homogeneous aqueous solutions in which such solids are not present. The reactive solids in the above systems are thought to be chemically involved in the transformation of the chlorinated organics but the exact reaction mechanisms are not always known.

The heterogeneous transformation rates of HOCs are expected to be greater in environments that have low oxygen concentrations and an abundance of solids with reactive surface areas (Schwarzenbach et al., 1993; Kreigman-King and Reinhard, 1994). Such environments may exist in low permeability media where the low hydraulic conductivities are expected to be conducive to low oxygen concentrations and where reactive solids may be present, e.g. clay minerals and iron sulphides. Past research on

HOCs in low permeability media has largely focussed on the ability of the media to limit the advection of contaminants to underlying groundwater resources (Koerner, 1994). Research interests have shifted recently to the reactivity of the medium as a means to control the diffusive flux through low permeability media. In addition, the incorporation of reactive solids into engineered "aquitards" such as landfill liners has become of interest (Major, 1997).

Heterogeneous abiotic transformation reactions of HOCs, whether in engineered or natural low permeability media, may have great potential to reduce groundwater contamination. If the original contaminant (the reactant) undergoes transformations when diffusing through a low permeability medium containing reactive solids, the diffusive flux into the low permeability medium and the depletion rate of the contaminant from the source will be greater than in the case with no reaction. However, although the source will become depleted with respect to the parent contaminant(s), the products of the transformation that occurs in the reactive low permeability media may diffuse back into this source. Thus, the composition and strength of the source may change over time and the fate of the transformation products becomes a key issue in evaluation of risk or remediation. In the low permeability medium itself, the diffusive fluxes of constituents of the transformation series will be controlled by the rates of their generation, diffusion and subsequent transformation. Thus, for experimental investigations of such reactions in low permeability media, it would be advantageous to obtain temporal measurements of concentrations in both the source and the low permeability medium in a fast and efficient manner while having a minimal influence on the diffusion and reaction processes.

As described in Chapter 2, a laboratory diffusion cell technique using a single sample of a column of low permeability medium has been developed that allows for the temporal measurements of HOC concentrations in a reservoir source and in the profile without the removal of water or porous medium samples. The new design utilizes a vapour reservoir source, the establishment of negative porewater pressures and the creation of "mini-boreholes" containing vapour in equilibrium with the surrounding porewater in the low permeability medium (Figure 3.1). The concentration in the vapour reservoir and in the porewater is determined with a microsampling technique called Solid Phase Microextraction (SPME). SPME is a technique similar in concept to pentane extraction of water samples but in this case the extraction medium is a 1 cm long and typically 100 μm (or less) thick polymer coating on a similarly thin silica fibre. With this method, the coating on the fibre extracts analyte mass when the fibre is inserted into either the reservoir or the boreholes.

The analyte mass extracted in the coating is quantified after thermal desorption in a gas chromatograph and the concentrations in the vapour source or the porewater profile are then determined using an appropriate calibration factor. This laboratory diffusion cell technique allows for the measurement of sequential diffusion profiles with only a minimal generation of concentration and advection gradients and, thus, minimizes the disturbance to the diffusion and reaction processes in the low permeability medium. As shown in Chapter 2, this technique has provided temporal reservoir concentrations and sequential profiles of a suite of VOCs in a nonreactive low permeability medium.

3.1.1 Background, Goals and Objectives of the Study

This chapter examines the application of the new diffusion cell design to measure the diffusion and transformation of HOCs and their transformation products through a low permeability medium containing reactive solids. The transformation of carbon tetrachloride (CCl_4) in the presence of pyrite (FeS_2) was used as the model reactive system. This system was selected partly because some data was available on the reaction rates and pathways (i.e. in static batch experiments by Kreigman-King and Reinhard, 1991, 1993 and 1994). As well, these laboratory diffusion studies of CCl_4-pyrite systems are expected to have application to field conditions for both natural and engineered low permeability media.

According to Criddle and McCarty (1991), CCl_4 is a good model compound for abiotic transformation investigations as it is transformed under conditions that are not too extreme. Abiotic reactions that CCl_4 has been involved in include hydrolysis, nucleophilic substitution, hydrolytic reduction and reductive dechlorination (Vogel et al., 1987). It is expected that in low permeability media, the most likely transformation reactions for halogenated aliphatics (a subgroup of HOCs including CCl_4) will involve the removal of halogens as a result of either reduction or substitution (Vogel et al., 1987; Kuhn and Suflitia, 1989). Thus, since the CCl_4 transformation reactions in the presence of pyrite involve these kinds of reactions, the experimental systems in this study have relevance to reactions expected to be important in low permeability media. In addition, pyrite is one of the most prevalent sulphide minerals and its occurrence is widespread (Deer et al., 1966). In sedimentary environments, pyrite can occur as both a primary and a secondary mineral (Deer et al., 1966) and specifically in aquitards, pyrite in amounts of approximately 0.5 % have been reported for both the Southern Ontario St. Clair Clay Plain (Abbott, 1987) and the Western Canada Glaciated Till Plains (VanStempvoort et. al.,1994). As pyrite may have an important role in the natural abiotic transformation of many pollutants (Kreigman-King and Reinhard, 1993), it is

conceivable that even at these low abundances in aquitards, the long residence times might result in significant transformation of HOCs.

3.1.1.2 Background on the CCl_4-Pyrite Model Reactions

Based on the work of Kreigman-King and Reinhard (1991, 1993 and 1994), fast CCl_4 transformation rates can be achieved in pure pyrite systems with well-mixed solutions. In the Kreigman-King and Reinhard (1994) study, greater than 90% of the CCl_4 was transformed within 12 to 36 days for anaerobic and aerobic conditions, respectively at a temperature of 25°C and pyrite surface concentrations of 1.2 to 1.4 m^2/L. The major transformation products were identified as chloroform (CCl_3H), carbon disulphide (CS_2) and carbon dioxide (CO_2), and formate and an absorbed fraction were classified as minor transformation products. Mass balances of between 80 to 90 % of the initial CCl_4 were achieved by accounting for these 5 types of compounds. CCl_3H was not reported to undergo further transformation whereas CS_2 was reported to undergo a hydrolysis reaction to CO_2.

Kreigman-King and Reinhard (1994) found that the CCl_4 reaction rate was not very sensitive to the experimental reaction conditions studied (i.e. presence or absence of O_2 and HS^- in solution and pyrite surface pretreated with O_2 and acid) and varied by a factor of 2.5. However, the distribution of the transformation products (presented as a percentage of the initial CCl_4 mass) was sensitive to the experimental reaction conditions. For example, under anaerobic conditions with acid washed pyrite surfaces, there were similar amounts of the 3 main transformation products, CCl_3H, CS_2 and CO_2, with each accounting for approximately 20 % of the total CCl_4 initial mass. Whereas, if the pyrite was not pre-washed in acid but was still under anaerobic conditions, CCl_3H was the major product at 50 % of the CCl_4 initial mass, and CO_2 at 10 % and there was a CCl_3H :CS_2 ratio of 25:1. For aerobic conditions, CO_2 was the major transformation product at 50 % and CS_2 at 11 to 15 % and there was a CCl_3H :CS_2 ratio of 1:2. The half life for CS_2 transformation was also found to be dependant on the experimental conditions and ranged from 6 to 60 days, with the larger value occurring in the aerobic system. Although there was a variation in the distribution of the three major transformation products (CCl_3H, CS_2 and CO_2) for the different experimental conditions investigated, the measured masses of the 3 major transformation products in each type of experiment accounted for at least 80 % of the initial CCl_4 mass. Although the exact reaction mechanism was not determined from these studies, Kreigman-King and Reinhard (1994) propose that the sulphur at the pyrite surface

is the electron transfer site and that the first step may involve the formation of the trichoromethyl radical ($\bullet CCl_3$). After this step a complex series of steps along different pathways are proposed for the formation of the CCl_3H, CS_2, CO_2 and other products. A detailed schematic of the proposed pathways and mechanisms is provided in their study. A simplified daigram for CCl_3H, CS_2, and CO_2 formation without the many intermediates are shown in Figure 3.1.

3.1.1.3 Goals and Ojectives of Study

The goal of the study was to illustrate that the diffusion-cell technique can be applied to the study of diffusion and time-dependent processes. In this case, the time-dependant process was a chemical transformation (CCl_4 transformation in the presence of pyrite) that had been previously studied by others (in static batch experiments). The major objectives of the study presented in this chapter are 1) to obtain temporal observations of both source reservoir concentrations and concentration profiles of a heterogeneous abiotic HOC transformation series formed within a reactive, low permeability medium and 2) to conduct these experiments in duplicate to assess the reproducibility of the technique in the investigation of transformation processes. Two other objectives were also devised as based on the literature on pyrite oxidation in general and on the relatively smaller amount of research on the specific CCl_4-pyrite reaction. The data obtained in the current study was compared with model simulations of the conceptualized diffusion and reaction processes. In addition, estimates of rate constants from the model fitting of the diffusion results were compared to those from batch experiments obtained from the literature.

Month long duplicate reactive-diffusion experiments similar in design to the nonreactive experiments described in Chapter 2 were conducted. The diffusion of an abiotic heterogeneous transformation series, which was comprised of the initial reactant carbon tetrachloride (CCl_4) and two transformation products, chloroform (CCl_3H) and carbon disulphide (CS_2), through reactive medium containing pyrite (FeS_2) mixed with silica grains was studied. The CCl_4 source was added as a vapour to a reservoir overlying the reactive medium which was water-saturated. A conservative tracer, 1,2-dichloroethane (1,2-DCA) was also present in the vapour source. The concentrations of these 4 compounds were measured temporally in the reservoir and in the vertical profile in the reactive low permeability medium. Since the grain size of both the pyrite and silica was that of fine silt and clay, the porous medium in these experiments was considered to be a idealized analogue of field cores of low permeability media.

3.2 METHOD

3.2.1 Materials

Analytical reagent grade chemicals were used for stock standards for the four compounds. Standard stocks were prepared by dissolving the organic solvents in analytical grade methanol. Vapour and water calibration standards were prepared by dissolving specific volumes of the standard stocks in known volumes of vapour or water. All laboratory experiments were conducted with nanopure water produced by using an Easypure UV filter.

The reactive material in the experiments was pyrite (Colorado Locale; Ward Scientific) and the nonreactive material was Ottawa sand. To create a homogeneous, nonsorbing and nonreactive artificial low permeability medium, Ottawa sand was crushed with a ball mill and sieved through a 325 mesh screen to obtain grains less than 44 μm in diameter. Pore diameter distribution was conservatively estimated to range from 5 μm to 20 μm with the assumption that the medium was comprised mostly of grains with a diameter near the large end of the range (e.g. approximately 40 μm). This pore diameter estimate was based on the additional assumptions of "closest" packing of the grains, that the narrowest openings are expected to have a diameter approximately 1/10 of the grain diameter and that the widest opening are expected to have a diameter approximately 1/2 of this grain diameter (personal communication, Dr. P. Groenvelt, University of Guelph). The pyrite had a specific surface area of 0.2 m^2/g and the Ottawa sand 0.6 m^2/g based on N_2-BET analysis. It was assumed that the pyrite solids were comprised of 100 % pyrite mineral but this was not confirmed by any chemical analyses. The mineralogy was approximately 95 % silica according to XRD analysis. The solid organic carbon content (f_{oc}) of the silica was 0.07%. Batch sorption studies were conducted with dissolved PCE (a contaminant more hydrophobic that those used in this work) and the crushed Ottawa sand and with 1,2-DCA and the crushed pyrite. In both, there was minimal mass loss from solution and the loss was similar to control samples without solids (i.e. 10 % or less). This suggests that there should be minimal sorption in the diffusion studies.

The following general procedure was used for cleaning pyrite surfaces prior to the experiments (Nicholson, 1990): 1) approximately 10 g of solid was exposed to 30 to 40 mls of 1N HCl for up to 1 hour, after which the acid wash was decanted; 2) the solids were rinsed with up to a total 4 L of nanopure water which was decanted after the solids had settled; 3) the solids were mixed with 20 to 30 ml of methanol which was then decanted;

and 4) the solids were air dried and used within 24 hours. A recommended modification of this technique that would reduce the potential for oxidation, would be to dry the solids in a glove box under an oxygen-free atmosphere.

3.2.2 Analytical Technique

Gas chromatography (GC) was used for the analysis of the organic compounds. The samples were collected with SPME 100 μm or 7 μm fibre extractions and analyzed using a Photoionization Detector (PID). The quantitation limits for the two fibres for the reservoir and porewater concentrations are provided in Table 3.2. Standards were run several times daily for all methods and the precision was approximately ± 5%.

The following inorganic analyses were performed on selected samples of porewater. SO_4^{2-} and Cl^- were measured using a Dionex system 2000 ion chromatograph and a conductivity detector. With this method, standards were run daily and the detection limits were 0.5 μM for SO_4^{2-} and 1.4 μM for Cl^-. Measurements of pH were taken with a Combo pH on a mV/pH/Temperature meter. The pH probe was calibrated using standard buffer solutions (pH 4, 7, and 10). Eh measurements were taken with a sealed Ag/AgCl reference ORP (Redox)electrode on a mV/pH/Temperature meter.

3.2.3 Reactive-Diffusion Experiments

Duplicate reactive-diffusion experiments were conducted in the stainless steel cylindrical cells described in Chapter 2 and schematically illustrated in Figure 3.1. The water-saturated, packed porous medium in the cells was composed of 17% (by weight) pyrite mixed with nonreactive silica. The vapour source initially contained 74 μM CCl_4 and 21 μM tracer (1,2-DCA); the latter had been determined to be nonsorbing and unreactive in the presence of pyrite (and silica). The expected CCl_4 transformation products (CCl_3H and CS_2) were not initially present in the source.

The physiochemical properties and the SPME partitioning coefficients for the tracer (1,2-DCA) and the transformation series (CCl_4, CCl_3H and CS_2) are provided in Table 3.1. These compounds have moderate vapour pressures, solubilities and hydrophobicities. This resulted in partitioning capacities for the SPME fibre samples which were well-suited for this work (neither too great nor too small). A more detailed description of the SPME calibration methods was presented in Chapter 2.

The methods for setting up the reactive-diffusion experiment were similar to that of the control diffusion experiment with the exception of the method used for packing and water saturation of the solids. The idealized reactive low permeability medium was created with the use of a vibration table to pack the grains and saturate the solids with de-aired nanopure water. The pyrite and silica were premixed prior to their addition to the diffusion cell. The diffusion cell was packed in lifts (1 cm thick layers of medium) with approximately 15 ml of the nanopure water added. Each lift was vibrated for 1 minute to mix and consolidate the soil and water. The methods for the other steps of the experimental set-up are described in Chapter 2.

3.2.4 Modelling of the Reaction and Diffusion of the CCl_4 Transformation Series in Low Permeability Medium Containing Pyrite

The diffusive transport of the CCl_4 transformation series through the reactive medium containing pyrite is conceptualized assuming 1) Fickian diffusion, 2) first order kinetics with respect to the pyrite reactive surface concentration and 3) first order kinetics with respect to CCl_4 concentration. Fickian diffusion has been used by others to represent diffusion through porous media (Shackelford, 1991). Heterogenous reactions have been reported to be first order with respect to the concentration of the solid surface (Lasaga, 1983; Wieland et al., 1988). The order of the reaction with respect to reactant concentrations for heterogeneous systems has typically been represented by psuedo first order kinetics (Kreigman-King and Reinhard, 1991; Gillham and O'Hannesin, 1994). However, in some cases other models have been used. Kreigman-King and Reinhard (1994) report zero order kinetics for CCl_4 reacting with pyrite and Nicholson et al. (1988) found that the rate of reaction varied in a nonlinear way with the reactant concentration, which could be approximated successfully with a Langmuir-like relationship. Nevertheless, for reasons described in more detail later, we have utilized a first order reaction in our modeling.

The reservoir and profile simulations were obtained from a numerical solution to equations [3.1 to 3.3]. Cirkpa (1994) developed the finite volume numerical model. The reservoir concentrations were not explicitly generated in the model but were obtained by multiplying the porewater concentrations determined for the top node in the profile simulation by the vapour-water equilibrium partition coefficients. The diffusion cell dimensions used in the model were 88 ml for the reservoir volume, 21.2 cm^2 for the cross-sectional area and 0.34 for the porosity.

Transport equations for a unit volume of saturated porous medium, for the transient one-dimensional diffusion of a CCl_4 transformation series are shown below, where the subscripts 1, 2, 3 and 4 refer to CCl_4, CCl_3H, CS_2,and CO_2, respectively. The system is modelled as CCl_4 transforming to both CCl_3H and CS_2 with CS_2 undergoing further transformation to an undetected product that is assumed to be CO_2.

Transport Equation for CCl_4 (the initial reactant)

$$\frac{\partial C_1}{\partial t} = De_1 \frac{\partial^2 C_1}{\partial x^2} - k_1 C_1 \qquad [3.1]$$

Transport Equation for CCl_3H

(CCl_4 transformation product which undergoes no further reaction)

$$\frac{\partial C_2}{\partial t} = De_2 \frac{\partial^2 C_2}{\partial x^2} + k_2 C_1 \qquad \text{where } k_2 = k_1 a \qquad [3.2]$$

Transport Equation for CS_2

(CCl_4 transformation products which undergoes a further reaction to CO_2)

$$\frac{\partial C_3}{\partial t} = De_3 \frac{\partial^2 C_3}{\partial x^2} + k_3 C_1 - k_4 C_3 \qquad \text{where } k_3 = k_1 b \qquad [3.3]$$

where C is the concentration in the porewater, D_e is the effective diffusion coefficient, k_1 is the overall first order rate constant where $k_1 = k_2 + k_3$ and a and b are the formation factors that determine the relative rates of transformation of CCl_4 to form CCl_3H and CS_2, respectively. As shown in equations [3.2] and [3.3], the fluxes of the transformation products are coupled to the fate of the reactant through the reaction term k_2C_1 and k_3C_1.

3.2.4.1 Selected Model Simulations of the Reactive-Diffusion Experiment

To illustrate some of the characteristic features expected for the CCl_4 heterogeneous transformation series, some select simulations using model parameters similar to those in the diffusion experiment are provided in Figures 3.3A and 3.3B. The CCl_4 source is finite, CCl_4 undergoes a heterogeneous transformation to CCl_3H and to CS_2 in a ratio of approximately 1:7 and CS_2 undergoes a transformation reaction at a rate approximately 15 times slower than that at which it is formed. Figure 3.3A illustrates the atypical diffusion profiles that are expected for the transformation products to have as a result of the back diffusion of these compounds into the reservoir at early times. A shown in Figure 3.3A, a zone of slight depletion is observed in the top of the profiles which results in a maximum concentration that is observed at about 0.5 cm from the top of the profile rather than at the

surface. There is greater depletion in the top of the profile for CS_2 than CCl_3H because CS_2 is forming at a greater rate and, thus, diffusing back into the reservoir at a greater rate. This zone of slight depletion is fairly distinct on Day 9, barely visible on Day 17 and has disappeared after about one month. The disappearance of this maximum at 0.5 cm after approximately two weeks occurs because the vapour in the reservoir and the porewater in the top of the profile have reached equilibrium concentrations and, thus, diffusion ceases to be bi-directional.

Figure 3.3B, with simulations for Day 9 and Day 34 using the same model parameters as for Figure 3.3A, illustrates that the relative differences in the rates of diffusion of the reactant and the products of a transformation series are dependent on the relative differences in their diffusion coefficients and in their rate constants. For this study and for these model simulations, the range in the diffusion coefficients is smaller than the range for the rate constants. As shown in Figure 3.3B, both transformation products diffuse ahead of CCl_4 because of the fast rate of the reaction producing them. Even at early times, the CS_2 profile concentrations, except at the top, are significantly greater than those of CCl_4. This is because CS_2 has the greater diffusion coefficient and, more importantly, CCl_4 has a faster rate of transformation. CS_2 diffuses ahead of CCl_3H because CS_2 is being formed at a faster rate resulting in greater concentration gradients. Even though CS_2 is undergoing transformation, its rate is slow enough at the end of the experiment so that the CS_2 profile concentrations remain greater than those of CCl_3H.

3.3 RESULTS AND DISCUSSION

Two types of temporal results were obtained with this diffusion cell design: the reservoir concentration changes with time and the sequential diffusion profiles. Reservoir and profile concentrations in both cells are shown in Figures 3.4 and 3.5 for the tracer (1,2-DCA) and in Figures 3.4, 3.6 and 3.7A, B and C for the transformation series (CCl_4, CCl_3H and CS_2). The experimental profile concentration data for the porewater just below the reservoir-solid interface were calculated by dividing the measured reservoir concentrations by the vapour-water equilibrium partition coefficients (H). The reservoir and profile samples were collected with SPME fibres having two different coating thicknesses, one of 7 μm and one of 100 μm. Figure 3.5 demonstrates that similar results were obtained with the two fibres. However, because of the higher quantitation limits for the thinner 7 μm coating, fewer quantifiable results were obtained with this fibre than with the 100 μm fibre, and, therefore, only concentrations obtained with the 100 μm fibre are provided for the transformation series.

For the two diffusion cells, the average initial vapour source reservoir concentrations were 73 μM ± 2.2 μM for the initial reactant (CCl_4) and 21 μM ± 1.1 μM for the tracer (1,2-DCA) and the average amount of pyrite (by weight) was 17 % ± 0.34. Two transformation products, CCl_3H and CS_2, were detected in both diffusion cells. The experiment was conducted for approximately one month during which time 5 sampling events were undertaken. Inorganic concentrations of the porewater obtained for samples collected along the profile at the end of the experiment were essentially constant with depth (SO_4^{-2} at 720 μM ± 108 μM and Cl^- at 620 μM ± 99 μM). Similarly, there was little variation in pH (6.6 ± 0.1) and Eh (188 ± 3).

3.3.1 Reservoir and Profile Concentrations Results with Time for the Transformation Series

The presence of 17 % pyrite in the porous medium resulted in a CCl_4 diffusive flux from the reservoir that was greater than expected for a medium with no transformations (Figure 3.4). For example, by the end of the experiment, more than 90 % of the CCl_4 had been depleted from the reservoir as compared to the 30 % decrease that would be expected in a nonreactive system. The CCl_4 reservoir results followed the expected trends of exponential decreases with time. The reservoir results for the two detected transformation products, CCl_3H and CS_2, followed the expected trends with time for this

experimental system, i.e. for a finite reservoir volume and for initially fast rates of formation, which decreased with time as the concentration of CCl_4 in the reservoir was depleted. CS_2 and CCl_3H were measured at early times in the reservoir because they underwent back diffusion from the reactive porous medium surface into the reservoir source (Figure 3.6). That CS_2 was detected earlier in the reservoir than CCl_3H, i.e. by 18 hours for CS_2 and by the next sample event at Day 5 for CCl_3H, reflects the faster rate of transformation and lower quantification limit for CS_2. Both transformation products increased with time until back diffusion ceased at about 2 weeks; thereafter, their reservoir concentrations remained constant or slowly started to decline for the remainder of the experiment. By the end of the experiment, the CCl_4, CCl_3H and CS_2 reservoir concentrations in diffusion cell 1 were 8 μM, 1 μM and 34 μM, respectively, and in diffusion cell 2 were 10 μM, 1.6 μM and 20 μM, respectively.

The profile results are provided in Figure 3.6. The CCl_4 diffusion profiles exhibited characteristics that were the result of a transformation rate that was fast relative to its diffusion rate. Thus, CCl_4 was not detected deeper than 5 cm and its concentrations in the sequential diffusion profiles decreased with time. The early time transformation product profiles, as expected, were not simple exponential curves because of the back diffusion into the reservoir. Instead, the CCl_3H and CS_2 concentrations were depleted in the top port in both cells (at less than 2 cm) relative to the ports immediately below. Although this depletion was only predicted for early times, it was observed for most of the CCl_3H and CS_2 data in this zone for the remainder of the experiment. As discussed in more detail later, these low concentrations may be a result of changes in the reaction conditions with time in this zone. For the deeper portions of the transformation product profiles, the expected changes with depth and time were observed for both CCl_3H and CS_2. CS_2 was formed at greater rates than CCl_3H and, thus, was present at greater concentrations and had diffused to greater depths than CCl_3H; the maximum CS_2 concentration measured in the profile was 48 μM and the maximum depth at which CS_2 was detected was 13.5 cm.

3.3.2 Comparison of Temporal Results from the Duplicate Diffusion Cells

The two diffusion cells yielded, for the most part, similar temporal results for both the reservoir and profile samples (Figures 3.4 to 3.7). Based on the similarity in concentration profiles, the rate of diffusive flux from the reservoir into and through the porous medium, for both CCl_4 and 1,2-DCA, was similar in both diffusion cells. The rates of accumulation of the

two detected transformation products (CCl_3H and CS_2) in the reservoir and their diffusive migration through the porous medium were less similar in the two diffusion cells.

In order to assess the reproducibility of the results in the two diffusion cells in a more detailed manner and to provide the formation factors for estimating the rate constants for the transformation products (a and b in equations 3.2 and 3.3), mass balances were calculated. These mass balances were calculated for each sample event and were then compared for the two diffusion cells. The equations used to calculate the mass balance are provided in Appendix A. The calculated mass for each compound was obtained by adding the mass in the reservoir, which was calculated by multiplying the concentration in the reservoir by the volume of the reservoir, to the mass in the porewater, which was calculated by integrating the area under the concentration curves for the porewater profile. In order to compare the transformation series results for the two diffusion cells, we needed to account for 1) the slight differences in the initial CCl_4 mass in the reservoir of each cell, and 2) the slight differences in tracer mass recovery. This double normalization was accomplished by dividing the calculated mass for each compound in the transformation series by 1) the initial CCl_4 mass in the respective diffusion cell, and 2) the fraction of tracer mass recovered, which was greater than 90 % in both diffusion cells for all sample events.

Figure 3.8 is a cumulative histogram of the double-normalized mass estimates for each diffusion cell and for 4 sampling events (Days 9, 17, 24 and 30/34). In both diffusion cells, a fast CCl_4 transformation rate was achieved with the 17 % (by weight) pyrite-rich medium since by the end of the experiment both had less than 15 % of the initial CCl_4 remaining. The rate of CCl_4 transformations was slightly faster in cell 1 as by the end of the experiment there was 11 % left in cell 1 and 14 % left in cell 2. CCl_3H was the minor transformation product detected in both cells as by the end of the experiment, the CCl_3H mass accounted for less than 10 % of the initial CCl_4 mass. The rate of formation of CCl_3H was less in cell 1 than cell 2 by about 40 % and this difference was constant with time. CS_2 was the major transformation product detected such that, in cell 1 at the end of the experiment, its total mass represented 70 % of the initial CCl_4 mass. CS_2 was measured in different amounts in the two cells and this difference increased with time such that by the end of the experiment there was 60 % more CS_2 in cell 1 than in cell 2. The possible causes of these differences between the two cells is in the rate of formation of the transformation products even though the rate of transformation of the parent was similar as discussed in section 3.3.5.

Figure 3.8 indicates that there was mass unaccounted for in the CCl_4 transformation series. This unaccounted-for mass was greater in cell 2 and increased to a 2 fold difference by the end of the experiment where 35% of the mass was unaccounted for in this cell. The average ratio of CCl_3H:(CS_2 + unaccounted-for mass) for the 4 sample events was 1:17 (with a relative standard deviation of ± 3 %) for cell 1 and 1:7 (with a relative standard deviation of ± 7 %) for cell 2. Based on the studies of Kreigman-King and Reinhard (1994), this missing mass may have been CO_2, formate, an adsorbed fraction or some other product not specifically identified. Due to the following lines of evidence, the missing mass in the transformation series is likely, at least in part, due to the tranformation of CS_2 to CO_2: 1) an increasing CCl_3H/CS_2 ratio throughout the experiment; 2) batch results conducted in this study that showed a decline in CS_2 control vial concentrations (no pyrite or silica) with time and 3) batch results of others that report that CS_2 hydrolyzes to CO_2 (Adewuyi and Carmichael, 1987).

3.3.3 Modelling of the Reactive-Diffusion Experiments

The CCl_4, CCl_3H and CS_2 model simulations for the reservoir concentrations are provided in Figures 3.4 and 3.6 and for the profile concentrations in Figure 3.7A, B and C, respectively. The experimental reactions, as presented in equations [3.1], [3.2] and [3.3], were modelled as CCl_4 transforming to both CCl_3H and CS_2 and with CS_2 undergoing further reaction to form CO_2. The model required three effective diffusion coefficients (D_e values) and four first order rate constants (*k* values).

3.3.3.1 D_e and *k* Model Values

The values of D_e and *k* used in the model simulations are provided in Table 3.2. The D_e values used in the model simulations were obtained from the control experiment described in Chapter 2 in which a nonreactive porous medium was used. In these nonreactive experiments, the D_e obtained from the reservoir (D_{e-R}) could be used to fit the diffusion profiles for the majority of the results. As both the tracer reservoir and profile model simulations generally agreed well with the experimental results (Figure 3.2 and 3.3), the addition of 17 % pyrite to this nonreactive porous medium for the reactive experiments did not appear to change the D_e from the control values. The same D_e value was used in the simulations of the transformation series results for each diffusion cell. The basis for this approach was that two diffusion cells had similar tracer reservoir results (Figure 3.4) and similar tracer profile concentrations (Figure 3.5).

The k values were the only fitting parameters in the model simulations. In Table 3.2 the four k values are: k_{CCl_4} for the overall rate constant for CCl_4 transformation, k_{CCl_3H} for the transformation of CCl_4 to CCl_3H, k_{CS_2} for the transformation of CCl_4 to CS_2 and k_{CO_2} for the transformation of CS_2 to an undetected compound that is assumed to be CO_2. The first step in simulating the experimental results involved determining the k_{CCl_4} since the fittings for the other three k values were dependent on this first k value. The same k_{CCl_4} was used in simulations for both diffusion cells. The k_{CCl_4} was determined from a fit "by eye" of the model simulations to the diffusion results. The initial estimate of the k_{CCl_4} was taken from some batch results conducted at the beginning stage of this research. These results have not been included because of their preliminary nature. The other three k values were based on the mass balance assessments discussed in section 3.3.2. Estimates of k_{CCl_3H} and k_{CS_2} were obtained by multiplying the k_{CCl_4} value by the respective ratio in which CCl_3H and CS_2 were formed in the transformation of CCl_4. Because CS_2 was expected to undergo further reaction to CO_2, this transformed CS_2 mass (or CO_2) needed to be accounted for in the determination of the ratio at which CCl_3H and CS_2 were initially formed. Assuming that the CO_2 formed from the CS_2 reaction represented the unaccounted-for mass resulted in a better correspondence of the simulations to the results than incorporating a third CCl_4 transformation reaction in the model and a slower k_{CS_2}. Thus the mass balance ratios presented above for CCl_3H:(CS_2 + unaccounted-for mass) were used to calculate the formation factors, a and b in each cell. These a and b values were 0.06 and 0.94 for cell 1 and 0.14 and 0.86 for cell 2, respectively. It is recognized that with additional detailed studies of the reaction, this model of the transformations may be revised at some later date. However, for the current study, the goal was to assess whether the data could be fit with this initial assessment of the possible reactions occurring in the diffusion experiment.

3.3.4 Comparison of Experimental Reactive-Diffusion Results and Model Simulations

The simulations, including the trends with time, corresponded well with the majority of the reservoir and the profile results (Figure 3.4 and 3.5, respectively). The best model fits were for profile results below a depth of 2 cm. Better fits at greater depths and with later times is consistent with the literature (personal communication, Dr. Shackleford, Colorado State University)

There appear to be some problems with the model fits of the concentrations in the reservoir (mostly at later times) and in the top 1 to 2 cm of the profile (for many samples collected over the entire experiment). Although there was some variability in the trends with

time, in general for these samples, the CCl_4 model concentrations were too low and CCl_3H and CS_2 model concentrations were too high. However, the model simulations were different from the experimental results by, at most, a factor of 1.5; CS_2 concentrations were the most poorly modelled as they were over estimated by a factor of 1.5 in the top port of both diffusion cells by the end of the experiment. The differences between the model and these results suggest that the model's calculated rate of CCl_4 transformation is greater than what was actually occurring in the top part of the profile. This poorer fits can be explained by changing reaction conditions in this zone that are not accounted for in the model. The processes thought to be responsible for these changes are discussed in the next section.

3.3.5 Suitability of the Technique to Study Transformation Processes in Low Permeability Media

Three types of comparisons were used to evaluate the suitability of the technique to study transformation processes in low permeability media. The first compared the results of the two diffusion cells which were conducted as duplicate reactive-diffusion experiments, the second compared the results with model simulations and the third compared the results with those from the literature.

The technique provided an estimate of the CCl_4 rate constant that was similar for the two diffusion cells used in the reactive-diffusion experiments. The other three rate constants, when their estimated values for each diffusion cell were compared, differed by a factor of 1.5 or less. This similarity in the overall rate constant but with differences in the rate of formation of the transformation products was also observed in the Kreigman-King and Reinhard (1994) study of the effect of different reaction conditions on the rates of reaction of the CCl_4 transformation series. The variations in the mass distribution of the transformation products observed in the Kreigman-King and Reinhard (1994) studies are larger than those observed between the results from the two diffusion cells. For example, for the two diffusion cells, the greatest difference was in the amount of CS_2, which was at most 0.6 times greater in cell 1 than in cell 2. However, Kreigman-King and Reinhard (1994) found, under the different reaction conditions studied (the extent of the exposure of the pyrite to oxygen, the amount of oxygen in the solution and the presence or absence of HS^- in solution), that there was a 10-fold difference in the CS_2 relative mass balance. Kreigman-King and Reinhard (1994) also report that the presence of O_2 significantly effects the CCl_4 tranformation pathway. It may be that a slight difference in the amount of O_2 in the two diffusion cells was partially responsible for the slight differences in the distribution of the

transformation products in the two diffusion cells. The Kreigman-King and Reinhard (1994) study suggests that the differences in the relative mass balances of the transformation products in the two diffusion cells, more likely reflects real but slight differences in the reaction conditions between the two diffusion cells rather than indicating some limitation in the precision of the diffusion cell technique.

The majority of the reactive-diffusion experimental results could be predicted by the model that assumed first order kinetics with respect to the concentration of the CCl_4 in the porewater and a constant and uniform reactive pyrite surface concentration. The poorest model fit, i.e. in the top 2 cm or less in the profile, had at most a factor of 1.5 disparity. This amount of disparity in this restricted zone was interpreted to be a further indication of variable reaction conditions rather than an unsuccessful application of the diffusion cell technique. The disparity suggested that the rate of transformation of CCl_4 was over predicted. This difference between the model fit and the results in the top 2 cm of the profile could be explained by zero order reaction kinetics and/or temporal decreases in reactive pyrite surface concentrations. These two processes are discussed in turn with respect to explaining the poorer model fit of results in the top of the profile.

First order kinetics with respect to CCl_4 porewater concentrations are expected when the pyrite solid surface sites are well below saturation with CCl_4. In this case, the rate of the heterogeneous reaction is dependent on the CCl_4 concentration in the water. This kinetic order was expected for deeper zones within the profile of the reactive-diffusion experiment, where the rate of diffusion through the porewater will control the CCl_4 concentration on the pyrite surface. However, at and near the reservoir/porous medium interface, the pyrite surfaces may always have been at or near saturation with CCl_4, because the adjacent vapour reservoir could readily replenish CCl_4. Thus, the reaction in the top of the profile might be better described by a zero order kinetic model with respect to the concentration of CCl_4 in the porewater. Similar changes in kinetics have been reported for pyrite oxidation in batch experiments in which first order kinetics are applied when the oxidant concentrations are low whereas at higher concentrations zero order kinetics are thought to better represent the reaction (Nicholson, 1994). For CCl_4-pyrite batch studies, Kreigman-King and Reinhard (1991; 1994) used a first order reaction model in early studies but they report that zero order kinetics better described the reaction in later and more detailed analyses. It is not clear from the Kreigman-King and Reinhard (1994) study whether the observed correspondence with the zero order kinetic model was a result of pyrite surface saturation

with CCl_4. However, as indicated above, the transformation reactions with pyrite may not always be first order with respect to the reactant concentration in solution.

The rate of transformation of CCl_4 may also have been affected by a decrease in pyrite reactivity with time in the top 2 cm or less of the profile due to the possibility of an accumulation of an iron oxide layer on the surface of the pyrite grains. The iron oxide coating could have formed as a by-product of the reaction of CCl_4 with the pyrite surface and the extent of its accumulation would be the greatest in this zone since here the rate of CCl_4 transformation was the fastest. Although no surface analysis was conducted on the pyrite in this study, Kreigman-King and Reinhard (1994) detected the presence of such a coating on pyrite grains after reacting with CCl_4. They did not report, however, on the thickness or distribution of the iron oxide layer. With the presence of an iron oxide coating, the CCl_4 access to the pyrite molecule is decreased and hence, a decrease in the rate of transformation may be observed depending on the thickness of this oxide layer. A decrease in pyrite reactivity and the accumulation of an oxide layer have been observed by Nicholson et al. (1990) in continuous flow oxidation laboratory experiments. The extent to which an oxide layer could have accumulated in the reactive-diffusion experiments is dependent on the extent of the reactive surface area of pyrite. In other work, SEM micrographs of oxidized pyrite grains suggested that the reaction is favoured to occur at high free energy sites such as edges or corners of the grain (McKibben and Barnes, 1986). In our case, most of the oxide layers in the reactive-diffusion experiments would have been formed in restricted portions of the medium (at shallow depths) and possibly acquired a thickness significant enough to slow the diffusion of CCl_4 to the reaction surface of the pyrite. Thus, in our experiments a lower overall reactivity may have resulted due to 1) reduced access to the higher energy sites, and 2) higher proportion of reactions occurring at lower energy sites.

The k_{CCl_4}, k_{CCl_3H}, k_{CS_2} and k_{CO_2} values obtained from the model fitting of the reactive-diffusion experiments are lower but within an order of magnitude of the values reported in Kreigman-King and Reinhard (1994). This difference with the Kreigman-King and Reinhard results is thought to reflect the sensitivity of the transformation rate to the presence of oxide coatings on the pyrite surface as reported by Nicholson (1990) for pyrite oxidation studies. It is likely that the pretreatment technique in our study was more prone to the subsequent generation of oxide coatings because the solids were not dried in a anaerobic glove box as they were for the Kreigman-King and Reinhard study. Nicholson (1994) reported the variability in the pretreatment techniques as the major cause of the variation in the pyrite

oxidation rate found in the literature. Although the rates are lower, the CCl_3H:(CS_2 + CO_2) ratios are similar to those from Kreigman-King and Reinhard (1994) study for their reaction conditions that are expected to be most similar to those in the diffusion experiment.

Even with the possibility of variable reaction conditions, the technique was able to provide a narrow range for estimates of rate constants and for the most part, predictable diffusive losses from the reservoir and diffusive profiles in the reactive low permeability medium. By accounting for the sensitivity of the distribution of the transformation products to reaction conditions, the slight variability between the two cells could be explained. Also, by accounting for the likelihood of the occurrence of zero order kinetics with respect to CCl_4 porewater concentration and/or a decrease in pyrite reactivity in the top of the profile, the poorer model fits could be explained. Because of the two types of sample measurements and because they were collected over time, the technique was able to discern apparent subtle differences in reaction processes. The technique has some definite advantages over more conventional methods because of the relative efficiency with which temporal measurements are obtained enabling such issues as changes in reaction kinetics to be identified.

3.4 CONCLUSIONS

The diffusion of a transformation series consisting of CCl_4 (the initial reactant) and CCl_3H and CS_2 (the transformation products) through a reactive low permeability medium containing pyrite was measured over time with a new diffusion cell design and micro-sampling procedure. Duplicate reactive-diffusion experiments and sequential reservoir and profile measurements indicated that reproducible results can be obtained with this technique.

The estimates of first order rate constants from the model fits from the diffusion experiment are within the same order of magnitude as those from the literature for batch experiments. However, the use of a large, well-mixed vapour source may have resulted in a lower order of reaction kinetics and/or a decrease in pyrite reactivity in the top portion of the profile. A zero order of kinetic reaction is believed to appropriately model the results in the top of the profile due the fact that CCl_4 can be readily replenished from the vapour source. The technique discerned these changes in reaction conditions with depth and with time because of the ability to collect temporal and nondestructive measurements.

First order kinetic rate constants for the overall reaction from batch experiments were utilized to provide an initial estimate for the artificial reactive low permeability media. Future work using a modified diffusion cell design to allow for the collection of field core samples could investigate the more complicated geochemical conditions in low permeability media. As the rate of CCl_4 transformation may be sensitive to oxide coatings on the pyrite, field rate constants may be lower than those obtained in these reactive-diffusion experiments with freshly cleaned pyrite.

REFERENCES

Abbott, D.E., 1987. The Origin of Sulphate and the Isotope Geochemistry of Sulphate-Rich Shallow Groundwater Of The St. Clair Clay Plain, Southwestern Ontario. M.Sc. Thesis, University of Waterloo.

Adewuyi, Y.G.and Carmichael, G.R. 1987. Kinetics and Oxidation of Carbon Disulfide by Hydrogen Peroxide in Alkaline Medium and Application to Carbonyl Sulfide. ES&T 21:170-177.

Cirpka, O. 1996. CONTRACT - A Numerical Tool for Contaminant Transport and Chemical Transformations. Mitteilungen des Instituts fuer Wasserbau der Universitaet Stuttgart, Heft 88. Eigenverlag des Institutes fuer Wasserbau, Stuttgart.

Criddle, C.S. and McCarty, P.L. 1991. Electrolytic Model Systems for Reductive Dehalogenation in Aqueous Environments. ES&T, 25(5):973.

Deer, W.A., Howie, R.A. and Zussman, J. 1966. An Introduction to the Rock-Forming Minerals. John Wiley and Sons, Inc, Suffolk, Great Britain.

Gillham, R.W. and O'Hannesin. S.F. 1994. Enhanced Degradation of Halogenated Aliphatics by Zero Valent Iron. Ground Water 32:958.

Koerner, R.M. 1994. Designing with Geosynthetics. 3rd addition. Prentice-Hall, Englewood Cliffs, New Jersey.

Kreigman-King, M.R. and Reinhard, M. 1991. Reduction of Hexachloroethane and Carbon Tetrachloride at Surfaces of Biotite, Vermiculite, Pyrite and Marcasite. In: Organic Substances and Sediments in Water. Baker, R.A. Ed. Lewis Publishers. Volume 2, Chapter 16.

Kreigman-King, M.R. and Reinhard, M. 1993. Reduction of Carbon Tetrachloride by Pyrite. 205th ACS National Meeting, Division of Geochemistry, Denver, Co. March 28-April 2, 1993.

Kreigman-King, M. and Reinhard, M. 1994. Transformation of Carbon Tetrachloride by Pyrite in Aqueous Solution. ES&T 28(4):692-700.

Kuhn, E.P. and Suflitia, J.M. 1989. Dehalogenation of Pesticides by Anaerobic Microorganisms in Soils and Groundwater - A Review. In: Reactions and Movement of Organic Chemicals in Soils. Soil Science of America and American Society of Agronomy Special Publication No. 22, p. 111.

Lasaga, A.J. 1983. Rate Laws of Chemical Reactions. In Reviews of Mineralogy 8, Kinetics of Geochemical Processes, Mineralogical Society, Washington D.C.

Mackay, D and Shiu, Wan Ying. 1981. A Critical Review of Henry's Law Constants for Chemicals of Environmental Interest. J. Phys. Chem. Ref. Data 10(4):1175-1193.

Major, L. 1997. Granular Iron as an Inhibitor to Tricholorethene Transport Through Geosynthetic Clay Liners. University of Waterloo, M.Sc. Thesis.

McKibben, M.A. and Barnes, H.L. 1986. Oxidation of Pyrite in Low Temperature Acidic Solutions: Rate Laws and Surface Textures. Geochimica Cosmochimica Acta 50:1509-1520.

Montgomery, J.H. 1990. Groundwater Chemicals Desk Reference Vol 1. John Wiley and Sons, Inc., Toronto.

Nicholson, R.V., Gillham, R.W. and Reardon. E.J. 1988. Pyrite Oxidation in Carbonate-Buffered Solution: 1. Experimental Kinetics. Geochimica Cosmochimica Acta 52:1077-1085.

Nicholson, R.V., Gillham, R.W. and Reardon. E.J. 1990. Pyrite Oxidation in Carbonate-Buffered Solution: 2. Rate Control by Oxide Coating. Geochimica Cosmochimica Acta 54:395-402.

Nicholson, R.V. 1994. Iron-Sulphide Oxidation Mechanisms: Laboratory Studies. Min. Assoc. of Can Short Course, 22:163-183.

Schwarzenbach, R.P., Gschwend, P.M., and Imboden, D.M. 1993. Environmental Organic Chemistry. John Wiley and Sons, Inc., Toronto.

Shackelford, C.D. 1991. Laboratory Diffusion Testing for Waste Disposal - A Review. J. of Contaminant Hydrology 7:177-217.

VanStempvoort, D.R., Hendry, M.J., Schoenau, J.J., and Krouse, H.R. 1994. Sources and Dynamics of Sulfur in Weathered Till, Western Glaciated Plains of North America. Chemical Geology,111:35-56.

Vogel, T.M., Criddle, C.S. and McCarty, P.L. 1987. Transformations of Halogenated Aliphatic Compounds. ES&T 21(8):722.

Wieland, E., Wehrli, B., Stumm, W. 1988. Geochimica Cosmochimica Acta 52:1969-1981.

Table 3.1. Physicochemical Properties of Compounds

Literature Values						Experimental Values					
Compound	D_W	V_P	S	K_{ow}	H	K_V		K_W	K_B		H_{exp}
						100 μm	7 μm	100 μm	100 μm	7 μm	
1,2-DCA	89.7	0.11	85 (5100)	30	0.04	315	355	15	9	16	0.05
CCl_4	8.5	0.12	5 (1150)	250	0.82	405	465	325	150	673	0.8
$CHCl_3$	9.9	0.21	85 (1000)	90	0.13	230	295	35	22	44	0.15
CS_2	11	0.39	40 (2900)	70	0.5	90	115	46	31	67	0.5

NOTES:

D_W Estimated Free Solution Diffusion Coefficient (value x 10^{-6} cm^2/s)

V_P Vapour Pressure atm 25°C (Mackay and Shui, 1981; Montgomery, 1990)

S Water Solubility mM (μg/l) 25°C (Mackay and Shui, 1981; Montgomery, 1990)

K_{ow} Octanol-Water Partition Coefficient 25°C (Schwarzenbach et al., 1993; Montgomery, 1990)

H C_V / C_W Equilibrium Partition Coefficients 25°C (Mackay and Shui, 1981; Montgomery, 1990)

K_V C_C / C_V Equilibrium Partition Coefficient (22°C ± 1.5°C)

K_W C_C / C_W Equilibrium Partition Coefficients (22°C ± 1.5)

K_B C_C / C_W^0 Calibration Coefficient (22°C ± 1.5)

H_{exp} $K_{W\ 100\ \mu m} / K_{V\ 100\ \mu m}$

Table 3.2. Experimental and Model Parameter Values for Reactive Diffusion Experiment

	Units	1,2-DCA	CCl_4	CCl_3H	CS_2	CO_2 [a]
		Diffusion Cell Experimental Parameters				
Quantitation limits for conc. in reservoir 7 μm fibre	μM	1.7	4.1	7.4	4.0	NA
Quantitation limits for conc. in reservoir 100 μm fibre	μM	0.08	0.21	0.34	0.18	NA
Quantitiation limits for conc. in porewater 7 μm fibre	μM	36.4	2.5	41.5	5.1	NA
Quantitiation limits for conc. in porewater 100 μm fibre	μM	2.6	0.45	3.4	0.45	NA
Initial concentration in reservoir	μM	21	73	0	0	0
		Reactive-Diffusion Model Parameters				
Effective diffusion coefficient (D_e) [b]	$x10^{-6}$ cm^2s^{-1}	6	4	6	7	ND
Reaction coefficients cell 1 (k) [c]	$x\ 10^{-5}$ s^{-1}	0	1.9	0.13	1.8	0.04
Reaction coefficients cell 2 (k) [c]	$x\ 10^{-5}$ s^{-1}	0	1.9	0.26	1.6	0.07

[a] CO_2 was not experimentally measured but was assumed to equal the % unaccounted-for mass / initial CCl_4 mass in the cell

[b] D_e from nonreactive experiment reservoir model simulations

[c] k values under CCl_4, CCl_3H, CS_2 and CO_2 columns represent k_{CCl4}, k_{CCl3H}, k_{CS2} and k_{CO2}, respectively

NA Not Applicable

ND Not Determined

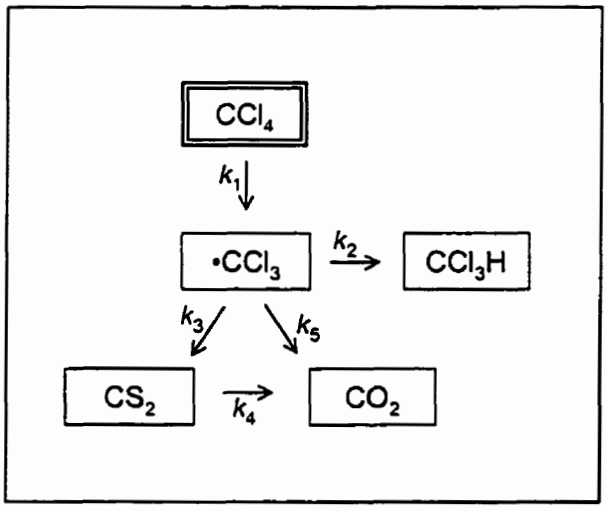

Figure 3.1. CCl_4 Transformation Pathway for Formation of CCl_3H, CS_2, and CO_3. Diagram modified from Kreigman-King and Reinhard (1994).

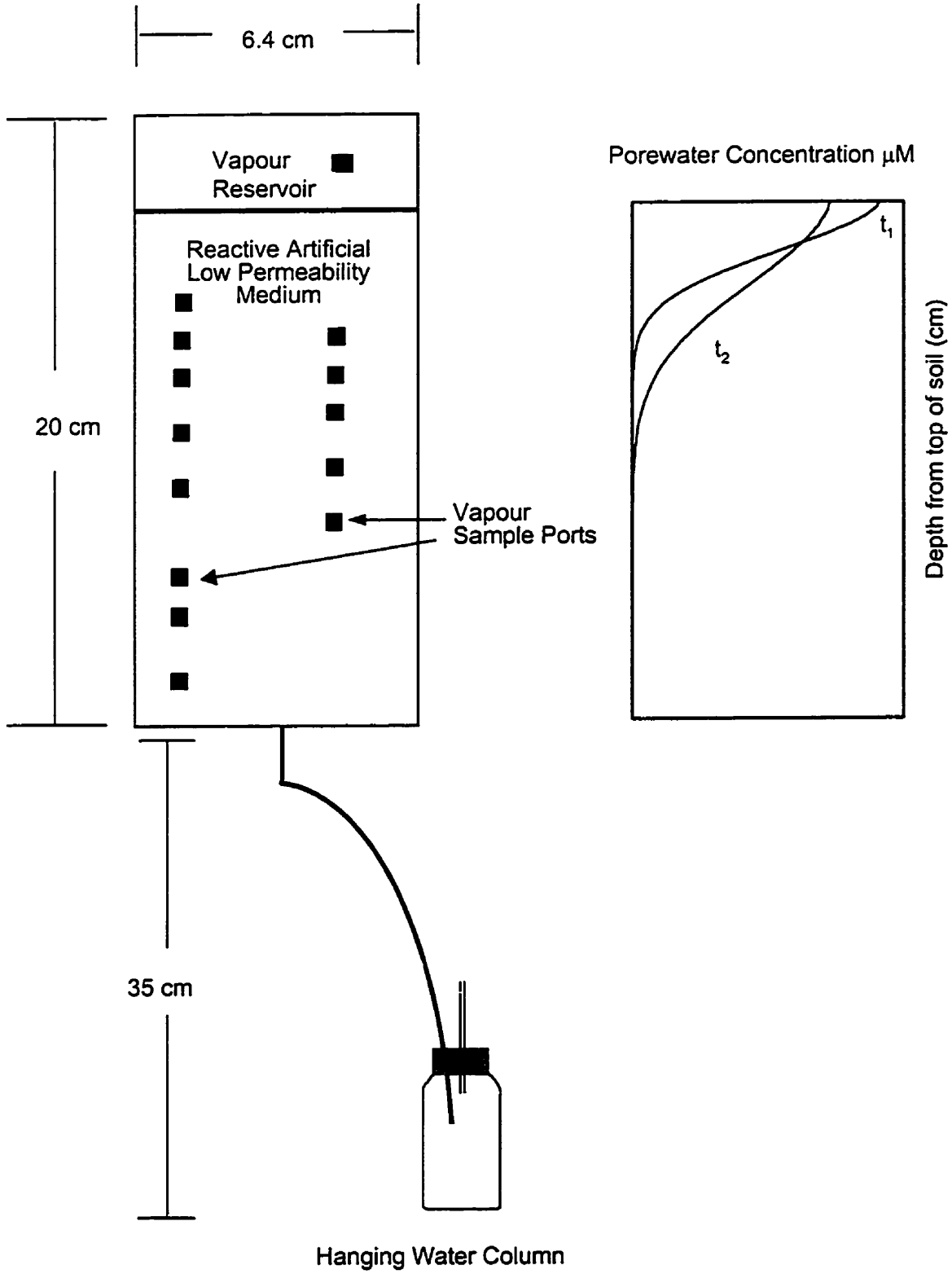

Figure 3.2. Schematic of Reactive-Diffusion Cell Apparatus. Reactant added to reservoir and reactive material present in artificial low permeability medium. Figure on right is example of sequential diffusion profiles in the porewater (t_1 and t_2) obtained from temporal sampling of vapour in boreholes in the artificial reactive medium.

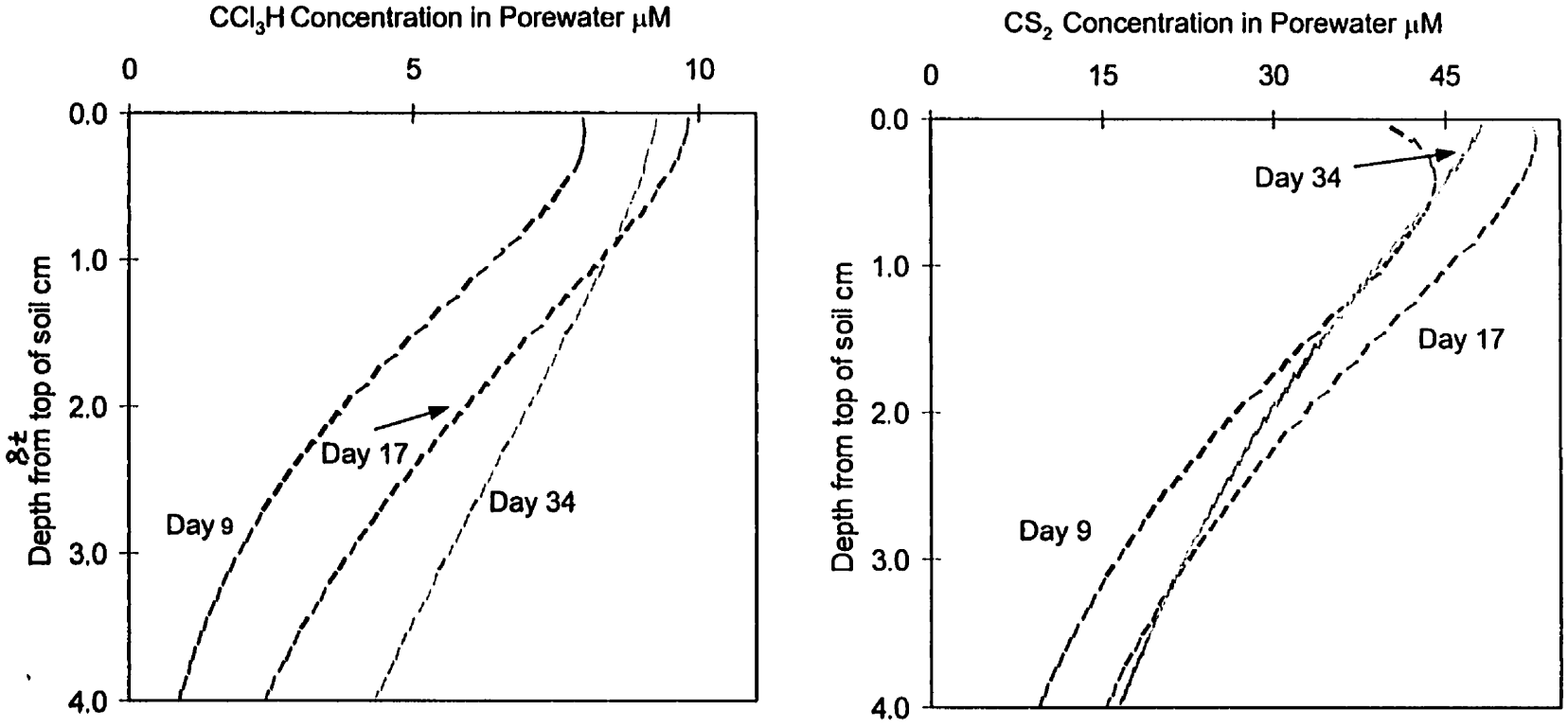

Figure 3.3A. Selected Model Simulations of Reactive-Diffusion Profiles for the Transformation Products. D_e and *k* values within range reported in Table 3.2.

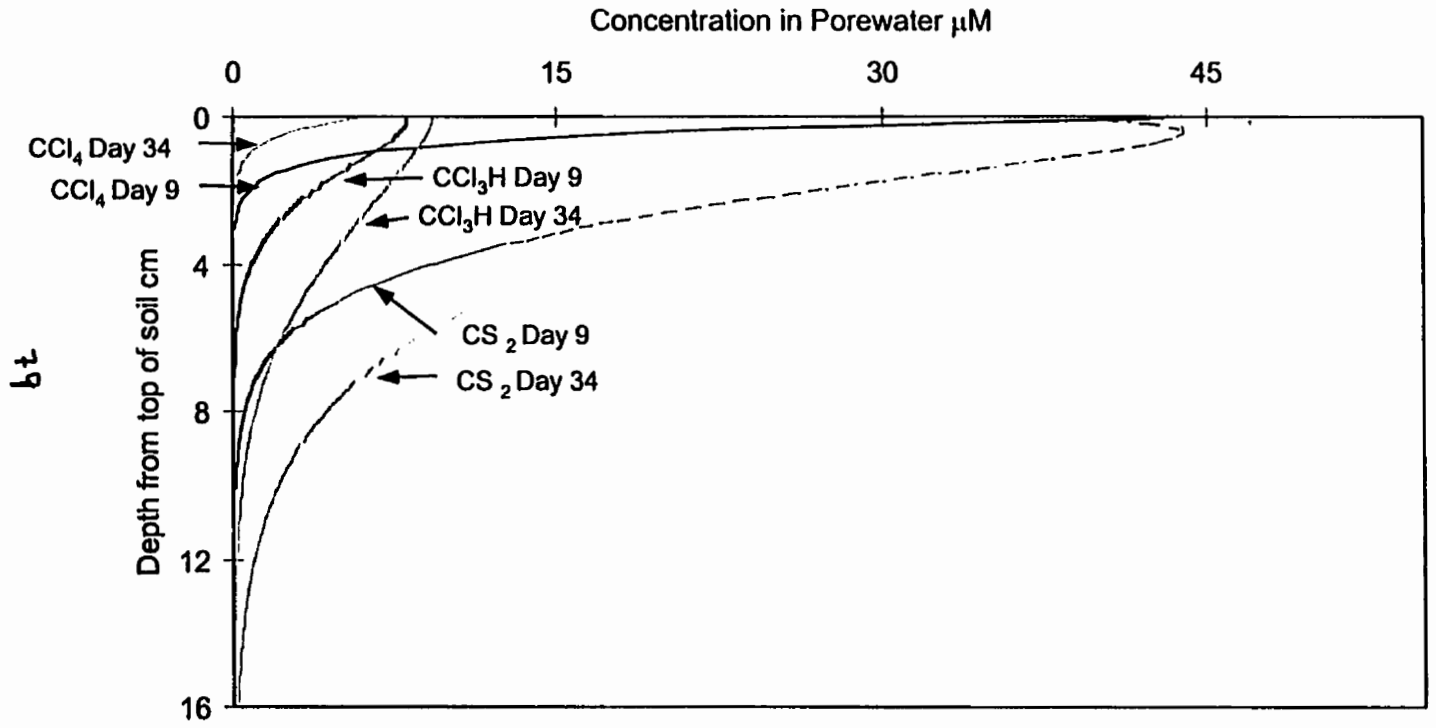

Figure 3.3B. Selected Model Simulations of Reactive-Diffusion Profiles for the Transformation Series. For Days 9 and 34. D_e and *k* values within range reported in Table 3.2.

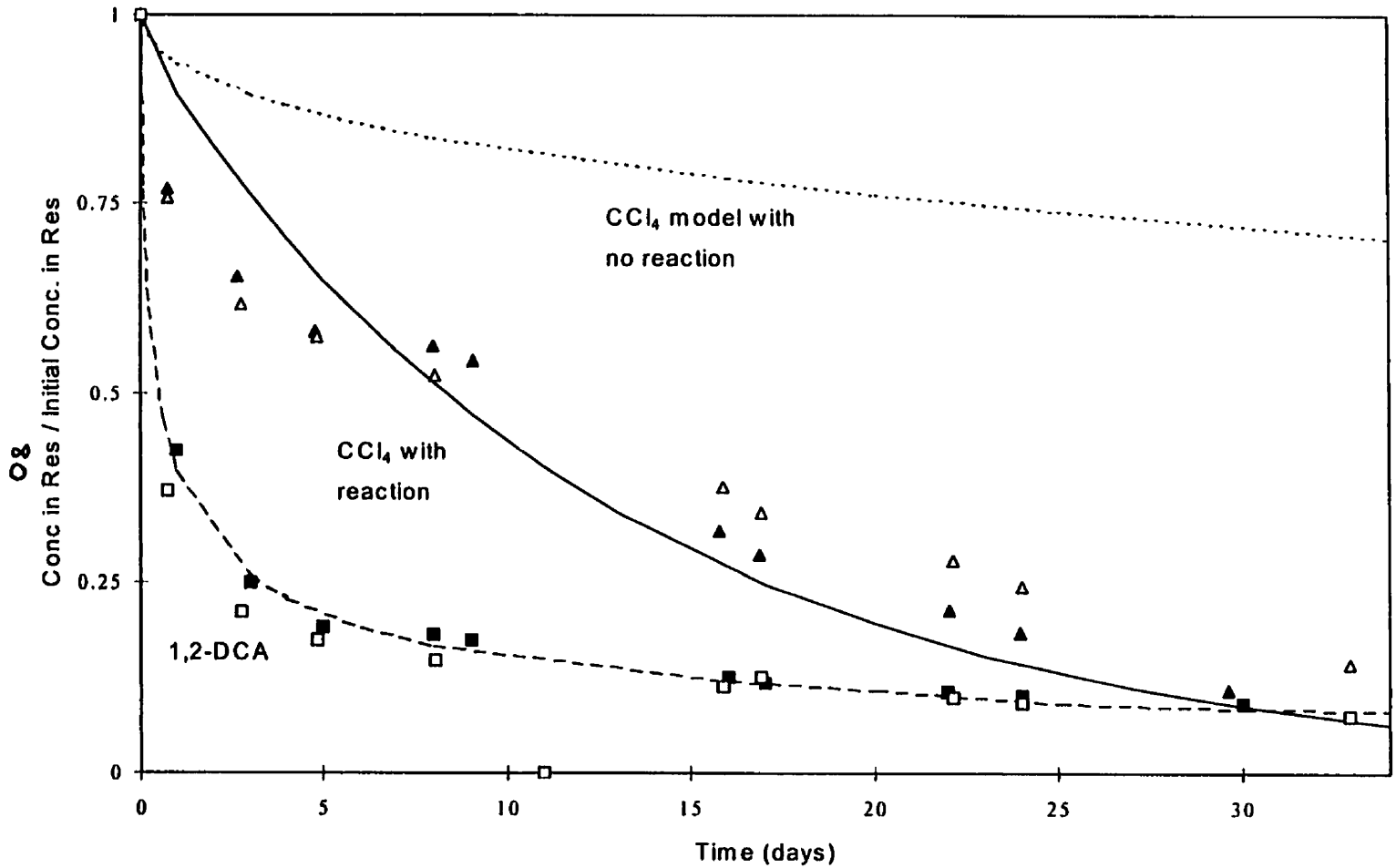

Figure 3.4. Tracer (1,2-DCA) and Reactant (CCl_4) Reservoir Concentrations With Time. Diffusion cell 1 = closed symbols, diffusion cell 2 = open symbols, model = lines. D_e values (and k for CCl_4) provided in Table 3.2. CCl_4 model results shown for both nonreactive and reactive conditions.

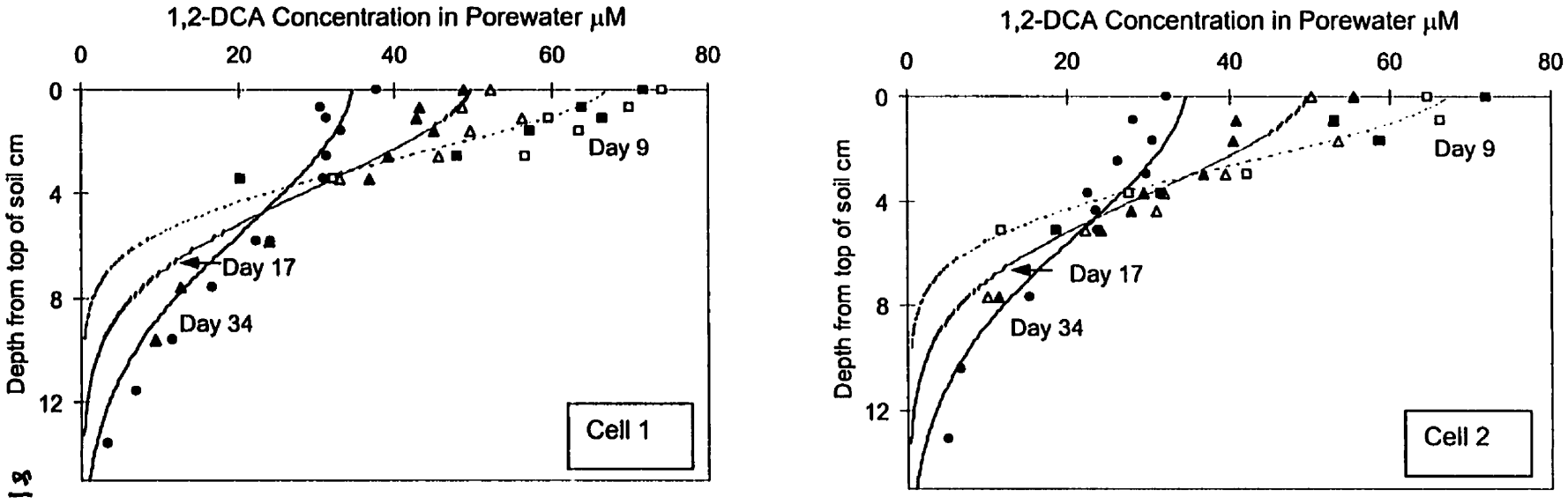

Figure 3.5. 1,2 DCA 100 µm and 7 µm Fibre Diffusion Profile Results. 7 µm = open symbols, 100 µm = closed symbols, model = lines. D_e values provided in Table 3.2.

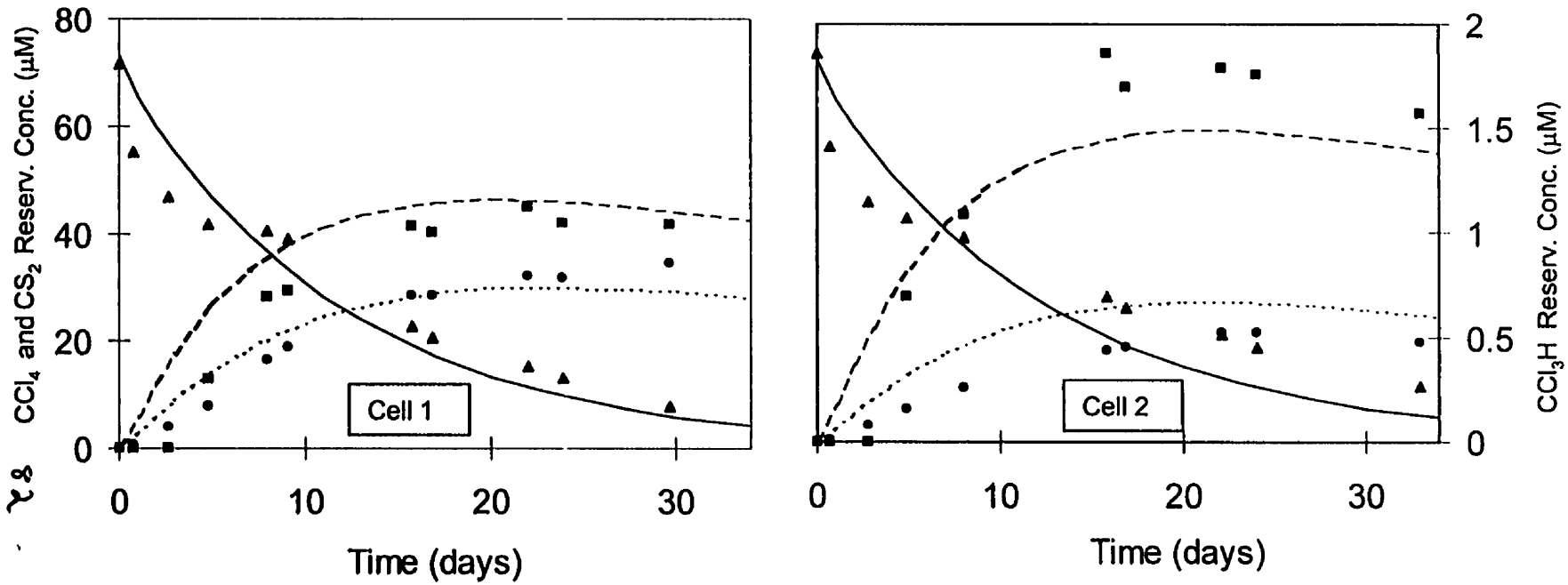

Figure 3.6. Reservoir Concentrations with time for Transformation Series (CCl_4, CCl_3H and CS_2).
Experimental results = symbol, model = lines. Refer to Table 3.2 for model D_e and *k* values

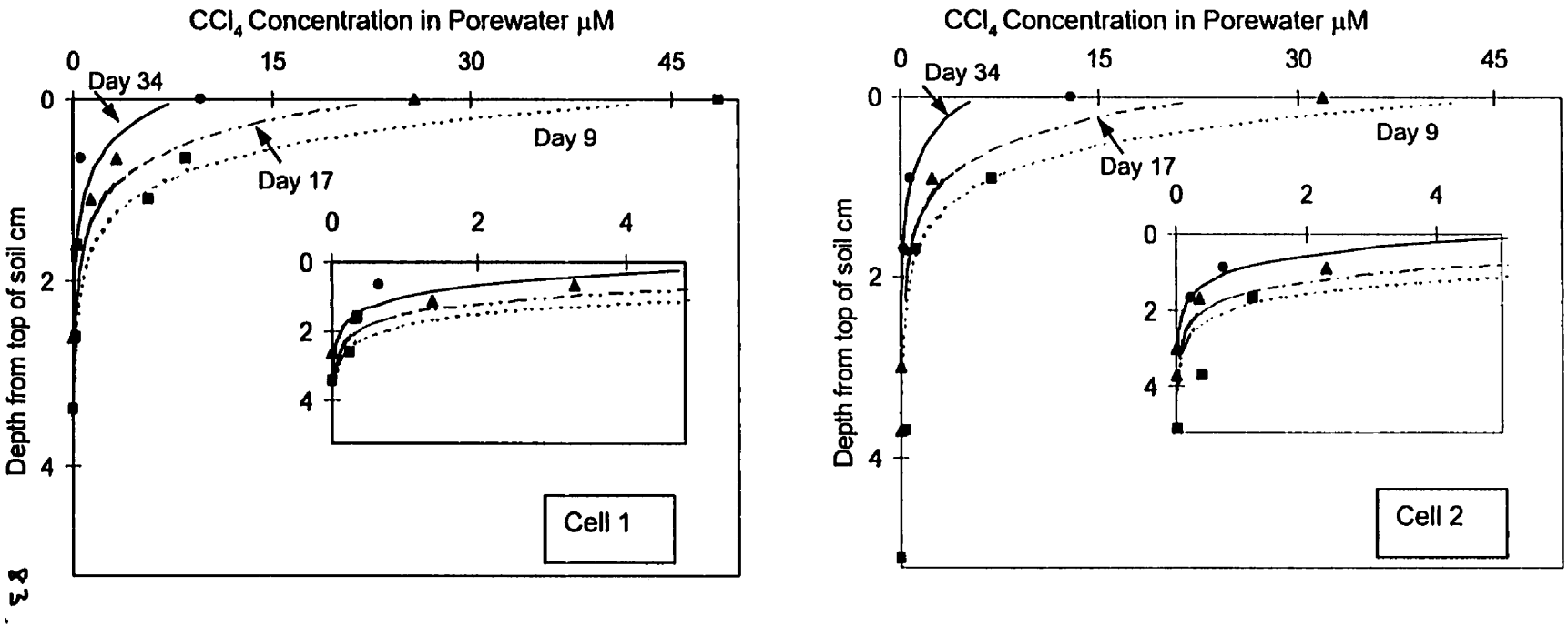

Figure 3.7A. CCl_4 Reactive-Diffusion Profiles. Experiment = symbols, model = lines. Refer to Table 3.2 for model D_e and *k* values.

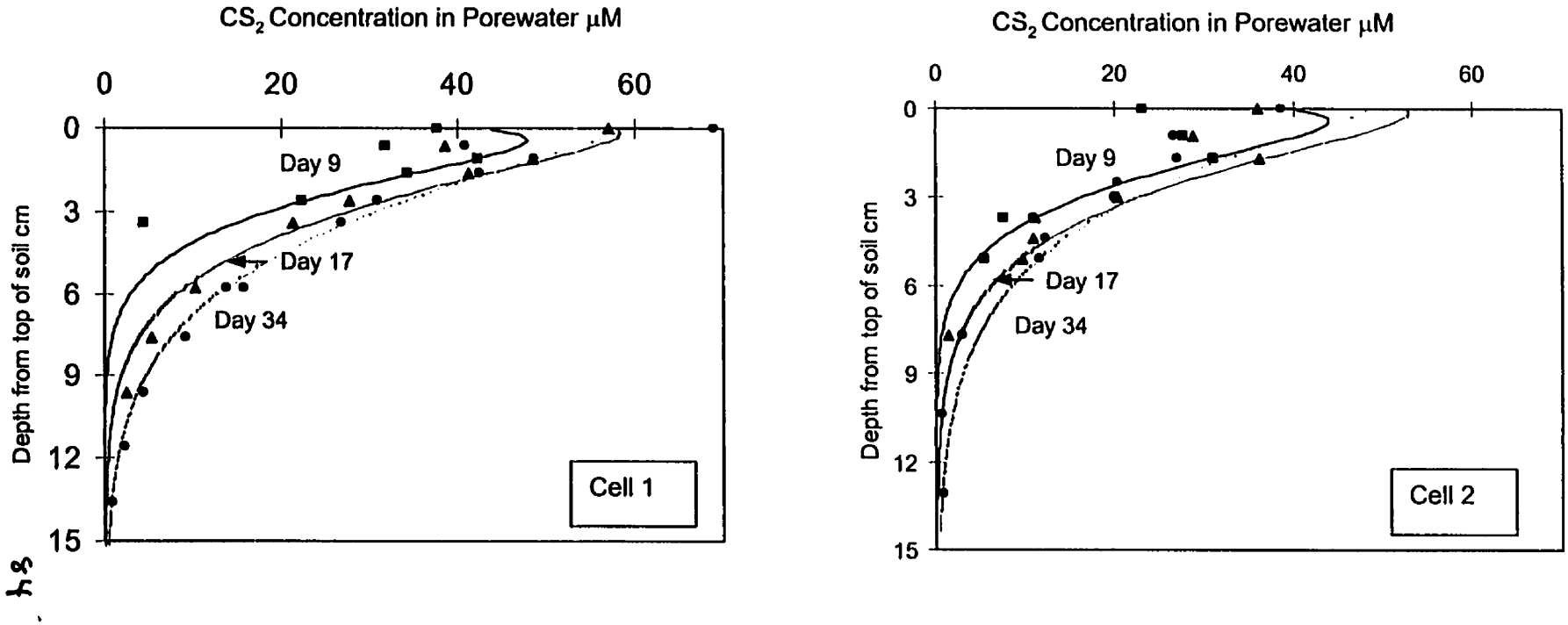

Figure 3.7B. CS_2 Reactive-Diffusion Profiles. Experiment = symbols, model = lines. Refer to Table 3.2 for model D_e and *k* values.

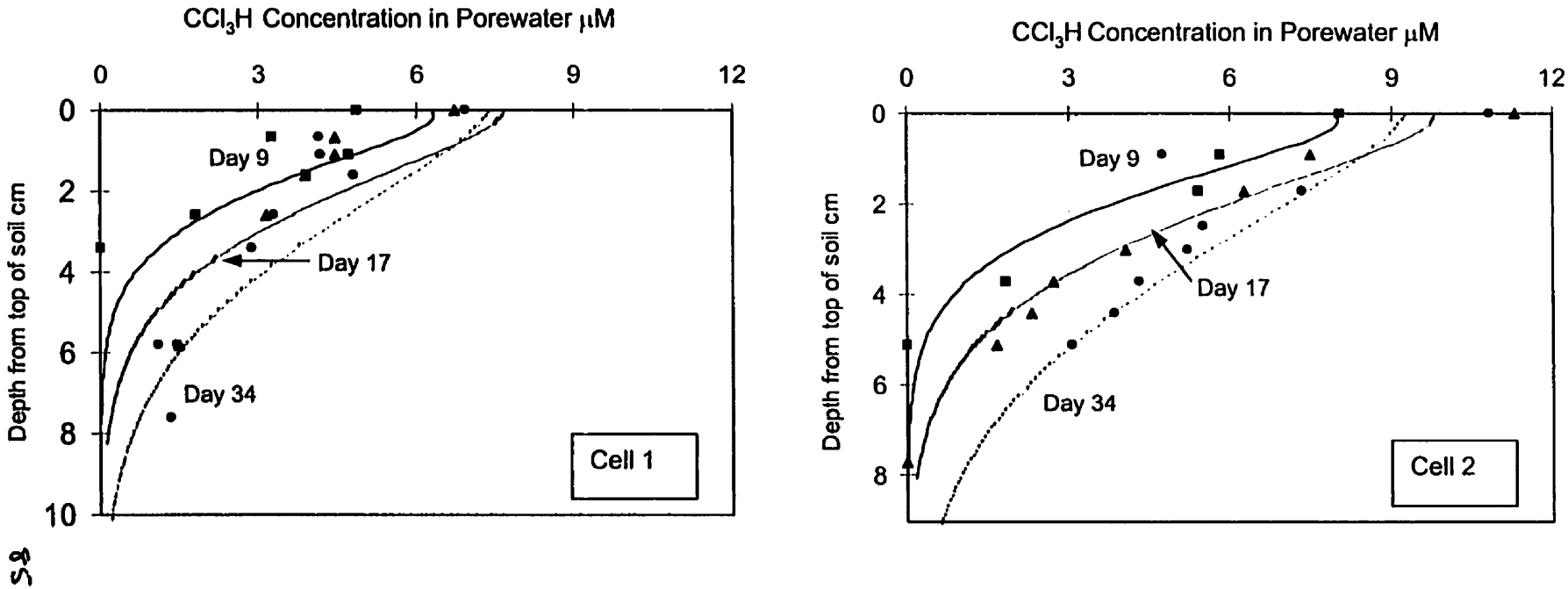

Figure 3.7C. CCl_3H Reactive-Diffusion Profiles. Experiment = symbols, model = lines. Refer to Table 3.2 for model D_e and *k* values.

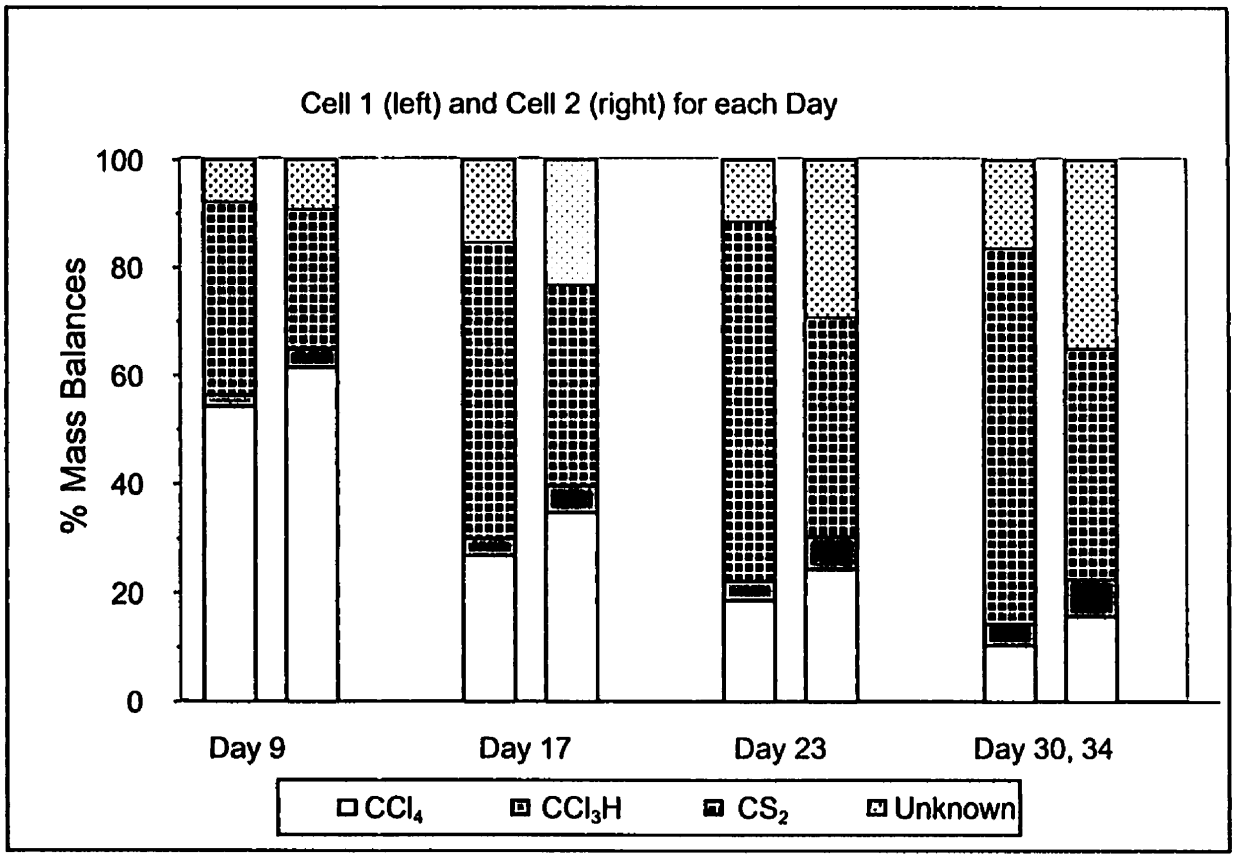

Figure 3.8. Evaluation of Mass Balance Over Time in the Duplicate Reactive-Diffusion Experiments. Unknown mass is the unaccounted-for mass described in text and is assumed to be CO_2 in modelling simulations.

CHAPTER 4
CONCLUSIONS

The goal of temporally evaluating VOC concentration measurements with minimal disturbances to the diffusion and transformation processes was attained with this laboratory diffusion cell design and SPME microsampling. As well, reproducible and predictable diffusive losses with time in the reservoir and sequential diffusion profiles for a single column of low permeability medium were obtained. This allowed for the estimation of D_e for 5 VOCs in a nonreactive low permeability medium and *k* values for a 3 member HOC abiotic heterogeneous transformation series in a reactive low permeability medium. The estimated values were within an order of magnitude of the range of literature values reported for similar conditions.

In the nonreactive and reactive experiments, the results were reasonably well predicted for the majority of the data by a one-dimensional diffusion model that assumed Fickian diffusion and a constant porosity with time and depth and, for the reactive experiments, first order reaction kinetics with respect to reactant concentration and a constant concentration of reactive solid surface. Differences between the model and results in both experiments may be due to inappropriate model assumptions for conditions in the top portion of the porous medium column.

For studies utilizing packed low permeability media, it is recommended that a vibration table be used to pack and saturate the solids thereby reducing the potential for consolidation in the top portion of the porous medium. For intact field cores (both clean and contaminated), consolidation is not expected to be a problem. For application to natural media collected in cores, this method would ideally use the coring container as the diffusion cell (with a space left on top for the vapour reservoir for clean cores). This would minimize the disturbance to the cores and likely ensure a much tighter seal between medium and cell walls. To further improve the general applicability of the technique to a wide range of compounds, the design needs to be modified so that less mass is extracted from the porewater during each SPME sampling.

This work has shown that first order kinetic rate constant for the overall reaction from batch experiments can be utilized to provide initial estimate for VOC transformation in artificial reactive low permeability media. Future work using a modified diffusion cell design to allow for the collection of field core samples could investigate whether batch results can be extrapolated to more complicated geochemical conditions in low permeability media. As

the rate of CCl_4 transformation may be sensitive to oxide coatings on the pyrite, field rate constants may be lower than those obtained in these reactive-diffusion experiments with freshly cleaned pyrite.

APPENDIX A

Mass Balance Calculations

M_{TOT} (the total mass of a compound in the diffusion cell)

$$M_{TOT} = C_R V_R + \int_{L_{PM}} C_{PW}\, dz\theta$$

M_{TOT} for Transformation Series

M_{TOT} for CCl_4 + M_{TOT} for CCl_3H + M_{TOT} for CS_2

M_{BAL} (the total mass relative to the initial mass)

$$M_{BAL} = \frac{C_R V_R + \int_{L_{PM}} C_R V_R\, dz\theta}{C_R{}^i V_R}$$

C_R Concentration in reservoir, superscript i refers to initial concentration
V_R Volume of reservoir
C_R Concentration in porewater reservoir
dz Depth in porous medium
θ Porosity